



# CLASS VI PERMIT

## APPLICATION NARRATIVE

**40 CFR 146.82(a)**

LAPIS ENERGY (AR DEVELOPMENT) LP  
PROJECT BLUE  
EL DORADO, ARKANSAS

Prepared By:  
GEOSTOCK SANDIA, LLC

Revision No. 1  
August 2023

## TABLE OF CONTENTS

1.0	Project Background and Facility Information.....	13
1.1	Facility Information.....	13
1.2	Project Goals and Stakeholders.....	13
1.3	Project CO <sub>2</sub> Details.....	14
1.4	Project Timeline .....	14
1.5	Project WELL DESIGNATION .....	15
2.0	Site Characterization.....	16
2.1	Regional Geology.....	17
2.1.1	Regional Maps and Cross Sections.....	22
2.1.2	Regional Stratigraphy .....	23
2.1.3	Regional Structural Geology.....	43
2.1.4	Regional Groundwater Flow in the Injection Zones .....	45
2.2	Local Geology of the El Dorado Site .....	47
2.2.1	Data Sets Used for Site Evaluation.....	47
2.2.2	Local Stratigraphy.....	49
2.2.3	Local Structure.....	53
2.2.4	Faulting in the Area of Review .....	55
2.3	Description of the Confining and Injection Zones .....	56
2.3.1	Confining Zones.....	57
2.3.2	Injection Zones.....	62
2.4	Geomechanics and Petrophysics .....	68
2.4.1	Ductility .....	68

2.4.2	Stresses and Rock Mechanics .....	73
2.4.3	Pore Pressures of the Injection Zone .....	77
2.4.4	Calculated Fracture Gradient .....	79
2.5	Seismicity .....	79
2.5.1	Regional Seismic Activity .....	82
2.5.2	Seismic Risk of the Project Site.....	84
2.5.3	Induced Seismicity.....	86
2.5.4	Seismic Risk Models for the Project Site .....	89
2.6	Hydrogeology.....	95
2.6.1	Regional Hydrogeology .....	95
2.6.2	Local Hydrogeology .....	106
2.6.3	Determination of the Base of the Lowermost USDW .....	107
2.6.4	Base of the Lowermost USDW.....	111
2.6.5	Water Well Data Sets.....	111
2.6.6	Local Water Usage.....	112
2.6.7	Injection Depth Waiver.....	113
2.7	Geochemistry .....	114
2.7.1	Formation Brine Properties.....	115
2.7.2	Compatibility of the CO <sub>2</sub> with Subsurface Fluids and Minerals .....	118
2.7.3	Site Specific Geochemical Modeling.....	123
2.8	Economic Geology of the Area.....	124
2.8.1	Lithium.....	124
2.8.2	Proximity to the Lapis Energy – Project Blue Site .....	126
2.8.3	Oil Fields.....	127
2.9	Site Suitability Summary .....	127

3.0	AoR and Corrective Action Plan .....	130
4.0	Financial Responsibility.....	132
5.0	Injection Well Construction.....	133
5.1	Proposed Stimulation Program.....	133
5.2	Construction Design.....	134
5.2.1	Casing String Details .....	134
5.2.2	Centralizers .....	135
5.2.3	Annular Fluid.....	136
5.2.4	Cementing Details.....	136
5.2.5	Tubing and Packer Details .....	136
5.3	Proposed Drilling Program – INJECTION WELLS.....	137
5.3.1	Injection Well Drilling Procedures – Project Blue Class VI Injection Well No. 1 (INJ-1) .....	138
5.3.2	Injection Well Drilling Procedures – Project Blue Class VI Injection Well No. 2 (INJ-2) .....	149
6.0	Pre-Operational Logging and Testing.....	160
7.0	Well Operation.....	161
8.0	Testing and Monitoring.....	162
9.0	Injection Well Plugging .....	164
10.0	Post Injection Site Care (PISC) and Site Closure .....	165
11.0	Emergency and Remedial Response .....	166
12.0	Injection Depth Waiver and Aquifer Exemption Expansion .....	167
13.0	Optional Additional Project Information .....	168

14.0 Other Relevant Information .....	169
REFERENCES .....	170

## **LIST OF TABLES**

### **Section 2.0 – Site Characterization**

Table 2-1 Listing of Local Geologic Maps in Appendix A

Table 2-2 Permeability and Porosity of Hosston Shales in Union County, Arkansas (data from Great Lakes WDW-5 Injection Well, 1995)

Table 2-3 Bishop No. 2 (Union County) – XRF Analysis of the Lower Hosston – Core Samples from the Bureau of Economic Geology

Table 2-4 Permeability and Porosity data on the Cotton Valley Formation (from Spain et al. 2011)

Table 2-5 Table of Geomechanical Properties

Table 2-6 Calculated Fracture Gradient and Operating Pressures

Table 2-7 Tabulation of Seismic Events within 160 km (~100 miles) of the Project Blue Site since 1900

Table 2-8 Calculated Critical Pressure to Induce Seismicity

Table 2-9 Tabulation of Water and Monitoring Wells within the Delineated AoR

Table 2-10 Formation Fluid Properties – Injection Zones

### **Section 4.0 – Financial Demonstration**

Table 4-1 Cost Estimates for Activities to be Covered by Financial Responsibility

### **Section 5.0 – Injection Well Construction**

Table 5-1 Proposed Casing String Details

Table 5-2 Proposed Tubing Details

Table 5-3 Proposed Well Fluids Program

Table 5-5 Water String Casing Cement Program

Table 5-5 Surface Casing Cement Program

Table 5-6 Protection Casing Cement Program

## **Section 7.0 – Well Operation**

Table 7-1 Proposed Operational Procedures – Cotton Valley Injection Interval CV1

Table 7-2 Proposed Operational Procedures – Cotton Valley Injection Interval CV2

Table 7-3 Proposed Operational Procedures – Cotton Valley Injection Interval CV3

Table 7-4 Proposed Operational Procedures – Lower Hosston

## **LIST OF FIGURES**

### **Section 1.0 – Facility Information**

Figure 1-1 Project location – El Dorado, Arkansas

### **Section 2.0 – Site Characterization**

Figure 2-1 Stratigraphic column of Arkansas (from the Arkansas Geological Survey)

Figure 2-2 Type Log – Schuler Drilling Company, EDC No. 1

Figure 2-3 Physiographic provinces of Arkansas

Figure 2-4 Schematic northwest-southeast cross section showing the evolutionary stages in the formation of the northern Gulf of Mexico and East Texas Basin (modified from Jackson and Galloway, 1984)

Figure 2-5 Distribution of Cretaceous and Cenozoic continental margins in the northwestern Gulf of Mexico (modified from Jackson and Galloway, 1984)

Figure 2-6 Gulf of Mexico and the Four Provinces (from Galloway, 2008)

Figure 2-7 Tectonic process and features associated with the formation of the Gulf of Mexico (Sawyer et al., 1991)

Figure 2-8 Location Map of Major Interior Structures in the northern Gulf Coast Region (from Hosman, 1996)

Figure 2-9 Regional Cross Section of Southern Arkansas (Imlay, 1949)

Figure 2-10 Paleodepositional environment for the Upper Jurassic (Cotton Valley Formation) and the associated depocenters (from Ewing and Galloway, 2019)

Figure 2-11 Paleodepositional Environment of the Lower Cretaceous for the lower Hosston Formation (from Ewing and Galloway, 2019)

Figure 2-12 Paleodepositional Environment and Uplift of the Upper Cretaceous for the Tuscaloosa Formation (from Ewing and Galloway, 2019)

Figure 2-13 Paleodepositional Environments Upper Cretaceous illustrating the Olmos and Nacatoch Delta systems (from Ewing and Galloway, 2019)

Figure 2-14 Regional configuration and thickness trends of the Midway Group (from Hosman, 1996)

Figure 2-15 Regional configuration and thickness trends of the Wilcox Group (from Hosman, 1996)

Figure 2-16 Regional configuration and thickness trends of the Cane River Formation (from Hosman, 1996)

Figure 2-17 Regional configuration and thickness trends of the Sparta Formation (from Hosman, 1996)

Figure 2-18 Regional configuration and thickness trends of the Cook Mountain Formation (from Hosman, 1996)

Figure 2-19 Regional configuration and thickness trends of the Cockfield Formation (from Hosman, 1996)

Figure 2-20 Regional Structural features around the Project Area of Interest (modified from Dutton and others, 1993)

Figure 2-21 Topographic Map of the Project Blue site and the LSB Industries facility

Figure 2-22 Data Acquisition and Quality Control (QC) workflow

Figure 2-23 Location of 2D Seismic Lines used for Project Blue Study

Figure 2-24 Sligo Porosity Distribution (from Kirkland, 1988)

Figure 2-25 Hosston Injection Zone – Core Porosity-Permeability Cross Plot (data from SPDA database)

Figure 2-26 Lower Hosston Injection Zone Capillary Pressure (from Dutton et al., 1993)

Figure 2-27 Lower Hosston Ternary Diagram

Figure 2-28 Cotton Valley Injection Zone – Core Porosity-Permeability Cross Plot (data from SPDA database)

Figure 2-29 Density Effects in Shale Ductility (from Hoshino et al., 1972)

Figure 2-30 Change in density and ductility of shales with increasing depth (from Hoshino et al. 1972)

Figure 2-31 Three different creep stages illustrated on a Strain vs Time Plot (modified from Brendsdal, 2017)

Figure 2-32 Schematic diagram of stress and strain concepts (from Han, 2021)

Figure 2-33 Principal horizontal stresses along the Gulf Coast Region (modified from Nicholson, 2012)

Figure 2-34 Modified Mercalli Intensity (MMI) Scale (from USGS, 2022)

Figure 2-35 Seismic risk map of the United States (from USGS, 2018)

Figure 2-36 Seismicity of Arkansas from 1699 to 2019 (from Arkansas Geological Survey, 2020)

Figure 2-37 Liquefaction susceptibility map of Arkansas (from Arkansas Geological Survey, 2010)

Figure 2-38 Location of Project Blue site in relation to the South Arkansas Fault Zone (from Jackson and Wilson, 1982)

Figure 2-39 Regional and local seismic events within 160 km (~100 miles) of El Dorado, Arkansas since 1900 (Data search compiled in November 2022 from the USGS National Earthquake Database)

Figure 2-40 Seismic events in Union County since 1900 (Data search compiled in November 2022 from the USGS National Earthquake Database)

Figure 2-41 Major aquifers of Arkansas (from USGS, 2014)

Figure 2-42 Regional hydrostratigraphic column for the Coast Plains Aquifer in Arkansas (modified from Kresse et al., 2014)

Figure 2-43 Regional extent of the Sparta Aquifer System within the Mississippi Embayment systems (modified from USGS Fact Sheet 111-05, 2002)

Figure 2-44 Potentiometric Map of the Sparta Aquifer System in Arkansas (from Schrader, 2014)

Figure 2-45 Graphic solution of the Spontaneous Potential Equation (Schlumberger, 1987)

Figure 2-46 Resistivity nomograph for NaCl Solutions (Schlumberger, 1979)

Figure 2-47 J.D. Reynolds Company, Byrd No. 1 – Example of base of the Lowermost USDW for the Project Blue site

Figure 2-48 Water well search map (USGS Topographic basemap)

Figure 2-49 Water levels in Union County, Arkansas (from Schrader, 2014)

Figure 2-50 Formation temperature gradient

Figure 2-51 Viscosity nomograph

Figure 2-52 Location of critical economic minerals in the State of Arkansas (from the Arkansas Department of Energy and Environment, 2022)

Figure 2-53 Projection of worldwide Lithium demand from 2019 to 203 (from <https://www.statista.com/statistics/452025/projected-total-demand-for-lithium-globally/> )

Figure 2-54 Lanxess property and regional lithium brine values (production from the Smackover) (from Worley Technical Report, 2019)

Figure 2-55 Location of industrial minerals in the State of Arkansas (from the Arkansas Geological Survey/USGS, 2012)

## **Section 5.0 – Injection Well Construction**

Figure 5-1 Proposed Project Blue Injection Well 1 (INJ-1) – Class VI Schematic

Figure 5-2 Proposed Project Blue Injection Well 2 (INJ-2) – Class VI Schematic

Figure 5-3 Proposed Wellhead Schematic

## **LIST OF APPENDICES**

- Appendix A      Local Geologic Maps and Cross sections
- Appendix B      Stratum Laboratory Thin Sections and Analysis on Hosston Core Samples
- Appendix C      Stress Calculations on the Injection Well Tubulars
- Appendix D      Environmental Justice Report

## INDEX OF SUBMITTED APPLICATION PLANS

GSDT Module	Report Plan Name
<b>Module A - Summary of Requirements</b>	A.1 – Project Narrative
<b>Module B – Area of Review &amp; Corrective Action Plan</b>	B.1 – Area of Review and Corrective Action Plan
<b>Module C – Financial Demonstration</b>	C.1 – Financial Demonstration Plan
<b>Module D – Pre-Operational Testing</b>	D.1 – Pre-Operation Testing Plan
<b>Module E – Project Plan Submission</b>	E.1 – Testing and Monitoring Plan
	E.2 – Injection Plugging Plan
	E.3 – Post-Injection Site Care and Site Closure Plan
	E.4 – Emergency and Remedial Response Plan

## **1.0 PROJECT BACKGROUND AND FACILITY INFORMATION**

### **1.1 FACILITY INFORMATION**

**Facility/Project Name:** El Dorado Chemical Company / Lapis Energy  
Project Blue Class VI Injection Wells No. 1 and No. 2

**Facility/Project Contact:** Stijn Konings, Chief Geoscientist  
Lapis Energy LP  
5420 LBJ Fwy, Bldg. 2  
Suite 1330  
Dallas, Texas 75240  
(972) 757-6529 / skonings@lapisenergy.com

**Well Locations:** Union County  
El Dorado, Arkansas  
Project Blue Class VI Injection Well No. 1 (Blue INJ-1)  
Latitude Coordinate (NAD-83): 33. 2613614642  
Longitude Coordinate (NAD-83): -92.6911515334  
  
Project Blue Class VI Injection Well No. 2 (Blue INJ-2)  
Latitude Coordinate (NAD-83): 33. 2613625494  
Longitude Coordinate (NAD-83): -92.6909878157

### **1.2 PROJECT GOALS AND STAKEHOLDERS**

On behalf of LSB Industries, Lapis Energy plans to sequester CO<sub>2</sub> emitted from the El Dorado Chemical Company (EDCC) in El Dorado (Union County), Arkansas (Figure 1-1), in saline aquifers underneath the facility. The project will be the first of its kind in Arkansas. The goal is to capture most of the process CO<sub>2</sub> generated during ammonia production, which will generate more than 375 thousand metric tons of low carbon ammonia per year. The project will permanently sequester more than 450 thousand metric tons of CO<sub>2</sub> per year and reduce LSB Industries' scope 1 greenhouse gas emissions by roughly 25% from current levels. To put this number in perspective, this equates to more than 5% of all the industrial related carbon dioxide emission in the state of Arkansas, as per the U.S. Energy Information Administration (EIA) 2020 data.

Low carbon ammonia produced with the aid of carbon sequestration is called ‘blue’ ammonia, hence the name Project Blue. With levelized CO<sub>2</sub> emissions of half that of LNG, diesel or coal, blue ammonia is an important fuel in the energy transition towards no-carbon. Carbon sequestration will give the EDCC an environmental and an economic edge over the competition, providing jobs and economic opportunity to the region while minimizing the amount of CO<sub>2</sub> emitted into the earth’s atmosphere.

### **1.3 PROJECT CO<sub>2</sub> DETAILS**

The geology underneath the LSB plant in Eldorado is ideally suited for hydrocarbon sequestration. A thick section of 3,000 ft of storage reservoir, approximately 3,500 to 6,500 ft below the surface, is capped by a 1,000 ft thick impermeable layers of shale, shielding the area drinking water supply and preventing upward migration of CO<sub>2</sub>.

The CO<sub>2</sub> will be sequestered via two injection wells located centrally on the property of the EDCC just south of the plant facilities. The source of the CO<sub>2</sub> is the Steam Methane Reforming (SMR) Process, which inputs natural gas, water and air and emits hydrogen and nitrogen as well as high purity process CO<sub>2</sub>. A small part of the process CO<sub>2</sub> is being captured to produce dry ice, but the majority is currently vented into the atmosphere. The SMR process also requires heat, which is generated by burning natural gas. The CO<sub>2</sub> generated by the heating process will not be captured as part of this Class VI Application, but studies are ongoing to evaluate the viability of capturing these emissions too.

Lapis Energy is committed to transparent and proactive stakeholder engagement. In this regard, Lapis has been engaging with industry, government and community stakeholders in both Little Rock and El Dorado and will continue to deepen those efforts throughout the Class VI Application process, as well as through project development and operation.

### **1.4 PROJECT TIMELINE**

This Class VI Application seeks the approval to sequester up to 500 thousand metric tons of CO<sub>2</sub> per year over the 20-year injection period of the project, with first injection planned as early as the beginning of 2025.

## 1.5 PROJECT WELL DESIGNATION

A tabulation of the well naming convention used in this permit application is shown below:

PROJECT BLUE WELL NAMING TABLE	
Well Identification	Well Name
Project Blue Class VI Injection Well No. 1	Blue INJ-1
Project Blue Class VI Injection Well No. 2	Blue INJ-2
Project Blue Above Confining Zone Monitor Well	Blue SM-1
Project Blue In Zone Monitor Well	Blue DM-2
Project Blue In Zone Contingent Monitor Well	Blue DM-1
Project Blue Type Well EDC #1	EDC #1
EDCC Water Source Well 4 (WSW4)	LSB WW-4
EDCC Water Source Well 6 (WSW6)	LSB WW-6
Project Blue North Monitor Well Pad Water Source Well	Blue WW-1
Project Blue Injection Well Pad Water Source Well	Blue WW-2
Project Blue Pond Water Source Well	Blue WW-3
Eastern Water Well (LSB WW-4 Alternate)	Blue WW-4
Eastern Water Well (LSB WW-6 Alternate)	Blue WW-5
Lawson Urbana W/S (Option for Blue WW-2)	Lawson Urbana W/S

- Wells in red fonts are existing Wells

## **2.0 SITE CHARACTERIZATION**

The geologic suitability of a specific stratigraphic interval for the injection and confinement of carbon dioxide (CO<sub>2</sub>) is determined primarily by the following criteria:

- Lateral extent, thickness, interconnected porosity, permeability, and geomechanical properties of the injection zone
- Lateral extent, thickness, minimal porosity, impermeability, and geomechanical properties of the overlying confining zone
- Hydrogeologic compatibility of the injected carbon dioxide with the rock formation material and in-situ brine solutions
- Faulting or fracturing of the injection zone, overlying aquiclude, and confining zone, and
- Seismic risk.

These criteria can be evaluated based on the regional and local depositional and structural histories of the geologic strata.

In this section, the subsurface geology at the Lapis Energy – Project Blue site, represented by the composite stratigraphic column in Figure 2-1, is presented and discussed to demonstrate the potential of the rocks underlying the project site to be used for the sequestration of carbon dioxide produced by EDCC. The data used in this permit application has been obtained from multiple sources, which include regional and local data interpretations performed for the study of the Area of Review (AoR), published literature, well logs, core evaluations, and empirical data where available.

An onsite well, EDC 1, drilled by the Schuler Drilling Company in 1996, has been designated as the type-log for Project Blue (Figure 2-2). The key regulatory intervals are reported in the below ground elevation. Geologic maps and cross sections illustrating the regional geology, hydrogeology, and the geologic structure of the local area are provided per 40 CFR 146.82(a)(3)(vi) standard.

## 2.1 REGIONAL GEOLOGY

The Lapis Energy – Project Blue site is situated just northwest of the municipality of El Dorado, in Union County, Arkansas. Sharing its southern border with the northern border of Louisiana, Union County, Arkansas is the most south-central county in the state and is geographically located within the West Gulf Coastal Plain province of Arkansas.

There are the two major physiographic provinces of Arkansas: the Interior Highlands and the Gulf Coastal Plain (Figure 2-3). The Interior Highlands province is subdivided into the Ozark Plateaus, the Arkansas Valley, and the Ouachita Mountains. The Gulf Coastal Plain province is subdivided into the Mississippi River Alluvial Plain and the West Gulf Coastal Plain (Figure 2-3). The West Gulf Coastal Plain province of Arkansas is part of the Gulf of Mexico Basin of the United States, which is a roughly circular structural basin that began forming along the southern margin of the North American Plate when, during the Late Triassic through the Middle Jurassic, southward rifting along the Atlantic spreading ridge caused the Paleozoic supercontinent of Pangea to separate.

Tensional deformation associated with crustal extension was the primary control on the development of the Gulf of Mexico during the Mesozoic Era. Figure 2-4 presents a series of cross sections that illustrate the structural evolution of the Gulf of Mexico during this time. Extension of the preexisting continental crust created a series of basement grabens and half grabens that filled with terrestrial red beds and volcanics early in the basin's development. Subsidence associated with crustal cooling and sediment loading continued to depress the basin, allowed the deposition of the thick sedimentary sequences, and formed a clearly defined shelf edge and slope that separates the abyssal plain from the coastal plain (Galloway, 2008). The rate of terrigenous sediment influx has been greater than the rate of basin subsidence since the termination of rifting during the Cretaceous and has resulted in a significant progradation of the continental shelf margin (Figure 2-5).

The stratigraphic-structural framework of the Gulf of Mexico basin can be subdivided into four provinces (Figure 2-6), which correspond to the major lithofacies provinces that persist from the Late Jurassic to the Holocene (Galloway, 2008).

- 1) The central basin deep water abyssal plain.
- 2) The eastern carbonate margins of the Florida and Yucatan platforms.
- 3) The Laramide-modified western compressional margin of Mexico.
- 4) The northwestern progradational margin from northeastern Mexico to Alabama.

The Western Gulf Coastal Plain of Arkansas (Figure 2-3) is physiographically located within the northwestern progradational margin structural province, which is an onshore broad coastal plain. It can be further divided along a subsidence hinge that formed along the trend of the Lower Cretaceous reef system, into an Interior Zone and a Coastal Zone. The reefs provided a focus for the development and stabilization of the Cretaceous continental shelf margin, and the reef trend is the inflection point between the Cretaceous shelf and slope and the processes that affected the development of each are inter-reliant. The Lapis Energy – Project Blue site is located near the upper extents of the interior zone in the north-central part of the coastal plain northwestern progradational margin region.

One of the major distinctions between the interior zone and the coastal zone, which is marked by the Cretaceous reef system subsidence hinge line, is the character of the crust, which is inherently related to the stratigraphic-structural framework of the basin. There are four classifications of crust in the Gulf of Mexico basin (Galloway, 2008).

- 1) Oceanic: created concurrent with the formation of the Gulf of Mexico basin from magma at the spreading center.
- 2) Thin transitional: predates the formation of the Gulf of Mexico basin and was significantly thinned and highly extended by Mesozoic rifting.
- 3) Thick transitional: crust that predates the formation of the Gulf of Mexico basin and was less attenuated than thin transitional crust during Mesozoic rifting.
- 4) Continental: predates the formation of the Gulf of Mexico basin and was not significantly modified by Mesozoic rifting.

Figures (2-7) illustrates the crustal extension, the tectonic subsidence, and the estimated crustal thickness around the basin, which are related to the formation of the Gulf of Mexico basin (Sawyer et al., 1991).

At the Lapis Energy – Project Blue site, in the interior zone of the northern progradational margin, the crustal thickness is estimated to be between 30 – 35 km, the highest endmember for the basin, and is classified as thick transitional crust (Galloway, 2008). This thick transitional crust is found as a somewhat concentric rim at the outer margins of the basin. The controls on the rate and the amount of crustal extension during basin formation were primarily related to subsidence and sediment influx, but at local and regional scales, secondary influences like preexisting structures, rock types, thermal state, and crustal or lithospheric weaknesses could also significantly impact the stratigraphic-structural development (Galloway, 2008). These localized and regional structural elements related to the West Gulf Coastal Plain region of Arkansas on the northwest progradational margin include:

- 1) Localized basins of enhanced subsidence and deposition.
- 2) Intervening uplifted platforms or arches related to cooling and loading.
- 3) Basin-margin fault systems related to flexing of the basin rim and uplift of adjacent provinces.
- 4) Structural basins, uplifts, erosional unconformities, and clastic wedges related to block faulting, epeirogenic doming, and the formation of fold-thrust belts.
- 5) Salt diapirs and structures formed from flow of Jurassic salt that lies at the base of the sediment column.
- 6) Syndepositional normal fault systems formed by gravitational failure of the thick clastic sedimentary wedges.

The interior zone of the northwestern progradational margin is characterized by a broad rift complex associated with tectonism, by differential subsidence associated with sedimentation, by the intrusion of interior salt diaper provinces associated with the movement of the underlying Jurassic salt in reaction to sediment loading, by Late Mesozoic igneous activity that caused a hiatus in subsidence, and by the minor reactivation of structures, gentle uplift, and tilting during the Cenozoic (Galloway, 2008).

The coastal zone of the northwestern progradational margin is characterized by extreme extension and subsidence, resulting in Mesozoic strata that is buried beneath a 10 to 15 km-thick sedimentary prism of Upper Cretaceous and Cenozoic deposits. Progradation of the shelf margin by hundreds of kilometers in seaward direction destabilized the Jurassic salt layer (Galloway,

2008). Listric, en echelon, and syndepositional growth fault systems, and diapir provinces formed as a result.

This region has an alternating series of Mesozoic subbasins and structural highs (Figure 2-8) that developed along the northern flank of the basin in response to rifting related tectonics. From west to east the structures are the East Texas Basin, the Sabine Uplift, the North Louisiana Salt Basin, the Monroe Uplift and the Mississippi Salt Basin. The origin of these features varies and is complex, and the geomorphology of the series spans tens of millions of years. These structures are secondary and superimposed on the larger Gulf of Mexico Basin, but they had significant influence on regional elements including sediment supply, accumulation patterns, and gravity tectonic structures. It reflects the dynamic interactions which took place between for example depositional loading, sediment and salt mobilization, creation or loss of accommodation space, and deformation.

Paleozoic, pre-rift, orogenic, structures are found on the periphery of the basin, further north and northeast, these features have less direct influence on the subsidence history of the Gulf Coastal Plain than the Mesozoic and Cenozoic structural features, however, pre-Jurassic transform fault lineations along northwest-southeast lines strongly influenced the shape and style of the resultant uplifts (Galloway, 2008), including the secondary structure closest to the Project Blue site, the Sabine Uplift.

The Sabine Uplift, a low-amplitude anticline/arch centered on the Texas-Louisiana border, originated as a mid-rift high during the Triassic rifting phase of the opening of the Gulf of Mexico. It has a northwest-southeast axis, supported by a large rhombic area of basement fault blocks that are bounded on the northeast and southwest by pre-Jurassic transform fault systems that parallel the opening of the Gulf of Mexico. Thin salt over the Sabine Arch shows that it was a positive area in the Middle Jurassic, but by the Late Jurassic this positive area had eroded and subsided. From the Late Jurassic through the late Early Cretaceous the Sabine Arch had no topographic expression, however three additional episodes of uplift during the Middle Cretaceous to lower Eocene created angular unconformities in strata surrounding the uplift (1990; Ewing, 2009).

During the Middle to Late Cretaceous lateral compression from the southwest, possibly associated with an early Laramide aged wrench fault system called the Saltillo–St. Lawrence Shear System of Mexico, re-initiated uplift of the Sabine by 550 ft and subsequently created the North Louisiana Salt Basin (Adams, 2009).

Also, during the Late Cretaceous, intrusive, and extrusive volcanism created volcanic clusters around the interior zone of the northwestern progradational margin (Byerly, 1991; Ewing, 2009). This volcanism formed a large dome, called the Southern Arkansas Uplift, which further protruded the existing highs on the flanks of the basin, including the Sabine Uplift. Subsidence and erosion caused another period of submergence after the Late Cretaceous and into the Paleocene.

During the Cenozoic era, the geometry of the deposition in the Gulf of Mexico Basin was primarily controlled by the interaction of the following factors:

- 1) Changes in the source locations and rates of sediment input, resulting in major shifts in the distribution of areas with maximum sedimentation.
- 2) Changes in the relative position of the sea level, resulting in the development of series of large-scale depositional cycles.
- 3) Diapiric intrusions of salt and mud rock material in response to sediment loading.
- 4) Flexures and growth faults caused by sediment loading and gravitational instability.

Sources for the terrigenous sediments for the northern portion of the Gulf Coastal region are primarily the Ouachita mountains and the ancestral Mississippi River. The continued regression of the sea is reflected through alternating sequences of lignitic sands and shales for the remainder of the Paleocene and Eocene on the norther Gulf Coast. By Oligocene time, deposition had increased to the northeast, suggesting that the ancestral Colorado, Brazos, Sabine, and Mississippi Rivers were increasing in importance. Miocene time is marked by an abrupt decrease in the amount of sediment supply entering the Rio Grande Embayment, with a coincident increase in the rate of sediment supply in southeast Texas, Louisiana, and Mississippi. Throughout the

Pliocene and Pleistocene epochs, large depocenters of sedimentation were controlled by the Mississippi River and developed offshore of Louisiana and Texas.

Tertiary sediments accumulated to great thickness where the continental platform began to build toward the Gulf of Mexico, beyond the underlying Mesozoic shelf margin and onto transitional oceanic crust. Rapid loading of sand on water-saturated pro-delta and continental slope muds resulted in contemporaneous growth faulting (Loucks et al., 1986). The effect of this syndepositional faulting was a significant expansion of the sedimentary section on the downthrown side of the faults. Sediment loading also led to salt diapirism, with its associated faulting and formation of large salt withdrawal basins (Galloway et al., 1982a).

Sediments of the Tertiary progradational wedges were deposited in continental, marginal marine, nearshore marine, and shelf environments in southern Arkansas and Northern Louisiana. The Pliocene and Quaternary mark the last major episodes of deposition in the northern Gulf Coastal region of Southern Arkansas and Northern Louisiana. In Southern Arkansas these sediments are found as alluvial floodplains and river terraces (Hosman, 1996). Pleistocene sedimentation occurred during a period of complex glacial activity and corresponding sea level changes. As the glaciers made their final retreat, Holocene sediments were being deposited under the influence of an irregular, but rising, sea level. Quaternary sedimentation along the Texas Gulf Coast occurred in fluvial, marginal marine, and marine environments.

### **2.1.1 Regional Maps and Cross Sections**

The maps and cross sections in this section were obtained from state agency open-file reports and from literature. Interpretations and analysis of the maps and cross sections in this permit application are based on numerous published studies that evaluate the history of the geological processes that controlled the formation of the stratigraphy in the West Gulf Coastal Plain of Arkansas. The regional geology section is based upon available published maps and cross sections, as well as published studies on the formation and deposition of the Gulf of Mexico. The data evaluated covers the Gulf Coast Region and the State of Arkansas. These regional maps are contained as “Figures” referenced within their respective description sections as follows.

The regional cross section map in Figure 2-9 demonstrates the structural and stratigraphic character of the geology for the Lapis Energy – Project Blue site. These cross sections (Imlay, 1949) are bounded to the north by the South Arkansas Fault Zone and to the south by the North Louisiana Salt Basin. This cross-section presents the regional stratigraphic and structural character of the geology within the primary area of interest in Union County.

## **2.1.2 Regional Stratigraphy**

In the following subsections, the regional formations and regulatory intervals that may be penetrated by the proposed Lapis Energy – Project Blue Class VI well are discussed. While the regional stratigraphic sections of southern Arkansas have been extensively studied and are well documented in the literature, the nomenclature of the Arkansas stratigraphic column has not always been standardized. The stratigraphic nomenclature and geologic ages used in this Class VI permit application are consistent with current stratigraphic divisions and care has been taken to ensure that the stratigraphic units have been correlated appropriately in situations where a published literature reference uses a name inconsistent with other references. The names have been cross-referenced to the USGS National Geologic Map Database Lexicon for accuracy.

The following sections only describe the regional formations that may be penetrated and form the regulatory intervals at the Project Blue site. These formations are described in ascending order beginning with the Jurassic Buckner Formation (Figure 2-1).

### **2.1.2.1 *Buckner Formation***

After the deposition of the Smackover Formation, in response to an increase in detritus and a slowing of sea level rise, the depositional environment of this region of the West Gulf Coastal Plain transitioned from a reefal setting to a large, narrow calcarenite beach shoreline and marginal lagoon, with normal marine dark shales toward the basin center (Imlay, 1949). The Buckner Formation, which was deposited landward of the calcarenite shoreline, is representative of supratidal evaporitic mudflats. These were formed when high-density seawater brines infiltrated the exposed inland mud, via storm waves above or capillary action below, and evaporated causing the precipitation of anhydrite nodules and anhydrite mud in the unconsolidated sediment on the mudflats (Bishop, 1973).

The Buckner Formation also thickens as it moves toward the distal part of the basin, indicating that basin subsidence accommodated the increase in sedimentation during this time. The southern limits of the Smackover Formation and Buckner Formation most likely represent a change in the slope of the sea floor due to underlying structural control.

### **2.1.2.2      *Cotton Valley Group***

The Cotton Valley Group is a sedimentary wedge that was deposited along the Gulf Coastal Plain from East Texas to Alabama (Thomas and Mann, 1966) over two Transgressive -Regressive cycles. One which started and ended in the Jurassic and one that started in the Jurassic and ended early in the Early Cretaceous. It pinches out in southern Arkansas and thickens basinward in Louisiana (Thomas and Mann, 1966). The thickness of the Cotton Valley Group ranges from 1,400 ft to 2,275 ft in Arkansas and is up to 3,175 ft in northern Louisiana (Imlay, 1949). The differences in thickness can be attributed to the combined effects of a drastic increase of terrigenous sediments, sediment loading, increased mobility of the Louann Salt Formation beneath the paleo sea floor, and subsidence in the Gulf of Mexico Basin (Bartberger et al. 2002).

The dominant lithologies are shale and sandstone, but they vary in color, cementing, fossil presence, and porosity. In the literature, the Cotton Valley Group has been classified by many authors into members and formations. Not all members and/or formations are present in all locations. The USGS names and locations of the Cotton Valley Group subdivisions are the Bodcaw Sand (LA), Bossier Formation (AL, AR, LA, MS, TX), Davis Sand (LA), Dorcheat Formation (LA), Hico Shale (LA), Knowles Limestone (LA), Schuler Formation (AL, AR, LA, MS, TX), Shongaloo Formation (LA), Terryville Sandstone (LA, TX), and Vaughn Sand (LA). Only the Bossier and Schuler Formations are present in Arkansas.

In Louisiana, the terrigenous sediments of the Cotton Valley Group were transported westward by longshore currents and formed an east-west oriented, vertically stacked, barrier island complex referred to as the Terryville (Bartberger, Dyman, and Condon, 2002), which accumulated within the Cotton Valley Group as a massive sandstone complex across northern Louisiana and to the south. This section of the Cotton Valley is capped by the Knowles Limestone, which is truncated

to the north and not present the northern portions of the West Gulf Coastal Plain, including Arkansas.

To the north of the (Terryville) barrier island complex, in Arkansas, the Bossier and Schuler Formations of the Cotton Valley Group are made up of sediments derived from the Terryville barrier island complex in Louisiana (Bartberger, Dyman, and Condon, 2002) (Figure 2-10).

The Bossier Formation is the lowermost member of the Cotton Valley Group and is classified as a transgressive marine deposit. In Louisiana it is present as a thick dark, calcareous, fossiliferous, marine shale; it grades to a fine to medium-grained gray and white sandstone and interbedded shales where it pinches out in southern Arkansas (Bishop, 1973; Swain, 1943).

The Schuler Formation is series of transgressive blanket sandstones that are (Dyman and Condon, 2006) interbedded with variegated shales and local basal conglomerates. The sandstones range from fine to coarse and are red to white, while shales are red, gray to brown and green; additionally, they contain pellets of siderite, which is distinctive for the Schuler Formation (Imlay, 1949). The sediments that form the Schuler Formation are derived from the barrier island complex, and the Schuler facies has a higher porosity than the barrier island complex. Regionally, the Schuler Formation thickens basinward at a rate of 50 ft per mile and ranges from about 50 ft thick in Nevada County, Arkansas to at least 2,300 ft thick in Union County, Arkansas and Union Parish, Louisiana. The Schuler Formation is the lowest member of the Lower Cretaceous stratigraphy and was exposed during the Early Cretaceous, denoted by the Comanchean Unconformity.

### ***2.1.2.3 Coahuila Group***

#### ***2.1.2.3.1 Hosston Formation***

The Hosston Formation is part of the Lower Cretaceous stratigraphy and unconformably overlies the Schuler Formation. The Hosston Formation was deposited in a shallow marine environment and is composed of fine-grained sandstones, interbedded with clays and sandy clays that contain oyster fossils (Figure 2-11). The clays of the Hosston Formation are distinct and range from pink to Red.

In Arkansas, the Hosston Formation often contains conglomerates with novaculite, and quartzite peddles from the erosion of the Ouachita Mountains (Imlay, 1949). In the upper two-thirds of the Hosston Formation, sand content decreases and red to greenish-gray shales become more prevalent. In southern Arkansas, the Hosston ranges from 800 – 1,600 ft thick and it thickens up to 2,300 ft basin ward in northern Louisiana.

#### ***2.1.2.3.2 Sligo Formation***

The Sligo Formation is also part of the Lower Cretaceous stratigraphy. It was deposited in a shallow marine environment during a transgressive episode after the deposition of the underlying Hosston Formation. The Sligo increases in thickness from 160 ft in south Arkansas to 300 ft in northern Louisiana. The Sligo Formation is composed of gray to brown shale with lenses of dense gray limestone with local oolitic argillaceous limestones and sandy limestones (Imlay, 1949).

#### ***2.1.2.4 Trinity Group***

##### ***2.1.2.4.1 Pine Island Formation***

The Lower Cretaceous Comanche Pine Island Formation is a continuation of the transgressive backstepping phase that is observed in the Sligo Formation. The lithology of the lower section of the Pine Island is dominated by calcareous shale beds that represent marine shelf deposits. The upper section, which is dominated by silty shale beds, is interpreted as shallow marine deposits (Mancini and Puckett, 2002). The Pine Island is a wedge that outcrops in Arkansas at about 50 ft thick and thickens basinward to 500 ft in northern Louisiana. In Arkansas the lithology is coarser and redder and grades into gray and yellow sandstone, shale, and gravels. In Louisiana it is finer and darker and has higher shale content.

##### ***2.1.2.4.2 James Formation***

The James Formation overlies the Pine Island Formation. The transition to the James Formation from the Pine Island was the result of a decrease in the amount of detrital material from the source areas. The James Formation is composed of fossiliferous, fragmental and bioclastic limestone on the shelf areas and grades to dense limestone basinward. It was deposited during a regressive sub-

phase, in a moderately low energy open shelf environment, and has a regionally varying lithology. In southwest Arkansas, the James Formation consists of a fossiliferous, dense limestone and red and gray shale. In southern Arkansas, North Louisiana, and East Texas, it is characterized by porous, oolitic, and fossiliferous to fossiliferous-fragmental limestone. In Texas, the Glen Rose is equivalent to the James Limestone. In places it has named and defined lenses that serve as aquifers. It thins in Arkansas to about 70 ft and is about 100 ft thick in northern Louisiana.

#### **2.1.2.4.3 Rodessa Formation**

The “Rodessa Formation” is a group within the Comanche/Trinity Group that includes, at the base, the lowermost beds of the James Limestone up through the bottom of the Ferry Lake anhydrite. It contains several named informal sub-members of lenses and tongues that are known productive reservoirs within the oil fields of southern Arkansas and the Ark-La-Tex region. The Rodessa Formation is interpreted as a nearshore, transitional marine sedimentary unit with oolitic and crystalline limestones, lenticular fine-grained sandy limestones, anhydrite, coquinoid limestones and gray shales.

#### **2.1.2.4.4 Ferry Lake Anhydrite**

The Arkansas Geologic Survey summarizes the Ferry Lake Anhydrite as “one of the most distinctive, widespread sedimentary units within the Gulf Coastal Plain”. It is correlative across the northwestern progradational margin and was deposited on top of the James Limestone and the Rodessa Formation in an extensive lagoonal sea. Regional deposition was controlled by water depth, development of a restrictive barrier, subsidence, duration of each evaporative pulse, and areal salinity variation across the basin. The general lithology is white to gray, finely crystalline anhydrite that contains minor amounts of interbedded gray to black shale, dense limestone, and dolomite. It has an average thickness of 250 ft on the Gulf Coastal Plain, however, in Arkansas the thickness is 10 ft at the outcrop, 150-250 ft in the southern counties, and 500 ft at the tri-state boundary of Arkansas, Texas, and Louisiana. The Ferry Lake Anhydrite is the sealing unit for the Rodessa and James Formations.

#### ***2.1.2.4.5 Mooringsport***

The Mooringsport Member is a subsidence hinge line reef complex that is a locally recognizable unit in the subsurface of northwest Louisiana where it is up to 1,600 ft thick and in the subsurface of southwest Arkansas where it is up to 730 ft thick. It is a shallow marine carbonate, consisting of predominantly crystalline and fossiliferous limestone interbedded with sandstone, red beds, anhydrite, and shale. It is time equivalent to other named formations on the Gulf Coastal Plain, but it is not a suitable stratigraphic unit for use in regional correlations, because it displays lateral facies changes across the Gulf Coastal Plain (Forgotson, 1963). It sits above the Ferry Lake anhydrite and below the red shales and sands of the Paluxy Formation. To the west, in the East Texas Basin, it corresponds to undifferentiated strata in the Rusk Formation. Further west, in Texas, it is part of the Upper Glen Rose Formation, where it is mostly carbonate. To the east, in Mississippi and Alabama, it has fluvial and deltaic clastic facies. The Northern edge includes shallow marine sands and shales. Carbonates and shales increase basinward. (Devery, 1982; Forgotson, 1963).

#### ***2.1.2.5 Fredericksburg Group***

The Fredericksburg Group (Lower Cretaceous Comanche) constitutes a terminal deepening with shoals and resurgent clastic influx onto the inner shelf. It is capped by an unconformity. The regional lithostratigraphic components of the Fredericksburg genetic sequence are the Paluxy and Dantzler Formations and the Edwards Group.

The Paluxy and Dantzler Formations are time-equivalent units and mark an early progradational episode of deltas and flanking shore-zone systems onto the inner- to middle shelf that spanned the plain from Texas to Alabama (Caughey, 1977). The Edwards Group transgressed landward over the Paluxy and is deposited as a shelf limestone and dolomite.

During the Fredericksburg episode, clastic bypass to the slope decreased and carbonate systems dominated the shelf margin and slope sedimentation. Relief of the continental slope greatly increased (Corso et al., 1989) and a steeply bounded carbonate margin around the northern Gulf Coastal Basin facilitated the development of the Mid-Cretaceous Unconformity (Galloway, 2008).

In the Project Blue region of southern Arkansas, the Fredericksburg episode equivalents are the Paluxy Formation and the Goodland Limestone.

#### ***2.1.2.5.1 Paluxy Formation***

The Paluxy Formation consists of non-fossiliferous, red, brown, and gray shales, gray to white cross-bedded lenticular sandstones, and gray lignitic limestone. The variegated shales and sands grade laterally and downward into the Mooringsport Formation and form thick recessive sections. Near the southern boundary of Arkansas, the Paluxy Formation becomes finer and more calcareous. The maximum reported thickness of the Paluxy Formation in Arkansas is 1,200 ft.

Regionally, the Paluxy Formation is present in the other Gulf Coastal Plain states. In northwestern Louisiana's Caddo and Bossier Parishes, it consists mainly of red shales and sands and grades southward into gray limestones and shales, thin sands, and some red beds, which are commonly classified as part of the Mooringsport Member of the Trinity Group. In Texas, the Paluxy has been interpreted as the shoreward sandy facies of the upper part of the Glen Rose Formation.

#### ***2.1.2.5.2 Goodland Limestone***

The Goodland Limestone is found in Texas, Oklahoma, and Arkansas, and it is considered synonymous with the Comanche Peak Limestone of Texas. Goodland is the name given to the thin northern section of Fredericksburg aged limestone that is observed in places where the Edwards Limestone is not recognizable (Imlay, 1949). In Arkansas, the Goodland Limestone is deposited on top of the Paluxy Formation. The Goodland Limestone is a medium to thick bedded, hard, sandy, light gray limestone with minor thin bedded calcareous sandstones with poorly preserved fossils. The lower contact does not outcrop in Arkansas, but the exposed thickness of the Goodland Limestone is 35 ft, where it consists of thick-bedded, gray, sandy limestone, containing some beds of hard, yellow-gray, calcareous sandstone. At some horizons, the Goodland beds are notably lenticular with lenses of limestone 6 ft long and 1 ft thick, of varying degrees of sandiness. The upper 8 ft of the formation, where exposed, is less sandy limestone. The top is a ft thick ledge of hard, white limestone, which weathers into cavernous slabs. It increases to more than 100 ft in the subsurface.

#### ***2.1.2.6 Washita Group***

The Washita depositional episode is marked by regional deepening of the northern shelf of the Gulf of Mexico Basin, resulting in widespread accumulation and deposition of dark, calcareous claystone and interbedded lime mudstone. The Washita episode spans the Early to Late Cretaceous time boundary. The formation in Arkansas is called the Kiamichi Formation and it has equivalents across the Gulf Coastal Plain.

The Kiamichi Formation of alternating marly clays and thin limestone overlies the Goodland Limestone in northeast Texas, southeast Oklahoma, and southwest Arkansas. It is characterized by closely packed oyster shell aggregates in a matrix of dense, hard, gray-green marl, interbedded with softer gray and green marls and discontinuous beds and lenses of fossiliferous limestone. Across the Gulf Coastal Plain, it ranges in thickness from 10 ft to 150 ft, and in the southern Arkansas subsurface, where it is about 100 ft thick, it has been described as a distal turbidite flow that serves as a regional seal. (Dennen and Hackley, 2012)

There were more formations deposited during the Washita episode, however, at the end of Comanchean time, regression of the Cretaceous Sea and uplift caused erosion of Washita deposits across east Texas, southern Arkansas, north Louisiana, and across into west-central portions of Mississippi. Up to 10,000 ft of Washita deposits were removed in Arkansas (Granata, 1963) and only the Kiamichi Formation was left. The erosional surface of the Kiamichi Formation is part of the Mid-Cretaceous Unconformity, the basin-wide boundary between the Early and Late Cretaceous, which is discussed in other parts of this permit application. In Arkansas the Mid-Cretaceous Unconformity separates the Washita Group from the overlying Tuscaloosa Group.

#### ***2.1.2.7 Tuscaloosa-Woodbine Episode***

After the Mid-Cretaceous Unconformity and through the Late Cretaceous, the Gulf Basin depositional sequences and depocenters were heavily influenced by the volcanic uplift of the eastern interior, beneath what is now the Mississippi Embayment, which parallels the modern Mississippi Valley (Cox and Van Arsdale, 2002) (Figure 2-12). The first depositional episode post-Mid-Cretaceous Unconformity is the Woodbine-Tuscaloosa. This is a major progradational fluvial-delta of terrigenous siliciclastics, divided into two laterally equivalent depocenters, the

Woodbine on the west and the Tuscaloosa on the east. Both are separated by the Sabine Uplift. In Louisiana, Mississippi and Alabama, the upper part of the Tuscaloosa Formation is predominantly a marine shale, which forms the regional seal for the reservoirs within the lower part of the Tuscaloosa Formation. These upper Tuscaloosa Formation shales correlate with the marine shales of the Eagle Ford Group in Texas, which overlay the Woodbine Formation and form the regional seal for the underlying Woodbine Formation reservoirs.

In Arkansas, the Woodbine Formation unconformably overlies the Kiamichi Formation and is composed of bedded gravel, sand, bedded clay, and water-lain volcanic tuff and ash. The basal part of this unit is marked by gravel of variable thickness. The overlying water-lain volcanic tuffs are sandy and cross-bedded. The Tuscaloosa sandstone is between 250 and 350 ft thick in southwestern Arkansas. The sandstones contain abundant smectite clay, formed by diagenesis of the volcanic material. It thickens basinward at the subsidence hinge line, and it was terminated by a basin-wide maximum flooding event.

#### ***2.1.2.8 Austin Group***

The Austin Group is a Late Cretaceous carbonate chalk sequence formed during a global eustatic highstand and extends from Texas to Mississippi and up into Oklahoma and Arkansas. It is composed of open-shelf carbonates and shoals bounded by periods of relatively deep water across the northwestern Gulf (Lundquist, 2000). In Arkansas, the Austin Group consists of the Tokio and Brownstown Formations.

##### ***2.1.2.8.1 Tokio Formation***

The Tokio Formation is separated from the underlying the Tuscaloosa Formation by a distinct bed of conglomerate, which is primarily composed of novaculite, indicative of the reworking of the Ouachita Mountain erosional detritus. The conglomerate grades upward into dark gray lignitic, fossiliferous clays and cross-bedded gray and brown coarse quartz sands, which are indicative of minor fluctuations in the maximum advancement of the Cretaceous Sea. The Tokio Formation is a high energy shallow marine deposit, with ripple marks, lenses of cross-bedded sand, lignite, and invertebrate fossils (Dane, 1929). The formation is 300 ft thick in the southwest

corner of Arkansas and thins toward the east. The Tokio Formation contains *Inoceramus* fossils, indicating the unit is time equivalent with the Austin Chalk Formation in Texas (Dane, 1929)

#### **2.1.2.8.2 Brownstown Formation**

The contact between the Brownstown and the Tokio is sharp. A biostratigraphic marker, the *Scaphite hippocrepis*, found in the Brownstown is of Taylor series age, indicating there is a significant time gap between the deposition of the Brownstown and the Tokio. The Brownstown records a slow and continued transgression of the Upper Cretaceous Sea across the Gulf Coastal Plain evidenced by the presence of limestone beds in the basal portion and a deepwater lithology of fossiliferous dark gray calcareous clay and marl in the upper portions.

In the Arkansas counties of Miller, Lafayette, Columbia and Nevada, the Brownstown Formation is composed of dark-gray calcareous clays, marls, and shales, generally in massive beds and free of sand, with some thin beds of impure limestone. To the east, in Ouachita and Union Counties, the formation becomes increasingly sandy and is composed of fine-grained, in part glauconitic quartz sand, with gray, fine, sandy marls and clays. At its easternmost extent, the Brownstown is dominated by fine-grained and argillaceous sands. It is 200 ft thick in Miller County but thins to the east toward Union and Ouachita Counties.

#### **2.1.2.9 Taylor Group**

The Late Cretaceous global rise in sea level reached its maximum extent soon after the end of Eutaw deposition. Much of the Gulf Coast (including most of Mississippi) was inundated and remained below sea level through the end of Cretaceous time.

The Campanian/Maastrichtian-aged Taylor Group is separated from the Austin Chalk by a regional disconformity at the base of the unit. The Lower Taylor Group is comprised of mud, calcareous claystone and fossiliferous limestone, indicating deposition in a deeper marine environment. Outcrops in Arkansas record glauconite, shells, and phosphorite, which are characteristic of a condensed zone. Though sea level was relatively high, there were smaller fluctuations. During Upper Taylor deposition, short episodes of sea level falls coincided with sandy terrigenous sediment influx in a shallow shoreface environment (Galloway, 2008).

The Taylor chalk sequence, in southern Arkansas and northern Louisiana, was deposited on the submerged Lower Cretaceous Shelf and includes the Saratoga Chalk, Marlbrook Marl, Annona Chalk and Ozan Formation, which have a combined thickness averaging 300 ft in south Arkansas.

#### ***2.1.2.9.1 Ozan Formation***

The Ozan Formation, the basal unit of the Taylor Group in Arkansas, is a glauconitic transgressive sandstone and marine mudstone. The basal unit contains a glauconitic marl, with thin lenses of sand containing highly polished pebbles and black chert. It transitions to a micaceous sandy mud. Near the top of the formation, the marls tend to become chalkier. An occasional bed of hard limestone has been noted in some outcrops near the top of the unit. The Ozan ranges from 150 to 250 ft thick.

#### ***2.1.2.9.2 Annona Chalk***

The Annona Chalk is characterized by a hard, white, thickly bedded, massive, slightly fossiliferous chalk. It has a sharp conformable contact with the underlying Ozan Formation (Dane, 1929). It weathers white, but is blue-gray when freshly exposed. The unit is commercially mined for cement. The unit is 0 to 100 ft thick.

#### ***2.1.2.9.3 Marlbrook Marl***

The Marlbrook is conformable to the Annona and is characterized as a uniform blue-gray chalky marl with an increase in argillaceous material relative to the Annona. In outcrop, the change from chalk to marl is abrupt indicating a possible cessation of sedimentation following the deposition of the chalk (Dane, 1929). The increase in argillaceous material in the Marlbrook may indicate that it was deposited in slightly shallower water than the Annona, in a low energy marine system where light and organic life in the water column were persistent. The upper portion of the Marlbrook is abundant in fossils and contains thin cemented coquina reefs (Dane, 1929). The Marlbrook is 50-220 ft thick.

#### ***2.1.2.9.4 Saratoga Chalk***

This formation is characterized as a hard, sandy, blue-gray glauconitic chalk. In the basal portion of the formation there are abundant phosphatic nodules and fossil casts (Dane, 1929). Overall, the formation grades upward from a sandy chalk to soft argillaceous sand, to a fossiliferous clay. The sand in the basal portion of the chalk marks a considerable change in sedimentation from the underlying Annona and Marlbrook Formations. Accompanying this change in lithology is a change in the character of the fauna. This basal conglomerate with glauconite and phosphatic nodules is indicative of deposition in a wave dominated zone. Based upon outcrop data it is difficult to determine if there was a regression of the sea between the Marlbrook and Saratoga, or a just a slight uplift due to igneous activity, which caused an increase of terrigenous sediment supply to the West Gulf Coastal Plain (Dane, 1929). This unit has an unconformable base, represented by a distinct break in lithology and fauna. The Saratoga is 20 to 70 ft thick in the Arkansas/Louisiana region.

#### ***2.1.2.10 Navarro Group***

The Uppermost Cretaceous-aged Navarro Group overlies the Taylor Group and is bound at the base by a maximum flooding surface, recording the end of a marine transgression. At the top it is bound by an erosional unconformity. As sea levels were falling, the Navarro Group records a forward stepping progradational and shoaling event, dominated by siliciclastic material provided from the Olmos Delta and Nacatoch clastic system (Figure 2-13). Lag deposits on the bounding erosional surface consist of shell debris, fish, shark teeth, and mud clasts, indicating deposition in a nearshore to inner shelf paleoenvironment (Galloway, 2008). The Nacatoch delta and shore-zone system provided a clastic pulse to north-east Texas, south-west Arkansas and north-west Louisiana. The larger Olmos delta prograded across the Rio Grande embayment from in northern Mexico (Galloway, 2008).

The Navarro Group extends through East Texas, Louisiana, and Arkansas and contains interbedded layers of sandstone, mudstone, and marls. In Arkansas the Navarro Group is split into the Nacatoch Sand and the Arkadelphia Marl.

#### **2.1.2.10.1 Nacatoch Sand**

In the subsurface of southern Arkansas, the Nacatoch Formation is white to light gray, calcitic to friable, glauconitic, well sorted, fine to medium grained, and contains shell fragments and some beds of white, finely crystalline limestone (Granata, 1963; Dolloff et al., 1967). In southwest Arkansas tidal-flat, shoreface, and shelf sequences have been described.

Downdip, in Louisiana, the Nacatoch Formation becomes increasingly calcareous, grading into a gray to white fossiliferous and argillaceous chalk containing thin beds of very fine-grained calcareous sandstone and siltstone (Granata, 1963; Berryhill et al., 1968).

#### **2.1.2.10.2 Arkadelphia Marl**

Overlying the Nacatoch Formation is the Arkadelphia Marl, which is characterized by dark-gray and black marl, with beds of calcareous gray sandstone. Sandy and fossiliferous limestones, concretionary limestones, and white chalk also occur (Dane, 1929). The presence of argillaceous and calcareous sandstones at the base of the Arkadelphia indicates that deposition was contemporaneous with rapid subsidence of the shelf. The Arkadelphia Marl is 120 – 160 ft thick in Arkansas. It is the last recorded sedimentation event in the Cretaceous on the West Gulf Coastal Plain in Arkansas and is unconformable with overlying Tertiary sediments.

#### **2.1.2.11 Midway Group**

The transition between the Mesozoic and Cenozoic in the Western Gulf Coastal Plain region is marked by a considerable unconformity. The Paleocene-aged Midway Group sediments were deposited during the first major Tertiary regressive cycle, which is associated with the Cretaceous -Tertiary (KT) boundary / mass extinction event. The Midway shale is regional in extent, thickening from the East Texas Basin toward the Gulf of Mexico. The Clayton Formation conformably overlies marine Cretaceous sediments within the Midway Group. The Midway Group is a thick calcareous to non-calcareous clay, locally containing minor amounts of sand. The succession across the Upper Cretaceous/Tertiary boundary shows a sharp break in both macro-fauna and micro-fauna types, making it possible to accurately determine the base of the Tertiary in the Gulf Coast Basin (Rainwater, 1964a). At the beginning of the Tertiary, an

epicontinental sea still covered most of the Mississippi Embayment, with the Clayton Formation being deposited in an open marine environment. The unit is generally less than 50 ft thick and is composed of thin marls, marly chalk, or calcareous clays (Rainwater, 1964a).

As the epicontinental sea became partially restricted in the Mississippi Embayment, the Porters Creek clay was deposited on the Clayton marl. Fossil evidence, although scarce, indicates a lagoonal to restricted marine environment for the Porters Creek Formation (Rainwater, 1964b). The Porters Creek Formation is composed mainly of massively bedded montmorillonitic clay. Open marine circulation was re-established in the Mississippi Embayment during the deposition of the shallow marine Matthews Landing Formation. The Matthews Landing Formation was deposited above the Porters Creek clay in a shallow marine environment, and is composed primarily of fossiliferous, glauconitic shales with minor sandstone beds (Rainwater, 1964a).

A major regression marks the deposition of the late Paleocene Naheola Formation that overlies the Matthews Landing Formation. Uplift in the sediment source areas of the Rocky Mountains, Plains, and Appalachian regions caused an abundant supply of coarse-grained fluvial sediments for the first time in the Tertiary. Sedimentation rates along the Gulf Coast exceeded subsidence rates and produced the first major regressive cycle in the Tertiary. Alluvial environments dominated throughout most of Naheola time. The Naheola Formation consists of alternating sand, silt, and shale, with lignite interbeds near the top of the unit (Rainwater, 1964a).

The upper contact with the overlying Wilcox Group is gradational. Wood and Guervara (1981) defined the top of the Midway as the base of the last Wilcox sand greater than 10 ft thick. In outcrop, the Midway Group subdivides into the Wills Point and Kincaid Formations (Wood and Guevara, 1981). Precise thickness of the Midway is difficult to measure because it often cannot be differentiated from the underlying upper Navarro Group (Upper Cretaceous). The Midway, upper Navarro Clay (also called Kemp Clay), and the Navarro Marl are generally grouped together during electric log correlations. The Midway-Navarro section serves as an aquiclude, isolating the shallower freshwater Eocene aquifers from the deeper saline flow systems except, perhaps, at fault zones and along flanks of salt domes where vertical avenues for flow may exist (Fogg and Kreitler, 1983).

In a regional published map from Hosman, 1996 (Figure 2-14) the Midway continues to thicken to greater than 2,000 ft towards the Gulf Coast at depths exceeding 14,000 ft. Outcrops of the Midways exist from north-central Alabama up into Tennessee in the east.

#### ***2.1.2.12 Wilcox Group***

The transgression of the sea during the early Tertiary onto the Western Gulf Coastal Plain marked the last major and continuous transgression of the shoreline through present day. Following the deposition of the Midway group the Gulf Coast region transitioned into a state of regression and sediment progradation for the remainder of the Tertiary (Dane, 1929). The Paleocene-aged Wilcox Group is a thick clastic succession that flanks the margin of the Gulf Coast Basin. This geologic group contains fluvial and deltaic channel-fill sand bodies distributed in a matrix of lower permeability inter-channel sands, silts, clays, and lignites. Most of the sands are distributed in a dendritic pattern, indicating a predominately fluvial depositional environment (Fogg et al., 1983). The marine clays of the underlying Midway Group grade upward into the fluvial and deltaic sediments of the Wilcox (Fogg and Kreitler, 1982).

The result of this sediment influx was a consistent progradation of the margin which was only interrupted in certain localities for brief periods by hyper subsidence due to salt withdrawal (Galloway, 2000). This massive progradational system of terrigenous sediments resulted in three main depositional systems tracts from proximal to distal locations in the Gulf of Mexico. Proximally, the depositional systems tracts are classified by fluvial to delta to delta fed apron tracts. The region of the Lower Cretaceous shelf margin yields coastal plain to shore zone to shelf fed apron deposits. In the distal portions of the basin the Wilcox is deposited in delta flank to sub marine fan environments (Galloway, 2000).

The Wilcox Group is divided into the Lower, Middle, and Upper intervals. The semi-regional Yoakum Shale divides the Upper and Middle Wilcox, and the Big Shale Marker separates the Middle and Lower Wilcox. During Wilcox Group deposition, the Laramide Orogeny formed the Laramide uplands, which sourced most of the sediment. The Paleocene shelf moved eastward, away from the relict Lower Cretaceous reef (Galloway et al., 2000; Galloway et al., 2011). The East Texas Basin ceased to be a marine basin during the Tertiary and Quaternary Periods, when

major Eocene, Oligocene, Pliocene, and Pleistocene depocenters shifted towards the Gulf of Mexico.

The Lower Wilcox sediments were transported to the Central Gulf via two ancestral fluvial-dominated delta systems, the Houston Delta and the Holly Springs Delta (Ewing and Galloway, 2019). These are major Gulf Coast prograding delta systems, located primarily in the ancestral Mississippi trough that encompassed central Louisiana, and southern Mississippi (Galloway, 1968). The Houston Delta, supplied by a bed-load fluvial system, was the largest and was sand dominated. East of the Houston Delta, shore-zone facies deposits separated the Houston Delta from the smaller Holly Springs Delta system. The Holly Springs Delta was the first Cenozoic Delta to be aligned with the axis of the later Central Mississippi fluvial-delta system. The very high rate of sediment influx (150,000 km<sup>3</sup>/Ma) rapidly prograded the delta and shore-zone deposits towards the shelf edge and off lapping onto the continental slope (Galloway et al., 2000; Galloway et al., 2011).

Two transgressive events bound the Middle Wilcox, one at the base and one at the top. The early transgressive event deposited the Big Shale, and the later transgressive episode deposited the Yoakum Shale. During Middle Wilcox deposition (Late Paleocene-Early Eocene), the LaSalle wave-dominated delta and the fluvially-dominated Calvert delta supplied sufficient sediment to prograde the ancestral Gulf shelf (Galloway et al., 2000). Relative to the Lower Wilcox, the Middle Wilcox sedimentation rate was roughly half (Galloway et al., 2000; Galloway et al., 2011).

During Upper Wilcox deposition, a wave-dominated delta in the Mississippi axis prograded onto the central Gulf shelf. Reworking shifted the delta westward and deposited shelf and shore zone sands over the central Gulf. An increase in the carbonate content and glauconite content in the upper Wilcox sediments suggests more marine conditions compared to the lower Wilcox. An examination of Wilcox hydrocarbon producing trends in Louisiana and Mississippi led Paulson (1972) concluded that the Wilcox is a transgressive sequence.

Figure 2-15 provides a published regional isopach and configuration map of the Wilcox Group from Hosman, 1996 as presented in the USGS Report 1416. The composite thickness of the

Wilcox Group is about 300 ft in south Arkansas and thickens to the south towards the Gulf of Mexico, where it can reach a maximum thickness of 4,000 ft (Lowry, 1988). Thickness trends mimic the Mississippi Embayment in the northeast and thicken to the south and southwest at the front of the Holly Springs Delta System.

#### ***2.1.2.13 Claiborne Group***

The Claiborne Group in the Western Gulf Coastal Plain is a classic example of strata produced by alternating marine-nonmarine depositional cycles (Hosman, 1996). The Claiborne Group comprises of multiple sand and shale units. These are (in ascending order) the Carrizo Formation, Cane River Formation, the Sparta Sand, the Cook Mountain Formation, and the Cockfield Formation. These units are also the hydro-stratigraphic units for southern Arkansas, with the Sparta Formation as the main source of fresh groundwater (See Section 2.6 for details).

Depending on the proximity to the margin of the Mississippi Embayment many of the formations of the Claiborne group have been eroded between deposition and current time in the northern region of the Gulf Coast. This is most likely a result of the meandering and development of the Mississippi river through the end of the Eocene and into the Pleistocene and Holocene time.

##### ***2.1.2.13.1 Carrizo Formation***

The lowermost formation of the Claiborne is the Carrizo Formation which unconformably overlies the Wilcox. Relatively narrow northern oriented and elongated sinuous bands of the Carrizo Formation are evidence for erosion on the top of the Wilcox. These narrow sinuous bands can be mapped throughout the Western Gulf Coastal Plain and were likely to be normal to the shoreline during early Claiborne time (Kresse et. Al, 2014). These are interpreted as valley and channel fill sands deposited on top of an irregular erosional surface, which was created by the ancestral Mississippi river system. This resulted in a highly variable thickness of the Carrizo Formation across the Western Gulf Coastal Plain. The lithology of the near shore channel fill Carrizo Formation is characterized by fine to coarse micaceous massively bedded quartz-rich sandstone with minor interbedded clays and occasional lenses of lignite.

### ***2.1.2.13.2 Cane River Formation***

The Cane River Formation represents the most extensive marine invasion during Claiborne time. In the central part of the Mississippi Embayment (Arkansas, Louisiana and Mississippi), the formation is composed of marine clays and shales. This sequence represents the maximum marine transgression of the Claiborne Sea as indicated by the lithology and relatively low sand content. In the subsurface the Cane River acts as a confining unit for the Carrizo Formation (Kresse et. Al, 2014). It is glauconitic and calcareous in parts, and also contains sandy clay, marl, and thin beds of fine sand. Well-developed sand bodies are found only around the margins of the Mississippi Embayment. Regionally, the sand percentage decreases markedly to the south and southwest, so that in southeastern Arkansas, southwestern Mississippi, and all of Louisiana, the Cane River Formation contains virtually no sand. Along the flanks of the Mississippi embayment and over the Wiggins arch area the formation is generally 200 to 350 ft thick (Payne, 1972). It ranges from a thickness of 200 ft to 600 ft and deepens in bands towards the Gulf of Mexico. The Cane River is absent from the regional Sabine Uplift structure in the northwestern part of Louisiana (Figure 2-16). In the northern Louisiana region, the Cane River Formation acts as an additional regional seal, isolating the upper Sparta Aquifer from the deeper saline formations.

### ***2.1.2.13.3 Sparta Formation***

The Sparta Formation is one of the Gulf Coastal Plain's most recognized geologic units, and the main freshwater aquifer in the Project Blue area. The Sparta formation overlies the Cane River Formation and extends northward to the central part of the Mississippi Embayment. It was deposited in a deltaic to shallow marine environment. The Sparta is characterized by varying amounts of well sorted, rounded to subrounded, fine to medium quartz sand with interspersed silt, clay, and lignite (Kresse et. Al, 2014). It comprises primarily beach and fluvial sands with subordinate beds of sandy clay and clay. The Sparta ranges in thickness from less than 100 ft at outcrop to more than 1,000 ft near the axis in the southern part of the Mississippi Embayment (Hosman, 1996, Figure 2-17). The Memphis sand is the equivalent formation in the northern part of Arkansas and southern Tennessee. Outcrops of the Sparta sands are located in north central Louisiana along the edge of the Sabine Uplift (to the west of the project site). The deposition of the formation mimics the ancestral Mississippi River.

#### ***2.1.2.13.4 Cook Mountain Formation***

The Cook Mountain Formation is predominantly a marine deposit that is present throughout the Gulf Coastal Plain. It is generally less than 200 ft thick in the Mississippi Embayment but thickens in southern Louisiana and Texas to more than 900 ft (Figure 2-18). Along the central and Eastern Gulf Coastal Plain, the Cook Mountain Formation is composed of two lithologic units. The lower unit is a glauconitic, calcareous, fossiliferous, sandy marl or limestone. The upper unit is a sandy carbonaceous clay or shale, which is locally glauconitic. The Cook Mountain Formation thickens downdip as the clay facies gradually becomes the predominant lithologic type. The Cook Mountain is present at surface outcrops in southwestern Arkansas.

#### ***2.1.2.13.5 Cockfield Formation***

Lithologically similar to the Wilcox Group, the Cockfield Formation is present throughout most of the Western Gulf Coastal Plain, but less expansive in the interior than other units of the Claiborne Group (Figure 2-19). It is composed of discontinuous and lenticular beds of lignitic to carbonaceous, fine to medium quartz sand, silt and clay. The Cockfield is generally sandier in the lower part. The sand units of the Cockfield demonstrate considerable variability in thickness and grain size and are possibly not hydraulically connected (Kresse et. Al, 2014). The Cockfield is thickest in the west-central part of Mississippi, with thicknesses ranging from 10 to 550 ft as it thins to the east and southeast. It is interpreted that these sand bodies were deposited by longshore currents and deltaic distributary channels in the near shore environment of the ancestral Mississippi Delta. It outcrops in all parts of Union Country (as well as the Project Blue site), except where overlain by Quaternary alluvium in stream lowlands (Broom et al., 1984).

#### ***2.1.2.14 Jackson Group***

Deposits or equivalents of the Jackson Group are present throughout the Gulf Coastal. The Jackson is divided into two distinct units in Arkansas: a lower marine unit called the White Bluff Formation, and an overlying non-marine unit called the Redfield Formation. The White Bluff has three dominant facies: an argillaceous sand containing glauconite and rich in molluscan fossils, a calcareous glauconitic clay with common invertebrate fossils, and a blocky clay with some silt and traces of sand and invertebrate (mostly molluscan) molds. The Redfield is typically a

sequence of light gray, thinly laminated silts, silty clays, and silty sands. The Jackson is up to 300 ft thick. *Note: at the project site in southern Arkansas, the Jackson Group is not present.*

#### **2.1.2.15 Pliocene-aged Formations**

Pliocene aged formations in the Gulf Coast Region, although separated into upper and lower units, are mostly undifferentiated and unnamed. Much of the Pliocene and younger sediments were deposited offshore, of the present coastline, and are absent from the southern Arkansas Region. Near shore, sediments were deposited under predominantly fluvial-deltaic conditions and exist as a complex of channel sands, splays, and overbank flood plain marsh deposits. *Note: at the project site, the Pliocene-aged Formations are not present.*

#### **2.1.2.16 Pleistocene Formation**

Pleistocene sediments were deposited during a period of fluctuating sea level and represent a fluvial sequence of post-glacial erosion and deposition. The formations were deposited in both fluvial and deltaic environments, and they thicken in a southeastward dip direction, as well as southwest along strike. Pleistocene sediments thicken along the Texas-Louisiana border and in a dip direction where there was significant deposition along growth faults during Pleistocene sea level low-stands (Aronow and Wesselman, 1971). The thickest portions of the formation are towards the Gulf of Mexico, where the Pleistocene can be up to 5,000 ft thick. Pleistocene sediments grade conformably into the overlying Holocene depositional units. *Note: at the southern Arkansas project site, the Pleistocene-aged Formations are not present.*

#### **2.1.2.17 Holocene Formations (Quaternary Alluvium)**

With the retreat of the Pleistocene glaciers, sea level began a final irregular rise to its present-day level. Holocene sediments were deposited following the final retreat of glacial ice. The slow rise of the Holocene sea level marked the beginning of the present-day geologic epoch, which has shaped the current Texas and Louisiana coastal zone. During recent times, sediment compaction, slow basin subsidence, and minor glacial fluctuations have resulted in insignificant, relative sea level changes. The coastal zone in Louisiana has evolved to its present condition through the continuing processes of erosion, deposition, compaction, and subsidence. *Note: at the project site,*

Holocene deposits consist of the Quaternary Alluvium and unconformably overlie the Eocene-aged Cockfield Formations in lowland areas near streams, and are characterized by unconsolidated sands, gravels, silts, and clays.

### **2.1.3 Regional Structural Geology**

The interaction between sediment accumulation and gravity has played a major role in contemporaneous and post-depositional deformation of Tertiary strata. However, the continental margins and deep ocean basin regions of the Gulf of Mexico, are relatively stable areas (Foote et al., 1984). During the Late Triassic to Early Jurassic, large volumes of eroded material were deposited in areas of regional subsidence. The sediments of the Gulf Coast generally possess a homo-clinal dip (southward) toward the Gulf of Mexico (Murray, 1957). Isolated basins formed where the Louann Salt deposits were buried by a period of continuous clastic deposition. Positive regions in the area include the Sabine Arch and Monroe uplifts. Structurally negative regions in the near regional area include the North Louisiana Basin (Figure 2-20).

Major continental red-bed and anhydrite deposits were laid down unconformably on the Late Paleozoic Ouachita Peneplain which experienced significant erosion during the Early Triassic, following the breakup of the super continent Pangea. The Pangea breakup was initiated by subsidence of the of the Paleozoic crust causing rifting and creating of a system of grabens and half-grabens (Salvador, 1991). The extensive rifting controlled the deposition of the terrigenous red-bed deposits throughout southern Arkansas and northern Louisiana. A Middle Jurassic phase of rifting, crustal attenuation and the formation of transitional crust, is characterized by a pattern of alternating basement paleo-topographic highs and lows and the accumulation of thick salt deposits (Mancini, 2008). Major structural features of the Western Gulf Coastal Plain that resulted from this extensive period of tensional force are the South Arkansas Fault Zone and the Northern Louisiana Fault Zone. Both fault zones were associated with gravity induced creeping of Middle Jurassic sediments, gliding along the Louann Salt. The Southern Arkansas Fault Zone is an extension of the Mexico-Talco Fault Zone in east Texas. It generally trends west-east and shows activity from the Jurassic through the Eocene, creating strike-parallel normal faults, which formed symmetrical grabens (Dutton and others, 1993).

Rifting resulting in subsidence as the primary tectonic force continued into the Early Cretaceous, developing a carbonate shelf margin along a tectonic hinge zone of differential subsidence between thick transitional crust and thin transitional crust (Mancini, 2008). This hinge zone and varying rates of subsidence resulted in different depositional environments and facies for time equivalent stratigraphic units in proximal and distal portions of the basin. The Late Mesozoic and Early Cretaceous are characterized by near shore clastic and shallow water carbonates. To the south and west sedimentation transitions to shallow water and offshore deposits (Imlay, 1949). This pattern of consistent near shore sedimentation due to contemporaneous subsidence and sediment influx continued throughout the Early Cretaceous. Igneous activity during the Late Cretaceous interrupted this pattern and new structural features developed along the Western Gulf Coastal Plain.

During the Middle to Late Cretaceous the intrusion of the Sabine, Southern Arkansas and Monroe Uplifts interrupted the subsidence of the Western Gulf Coastal Plain, in turn developing new basins which experienced varying eustatic influence, sediment influx, tectonic settings, and depositional environments. Examples of basins resulting from this intrusive activity are the Northern Louisiana Salt Basin, and the Mississippi Embayment.

The North Louisiana Salt Basin is a roughly rectangular structural trough some 100 miles long and 30 to 50 miles wide, centered in Webster, Bienville, and Winn Parishes Louisiana. This extensional basin is associated with early rifting linked with wrench faulting and actively subsiding depocenters throughout the Mesozoic and into the Cenozoic. The basin is situated between the Sabine and Monroe Uplifts and is located to the northwest – west of the proposed sequestration site.

The Monroe Uplift is a domal structure that spans northeastern Louisiana and extends into southeastern Arkansas and western Mississippi. The uplift is a large body of igneous rock that originated following deposition of the Cretaceous strata, creating an unconformity between the Upper Cretaceous and Lower Paleocene (Kose, 2013).

The Mississippi Embayment is characterized as a broad structural depression, which resulted from the Mid to Late Cretaceous igneous activity in the region. As a result of the uplift which created

the Embayment, there was significant erosion of Lower Cretaceous stratigraphy within the Embayment. Outcrops show evidence of southward tilting of Upper Cretaceous stratigraphy, followed by slight eastward tilting in southwestern Arkansas, as indicated by overlap in the Tokio formation (Dane, 1929). This eastward tilting during the Upper Cretaceous is inferred to be caused by a westward shift of the embayment axis (Dane, 1929). From the Exogyra Costata zone of the Upper Cretaceous through the Tertiary, the embayment continued the eastward down-warping.

Following the igneous activity in the Late Cretaceous, which formed the major structural features discussed above, the Western Gulf Coastal Plain was relatively tectonically stable. The Cenozoic is characterized by increased sedimentation from the ancestral Mississippi River. The Early Cenozoic (Eocene – Miocene) is dominated by a prograding terrigenous wedge of sediment, moving distally toward the Gulf of Mexico. During the Pliocene and Pleistocene multiple glacial and interglacial fluctuations drove eustatic and depositional rate changes. From this time period through present day the predominant sedimentation patterns in the Western Gulf Coastal Plain have been controlled by migrating deltas of the Mississippi River (Salvador, 1991).

#### **2.1.4 Regional Groundwater Flow in the Injection Zones**

Natural aquifer flows are well documented in shallow aquifers, but reliable data for deep, confined aquifers have not generally been available. Many of the studies for flow rates in deep saline aquifers come from the search for nuclear waste isolation sites. These studies show sluggish circulation to nearly static conditions in the deep subsurface (Clark, 1987). Studies in other areas, such as for the Mt. Simon Formation by Nealon (1982) and Clifford (1973), and the Frio Formation on the Texas Gulf Coast by Kreitler et al. (1988), demonstrate the complexities of the problem and limitations of conventional hydrological methods.

Late Cretaceous-aged sediments outcrop in the northwest area of Alabama. A southern (downdip) direction of regional flow is established for Gulf Coast sediments, consistent with the theory of deep basin flows and the physical mechanisms (topographic relief near outcrops and deep basin compaction) identified as contributing to natural formation drift (Bethke et al, 1988; Clark, 1988; Kreitler, 1986). Modifications to the general flow of groundwater, as indicated by Kreitler et al. (1988), have locally been modified by the production of oil and gas. Lateral facies changes, such

as unconformities and pinch outs, are projected to occur in the direction of the recharge area (updip). Therefore, background hydraulic gradients in the injection zones are likely to be highly restricted.

There are conservative estimates of background gradients for Miocene-aged sediments, which can be made from previous studies, and then applied to the project site. Data published by Clifford (1973 and 1975), Slaughter (1981), and Bently (1983) provide estimated natural hydraulic gradients from three aquifers that are approximately 3,000 ft deep. The natural hydraulic gradient in these aquifers ranged from 0.021 ft/yr to 1.58 ft/yr, averaging 0.70 ft/yr. For deeper Frio aquifers in the Texas Gulf Coast, approximately 6,000 ft below ground, the natural hydraulic gradient is estimated to be much smaller and can, as indicated by Kreitler et al. (1988), only be measured on a geologic time scale.

Clark (1988) found similar sluggish circulation in the Frio Formation in the Houston area, with groundwater velocities expected to be in the inches to a few feet per year in scale. Original formation pressure gradient data for Class I wells completed in the Frio Formation in the east Houston area substantiates the lack of a large hydraulic gradient within these deeper sandstones. Original formation pressure gradients from the Sasol Plant Well No. 1 (WDW147), from the Lyondell Chemical Company Plant Well 1 (WDW148) located approximately 33,000 ft northeast, and from the Equistar Plant Well 1 (WDW036) located approximately 49,500 ft north-northwest, are nearly identical (+0.001 psi/ft). Therefore, based on this information, estimates for the natural background reservoir velocity in the Injection Zones are placed at inches to feet per year and in a downdip direction.

The actual value for the natural hydraulic gradients in the injection Zone units of the El Dorado site are expected to be less than 1.0 ft/yr. There are no obvious natural sinks for the formation fluid except in regions where salt domes are being dissolved. According to Miller (1989), flow due to dissolution of salt domes is expected to be on the order of a few centimeters per year, or substantially less than 1.0 ft/yr, at distances greater than one mile from the source of dissolution. Therefore, the estimate of 1.0 ft/yr. in the south-easterly (downdip) direction for the natural hydraulic gradient near the proposed sequestration site is a conservative estimate.

## 2.2 LOCAL GEOLOGY OF THE EL DORADO SITE

The Lapis Energy – Project Blue site is located approximately 4.25 miles northwest of the town of El Dorado, Arkansas. The Project Blue site lies on the southern side of the Ouachita River by approximately 10 miles. Topographically, the region is relatively flat with local relief of less than 50 ft at the project site, with surface elevations ranging from 190 ft above sea level at the plant facility to over 240 ft above sea level at the town of El Dorado (Figure 2-21). The Project Blue Injection Wells will be located on property owned by LSB Industries at the El Dorado Chemical Company (EDCC) facility. The following sections detail the geology on a local scale, specific to the area at and around the EDCC facility in Union County, Arkansas. Site specific geology maps in the following discussion are contained in Appendix A – Local Geologic Maps (see Table 2-1).

### 2.2.1 Data Sets Used for Site Evaluation

Multiple sets of data were used to evaluate and characterize the geology for the Project Blue site. Various forms of input data were available (publicly, commercially, and internal to Lapis Energy) for generating the integrated subsurface description of the Project Blue site. An initial larger extent of 6 miles was investigated to develop the local geology maps and cross sections. A workflow was developed to incorporate multiple public and commercial data sets and is presented in Figure 2-22.

#### 2.2.1.1 *Base Maps and Well Locations*

An initial basemap was acquired from a third-party commercial service (P2 Energy Services Tobin basemap) and is used as the primary source for oil and gas (legacy) surface and bottom hole well locations. This primary source was then compared and updated with additional well data from other commercial and public sources: Enverus Drilling (source 2), Arkansas Oil and Gas Commission (source 3), and Markit (source 4). An additional final check was compared with historical maps provided by Geomap (Cambe Maps), which was used as a quality check for historical well locations. Locations were cross checked with data provided from log headers and drilling records to resolve discrepancies.

### ***2.2.1.2 Offset Well Logs***

Well log data was acquired for wells within an approximately 14 square-mile area surrounding the proposed sequestration site. Formation tops were correlated across the area and used to develop structure maps, isopach maps, and cross sections. Within the study area, there are multiple oil and gas fields that produce from Jurassic to Upper Cretaceous sandstones, as well as a lithium and bromine production field from the Smackover. Within the 14-mile investigation area, there are seven defined Upper Cretaceous fields, one Lower Cretaceous field, and nine Jurassic fields. The nearest of the Upper Cretaceous fields is the Smackover Oil Field to the north of the Project Blue site. Its southern boundary is roughly 2 miles from the Project Blue site. The nearest Lower Cretaceous production comes from the El Dorado East Field, which is approximately 4 miles southeast of the Project Blue site. The nearest defined Jurassic field is the Schuler East Field, which is roughly 9 miles to the southwest of the Project Blue site. The Schuler East Field is in a similar location as the active lithium and bromine production and re-injection into the Smackover, with the closest active producer being approximately 4 miles to the southeast of the Project Blue site.

Within the study area, there is significantly more well control for the Upper and Lower Cretaceous stratigraphy than for the Jurassic stratigraphy. Along with deeper well control limitations, there were no logs found that fully penetrate the Smackover. There are fifty penetrations of the Smackover within 14 square-miles; 44 of which have digital (LAS) log data. These wells are used to provide information on the lateral extent and continuity of the Confining Zone and Injection Zones for Project Blue. Well logs for the project come from multiple data sources including: the Arkansas Geological Survey, the Arkansas Oil and Gas Commission, TGS, SPDA, and via the Freedom of Information Act (FOIA) at USEPA Region 6.

### ***2.2.1.3 Seismic Data***

Seismic data was used to confirm general structural attitudes in the area and to confirm the absence of faulting in the area. A total of seven (business confidential) seismic lines were acquired from commercial vendors who own and license the data. The available 2D seismic data that

crosses the project area is of sufficient quality to be utilized in a seismic interpretation (Figure 2-23).

Out of the seven seismic lines, two crossed the Lapis Energy – Project Blue site:

- Seismic Line No. 850069, which runs north - south across dip. Data was recorded in January 1988.
- Seismic Line No. 12, which runs east - west, parallel to strike. Data was recorded in March 1981.

Due to the vintage of the seismic lines, the data was reprocessed prior to interpretation. The objective of the reprocessing of the data was to derive consistent wave equation pre-stack time migrations of utilized lines. Time-depth conversion was based on a check shot at T. F. Russel No. 1 (API No. 0313902313), which was acquired along Seismic Line No. 3.25 and a seismic well tie to J & M Poultry Packing No. 1 (API No. 03139023130) (Figure 2-23).

The reprocessed 2D seismic data was loaded into the static model (Petrel) using the Arkansas South NAD27 projection. Because of the relative lack of surface anomalies and only moderate subsurface dip rates, the data was able to be used as a calibration for structural control and identify potential subsurface anomalies. Interpretations are made in two-way time mode. The primary objective of this mapping effort was to determine the presence or absence of faulting in the zones of interest and to confirm structural attitudes (strike and dip).

## 2.2.2 Local Stratigraphy

The injection and confinement system present beneath the Project Blue site is composed of sediments that range in age from Jurassic to Lower Cretaceous, which underlie Upper Cretaceous sands, Tertiary sands and shales, and Holocene alluvium. The local stratigraphy is established on a type-log (Figure 2-2) and is used as a basis for correlation with the offset well data. Using this type-log, and nearby logs, which represent the shallower stratigraphy, including the lowermost underground source of drinking water (USDW) (which is not observed in the type-log), the following local stratigraphic formations were evaluated:

- Wilcox Group

- Midway Group
- Lower Cretaceous Sequence Boundary (Sligo/Pine Island/Rodessa/Lower Hosston)
- Hosston Formation
- Cotton Valley Group

The proposed Injection Zone encompasses the Lower Hosston Formation and the Cotton Valley Group. The Injection Zone portion of the storage complex is confined by the overlying shale units of the Lower Cretaceous Sequence Boundary and the unconformity identified as the top horizon in the static and dynamic models, which together are identified as the Confining Zone. All injection is confined between 3,600 ft and 6,500 ft across the local area.

Most hydrocarbon production in the area has been from units deeper than the Confining Zone. South and southwest of the Project Blue site. There are Hosston Formation Class I injection operations and Smackover Formation Class II brine operations.

Isopach maps referenced in this section are contained in Appendix A – Local Geologic Maps (see Table 2-1) and discussed in descending depth.

#### ***2.2.2.1 Wilcox Formation***

The Upper Paleocene / Lower Eocene Wilcox Formation is composed of series of sandstones, lignites, and shales that range in thickness from less than 400 ft in the most southeastern part of the project area to over 500 ft in the northeastern most part of the project area. This change in isopach thickness can be attributed to proximity to the ancestral Mississippi River, which was the primary source of sediments for the Wilcox Formation. At the Project Blue site, the base of the Wilcox Formation is the lowermost USDW. Though not historically or currently used as a source of municipal water in Union County, salinity data for the Wilcox has been reported to be at or less than the 10,000-ppm cutoff set by the USEPA.

#### ***2.2.2.2 Midway Shale Formation***

The Paleocene Midway Shale Formation separates the overlying Wilcox Formation from the underlying Arkadelphia Formation, which is the shallowest of the Upper Cretaceous formations in the Lapis Energy – Project Blue AoR. The Midway Shale is approximately 600 ft thick across the project area and is laterally extensive throughout Union County and into Louisiana. The

Midway Group interval is divided into two formations in Arkansas, the Clayton Formation, and the Porters Creek Formation. The Clayton Formation is the basal member of the Midway Group and has calcareous and sandy lithologies. It underlies the Porters Creek Shale, which is a thick, dense, black, impermeable terrigenous shale that grades upward into a slightly calcareous shale. The fossils of the Midway Group include a rich fauna of bivalves, gastropods, foraminifera, and ostracods with bryozoa, brachiopods, echinoids, crabs, fish, and crocodile teeth fossils also present. The lower boundary of the Midway Group is unconformable. The thickness ranges from a feather-edge to 130 ft in the outcrop. In the subsurface, the unit is usually much thicker. The top of Midway Shale serves as the base of the lowermost USDW for Project Blue Lower Cretaceous Sequence Boundary – Upper Confining Zone (Figure A.1).

#### ***2.2.2.3 Lower Cretaceous Sequence Boundary – Upper Confining Zone (Figure A.1)***

At the Project Blue site, the Mid-Cenomanian Unconformity caused the erosion or partial erosion of formations in the Trinity, Fredericksburg, and Washita Groups. As a result, Lower Cretaceous formations that are present on the western edge of the project area are not always present on north and/or east parts of the project area. For this permit application, this Mid-Cenomanian Unconformity erosional surface and the underlying shales and low permeability formations of the Pine Island, Sligo, and Upper Hosston have been designated as the Lower Cretaceous Sequence Boundary (LCSB) and the Confining Zone for the Lapis Energy – Project Blue. Together, they have a combined thickness of approximately 500 to 1,500 ft in the project area and are laterally extensive over Union County.

The Pine Island Shale Member, the upper member of the Confining Zone, is present throughout southern Arkansas, southern Louisiana, and east Texas and south-central Texas (Granata, 1963). The Pine Island extends northwest to southeast through central Union County and it has a thickness of 100 to 160 ft (Imlay, 1949; Enomoto et al., 2012) in southern Arkansas. The formation is composed of dark (brown, gray, dark gray, black) shale and black calcareous shale that is interbedded with stringers of dense, gray limestone and fine-grained sandstones.

The Sligo Formation has a thickness of about 100 ft throughout southern Arkansas and thickens towards the south. In Union County, the depth to the top of the Sligo Formation is at

approximately 3,000 ft and dips towards the south. The formation consists of gray to brown shales, calcareous shales and limestones, and locally may contain lenses of dark gray oolitic argillaceous fossiliferous and sandy limestones and light to dark gray and brown fossiliferous shales (Nichols, 1958).

The shales of the Upper Hosston form the base of the LCSB Confining Zone for the Project Blue site. There is an active Class I injection facility, permitted by Lanxess, six miles south of the Project Blue site. It has two active waste disposal wells that inject into the sands of the Upper Hosston Formation. The shales of the Upper Hosston and the younger Lower Cretaceous formations have been demonstrated as providing an effect containment barrier in the near Class I injection operations for over 25 years. The LCSB Confining Zone thickens down dip (towards the southwest) from approximately 750 ft to 1,000 ft thick across the AoR (Figure A.1)

#### ***2.2.2.4 Lower Hosston Formation – Injection Zone (Figure A.2)***

The Lower Hosston Formation is comprised of alternating sands and shale packages. The sands are the uppermost Injection Zone for Project Blue. The net sand thickness range is approximately 700 ft in the southwestern portion of the AoR to approximately 400 ft in the northeast portion of the AoR. Like the LCSB Confining Zone, the formation thickens down dip.

#### ***2.2.2.5 Cotton Valley Formation – Injection Zone (Figure A.3)***

The Cotton Valley Formation is the final transgressive deposit of the Jurassic Period and ranges in thickness across the AoR (S-N) from 1,700 ft thick to 1,200 ft and displays sub-regional thickening similar to what is observed in the Lower Hosston and the LCSB units. The depositional environment for the sands of the Cotton Valley is interpreted as a stacked shallow marine barrier-island complex, with individual sand bodies ranging in thickness from 10 to nearly 100 ft thick. These barrier-island complexes display basal conglomerates, grading into sandstones with interbedded variegated shales. The Cotton Valley has a significant thickness of sand with porosities in excess of 15% and is part of the Injection Zone for Project Blue. The Cotton Valley overlies the Buckner Anhydrite (Figure A.4), which is the Lower Confining Unit for Project Blue, which is approximately 125 ft thick in the AoR, and isolates the proposed sequestration project from the deeper injection / production of the Smackover Formation.

Due to the overall thickness of the Cotton Valley portion of the Injection Zone, a sequence stratigraphic framework was used to define the modeling horizons. There are three correlative flooding surfaces in the Cotton Valley Formation, which can be identified sub-regionally. These horizons were correlated throughout the project area and help to define flow units, which are seen in the “*Area of Review and Corrective Action Plan*” submitted in Module B.

### **2.2.3 Local Structure**

The Lapis Energy – Project Blue site is located to the south of the South Arkansas Fault Zone, and to the northeast of the State Line Fault Zone, which is associated with the Sabine Uplift, and to the north of the North Louisiana Fault Zone, which demarcates the northern boundary of the North Louisiana Salt Basin (Figure 2-8). Though these fault zones bound the project area to the north and south, none of the regional scale faults are within the Lapis Energy – Project Blue delineated AoR. The Lapis Energy – Project Blue site displays a gentle monoclinal dip from the northeast towards the southwest. Near the Arkansas-Louisiana state line and approaching the North Louisiana Salt Basin the dip and structure becomes more complex, but these features are approximately 20 miles or more south of the project area.

Local Structure maps prepared for the project are contained in Appendix A and include:

- Top of the Midway Formation (Base of the Lowermost USDW) – Figure A.5
- Top of the Lower Cretaceous Sequence Boundary – Upper Confining Zone – Figure A.6
- Top of the Lower Hosston Formation – Injection Zone – Figure A.7
- Top of the Cotton Valley Formation - Injection Zone – Figure A.8
- Top of the Buckner Formation – Lower Confining Zone - Figure A.9

The structure maps are based on correlation of well log tops across the project area. The top of the LCSB Confining Zone (Figure A.6) is at least -2,700 ft (TVDSS) within the AoR, which is greater than 1,000 ft below the lowermost USDW. The top of the shallowest Injection Zone, the Lower Hosston (Figure A.7), ranges from -3,500 ft (TVDSS) in the northwest to deeper than -3,800 ft (TVDSS) in the southwest. Dip inclination is to the southwest for all mapped zones and is ~1 to ~1.5 degrees.

Additionally, 2-D seismic data was evaluated for both structure and evaluation of the presence or absence of any faulting in the Project Blue AoR. When completing the seismic to well tie (API

No. 03139023130, J & M Poultry Packing No. 1) there were three formations that were strong reflectors and provided a confident well tie: the Buckner Formation (peak), top Cotton Valley Formation (trough), and the top Annona Formation (peak). Additionally, well below the injection and confining system there are two horizons, which were mapped for the purposes of structural evaluation. The lowermost is interpreted to be the top of plutonic intrusions associated with the igneous activity of the Middle to Late Cretaceous and the seismic sequence boundary representing the first of the Jurassic sedimentation in the West Gulf Coastal Plain.

Analysis of the seismic data indicates there is no seismically visible faulting in the project area that would potentially cut and/or compartmentalize the proposed Hosston- -- Cotton Valley Injection Zone. In the AoR, there are no major structures, as shown by two perpendicular cross sections (Figures A.10 and A.11).

Cross Section A-A' (Figure A.10) is a dip line that runs from northeast to southwest across the project area which highlights the expansion of the Jurassic and Lower Cretaceous formations from north to south. The significant portion of stratigraphic expansion that occurs within the formations shallower than the Hosston, and the difference in the sub-regional dip of the LCSB and Annona units compared to the units of the Hosston and below.

Cross Section B-B' (Figure A.11) is a strike line that runs from northwest to southeast across the project area. It demonstrates less variation in thickness compared to the dip line and indicates that the stratigraphic and structural position was relatively stable from the onset of sedimentation in the Gulf of Mexico Basin through the Late Cretaceous Period. Additionally, this may be evidence that the effects of the Mid-Cenomanian Unconformity on Lower Cretaceous stratigraphy are primarily constrained to the northeast of the Lapis Energy – Project Blue AoR, due to proximity of the Mississippi Embayment.

## 2.2.4 Faulting in the Area of Review

The structure and isopach maps and the seismic data of the Project Blue AoR [40 CFR 146.82(a)(3)(ii)] indicate that there are no faults or subsurface structures above the Smackover Formation within the defined AoR plume for the project. However, there is a known system of grabens approximately 2.2 miles to the southeast of the Lapis Energy – Project Blue site (outside the delineated AoR). These graben systems are documented in stratigraphy from the Jurassic through the Tertiary, but these fault systems are approximately two miles to the southeast of the Project Blue site and are not impacted by the pressure or plume fronts in any of the proposed Injection Zones. The effect of these faults and their significance for the project is discussed in more detail in section 2.5 seismicity.

## 2.3 DESCRIPTION OF THE CONFINING AND INJECTION ZONES

This section contains the information on the confining and injection zones for the Project Blue sequestration site per the 40 CFR 146.82(a)(3)(iii) standard. Details pertaining to the formation characteristics, lateral and vertical extent, and mineralogy are identified for each zone of interest. Demonstration of security for injection includes a geologic containment demonstration and the absence of vertically transmissive faults that could form breaches of the containment system.

The Confining Zone is defined as “a geologic formation, part of a geologic formation, or a group of formations, which stratigraphically overlie the Injection Zone(s) and act as a barrier to fluid movement”. For the Project Blue site, the Upper Confining Zone has been designated as the stratigraphic section that includes the Pine Island Formation, the Sligo Formation, and the Upper Hosston Formation. In section 2.2.2. Local Stratigraphy, these formations are collectively referred to as the LCSB Confining Zone. For Project Blue, the Hosston Formation has been sub-divided into the Upper and Lower Hosston. The shales of the Upper Hosston comprise the lowermost layer of the Upper Confining Zone.

An injection zone is defined as “the geologic formation, group of formations, or part of a formation that is of sufficient areal extent, thickness, porosity, and permeability to receive carbon dioxide through a well or wells associated with a geologic sequestration project.” Injection targets have been usually identified as formations below a depth of 3,000 ft to ensure CO<sub>2</sub> stays in the supercritical phase. Two proposed Injection Zones have been identified and depths are based upon the type-log presented in Figure 2-2. Note: the site-specific depths will be updated with data from the injection wells. Formations are presented in descending order:

1. Lower Hosston Injection Zone
2. Cotton Valley Injection Zone

Based on the type-log for Project Blue, the sandstones of the Lower Hosston Formation and the Cotton Valley Formation, at depths between 3,900 ft and 6,300 ft, are able to accommodate the volumes and pressures associated with the injection of CO<sub>2</sub> and contain the necessary characteristics to serve as an effective Injection Zone for the project. All targeted geologic

intervals have the necessary characteristics to be effective sequestration reservoirs and are located more than 2,000 ft below the lowermost aquifer that meets the criteria for being a USDW (less than 10,000 mg/l total dissolved solids content) for the Project Blue site.

### 2.3.1 Confining Zones

In accordance with EPA 40 CFR §148.21(b), the Confining Zone is a lithologic layer that is laterally extensive and sufficiently low in permeability and porosity such that it restricts the vertical flow of injectate. The stratigraphic section composed, in descending order, of the Pine Island Formation, the Sligo Formation, and the Upper Hosston Formation has been designated as the Upper Confining Zone for the Project Blue site. This group of formations meet EPA standards and have the required rock properties to restrict the vertical flow of injectate within the designated Injection Zone(s).

At the Project Blue site, the Confining Zone is at a depth of approximately -2,800 ft (TVDSS) and averages 800 ft thick across the AoR (Figures A.1 and A.6 in Appendix A). The Buckner Anhydrite, a thick, regionally extensive evaporite (Figure A.4 and A.9 in Appendix A) and will act as lower confining unit for isolation of the sequestration complex.

As there is currently no site-specific data for the proposed Confining Zone, shale porosities via published literature were reviewed as part of the seal efficiency assessment. These published shale porosities were used to estimate permeabilities and entry pressures (via understanding textural components such as pore throat size) in the proposed confining zone. Although log evaluation of the shales may indicate high total porosity (as defined in the “*Area of Review and Corrective Action Plan*” submitted in **Module B**), a review of published literature was used to evaluate effective porosities as an indicator of the clay bound volume.

Core data and analysis, along with a comprehensive suite of logging and formation testing has been developed to collect data focused on the Confining Zone. This data will be updated into the site characterization and modeling to reduce uncertainties based upon lack of site-specific data. The injection and monitoring wells will be constructed, tested, and logged in accordance with Class VI standards set forth by the USEPA. Detailed information on the data acquisition is contained in the “*Pre-operational Testing and Logging Plan*” contained in **Module D**.

### ***2.3.1.1 Upper Confining Zone - Lower Cretaceous Sequence Boundary***

The lithostratigraphic characteristics of the rock units within the Confining Zone are the dominant control on the effectiveness of the stratigraphic section as a seal to vertical migration of injected CO<sub>2</sub>. This uppermost confining unit is comprised of the low permeability formation of the Pine Island, Sligo, and Upper Hosston (in descending order). The combined thickness of the Confining Zone is 750 ft to 1,000 ft (Figure A.1 in Appendix A).

#### **Pine Island Formation**

The Arkansas Geological Survey describes the Pine Island Shale in south Arkansas as a widespread, regionally transgressive deposit of marine shales associated with lagoon and nearshore marine environments, with 50 to 300 ft of thickness and lithofacies consisting predominantly of calcareous black shale with interbedded fine-grained sandstone and minor crystalline limestone layers. It has doxic-anoxic properties important to seal efficacy. On the type-log for Project Blue, the top of the Pine Island Shale is observed at a depth of 3,000 to 3,100 ft, and thins towards the north.

Log curves, cuttings, core, thin-section, and XRD analysis demonstrate that the Pine Island Shale has a primary lithology (70 – 90 percent) of black argillaceous lime mudstone, bioturbated gray argillaceous lime wackestone, and siltstone with lesser amounts (10 – 30 percent) of light-gray, yellow, green, and red lime mudstone and siltstone (Hackley et al., 2014). Thin section analysis indicates the dominant cement in the Pine Island Shale Member is authigenic carbonate (Hackley, 2012).

#### **Sligo Formation**

In Arkansas the contact between the Sligo Formation and the overlying Pine Island Shale is conformable and the contact between the Sligo Formation and the underlying Hosston Formation is time-transgressive, evidenced by the dark, shallow water marine Sligo sediments overlying the non-marine Hosston sediments. “The lithologic contrast” between the Sligo limestone beds and the underlying Hosston sandstone beds is recorded in higher resistivity and more positive SP log responses for the Sligo limestone beds, as compared to the Hosston sandstone beds.

The Sligo Formation ranges in thickness from 100 ft and greater throughout southern Arkansas and thickens towards the south. In Union County, the depth to the top of the Sligo Formation is at approximately 3,000 ft and dips towards the South. The formation consists of gray to brown shales, calcareous shales, and limestones, and locally may contain lenses of dark gray oolitic argillaceous fossiliferous and sandy limestones and light to dark gray and brown fossiliferous shales (Nichols, 1958). The carbonates are gray, argillaceous, oolitic and pseudo oolitic. In local areas, porous well developed oolite limestones are petroleum reservoirs referred to as the Pettet Limestone (Nichols, 1958; Michell-Tapping, 1981; Dennen and Hackley, 2012). Hydrocarbon producing fields from the Sligo are predominantly located in east Texas and western Louisiana, with smaller fields in southern Arkansas.

Details on the muddy limestone and shale beds from the Sligo are provided from the Vivian Field in Columbia County, Arkansas (approximately 30 miles west-southwest of the project site). Kirkland, (1988) characterized the porosity distribution of multiple facies from low energy lagoons to higher energy reef deposits. The Sligo had average porosities ranging from 0 - 2.5 percent (Figure 2-24, Kirkland, 1988). It is expected that the shales in the Sligo will have porosities and permeabilities less than 2.5% and less than 0.1 mD, respectively, which is within range of effective seal properties (Warren, 2016).

### **Upper Hosston**

Formation characteristics for the sealing units of the Confining Zone, come from the Lanxess (*formally* Great Lakes Chemical Company) Class I WDW-5 and WDW-6 injection wells. Whole and rotary sidewall core was collected from the facility located southwest of the project area in Union County.

Thirty-six samples from the Class I WDW-5 were tested for permeability and porosity (Table 2-2). This table contains predominately shales and silty shales, with a few sands that were analyzed. The shale intervals had permeabilities on average of  $1 \times 10^{-2}$  md when measured with air in a horizontal orientation. Porosities range from 2.1 to 6.7 percent in the shales and slightly higher in the silty sands. The shales of the Hosston and the younger Lower Cretaceous formations have been demonstrated to provide an effect containment barrier in the near Class I injection operations for over 25 years.

Additionally, Dutton et al., 1993 performed core analysis and characterized the Hosston in east Texas along the border of southern Arkansas and northern Louisiana. The average composition of the sandstones are quartz, feldspar, and lithic fragments, which are classified as quartzarenites and subarkoses. Quartz is the most abundant detrital component, next to plagioclase. Chert and low-grade metamorphic rock fragments are the dominant rock fragments present (Dutton et al., 1993). XRD analysis on detrital mud matrix indicates that illite, chlorite, and varying amounts of fine sized quartz comprise the composition of muds (Dutton, 1986).

Of common authigenic minerals present (quartz, illite, chlorite, ankerite, and dolomite), quartz cement is the most abundant and increases with depth. Illite, chlorite, kaolinite, mixed-layer and illite-smectite clay minerals are also observed. Authigenic illite and chlorite surround detrital grains and prevent the nucleation of quartz overgrowths. In the Upper Hosston, illite and chlorite clay rims are thicker (14 percent volume) and reduce the volume of quartz overgrowths (0.5 percent), compared to the Lower Hosston, which have thinner clay rims and higher quartz cement (15 percent) (Dutton, 1990). Dolomite and ankerite cement are most abundant in the Upper Hosston and decrease with depth. The mean volume of ankerite and dolomite cement are respectively 1.1% and 2.4% (Dutton, 1986; Dutton, 1990).

### ***2.3.1.2 Lower Containment Unit – Buckner Formation***

The Buckner Formation of Late Jurassic age is an evaporitic mudstone and conformably overlies the Smackover Formation Injection Zone and underlies the Hosston / Cotton Valley Injection Zone. The lower seal is approximately 75 ft to 125 ft thick within the delineated AoR. (Figure A.4 in Appendix A), which isolates the proposed sequestration operations in the Lower Hosston and Cotton valley Formations, from the deeper production and mineral extraction from the Smackover Formation.

There is limited core and literature data accessible to the public regarding porosity, permeability, and capillary pressure measurements of the Buckner Formation. One reason is that quantitative measurements of evaporite porosity and permeability are beyond the technical capacity of standard lab instruments used in the oil industry (Warren, 2016). In lieu of direct core and

literature data of the Buckner Formation, the properties will be discussed based on hydrocarbon seal analogs of similar lithology, chiefly evaporites and shale.

Evaporites, such as the Buckner Anhydrite, are excellent seals due to their extremely high entry pressures, low permeabilities, high ductility, lateral extensiveness, and their ability to maintain seal integrity even when exposed to various temperatures and pressures in the subsurface (Warren, 2016). The Buckner Anhydrite is the primary seal in the Mt. Vernon Field (approximately 35 miles west-southwest of the project site) as it is for many surrounding small fields in southern Arkansas. The log response of the Buckner changes very little along depositional strike which indicates little lithologic variation (Harris and Dodman, 1987). The Lapis AoR is located along depositional strike to the Mt. Vernon field, and it is estimated that a similar sealing lithofacies is present, making the Buckner Anhydrite an effective seal.

Evaporites are excellent long-term seals with very low intrinsic permeability and constitute some of the strongest subsurface barriers to the vertical migration and accumulation of large columns of hydrocarbons and CO<sub>2</sub>. Although evaporites constitute less than 2% of the Earth's sedimentary rock volume, about half of the hydrocarbon reservoirs are sealed beneath evaporites, the other half are sealed by shale (Grunau, 1987).

The most abundant rock types in the Buckner Formation are nodular anhydrite mudstone and nodular anhydrite. The main distinction between the two lithologies is the proportion of anhydrite nodules in the matrix. The remaining rock types in decreasing abundance are micro-grained anhydrite, shale, oolitic and detrital limestone, rock salt, and micro-grained and medium-grained dolomite (Dickinson, 1968b). The nodular anhydrite mudstone and anhydrite, contain nodules of white, light-red, or light-gray anhydrite in a matrix of gray-red, gray, or green-gray mudstone. The red and white color of the nodules are due to the presence of, or lack of, hematite crystals, respectively. Similarly, mudstone lacking hematite crystals are gray to green in color (Dickinson, 1968b).

XRD analysis performed by Dickinson (1968b) shows that the clay minerals in the matrix are illite, chlorite, and trace amounts of kaolinite. The mudstone matrix also contains silt to sand sized

anhedral to rhombohedral dolomite grains and disseminated small pyrite crystals that have replaced quartz or anhydrite.

### **2.3.2 Injection Zones**

The Injection Zone is defined as “the geologic formation, group of formations, or part of a formation that is of sufficient areal extent, thickness, porosity, and permeability to receive carbon dioxide through a well or wells associated with a GS project”. Sandstones of the Lower Hosston and Cotton Valley Group have the necessary characteristics to be an effective injection zone at the Project Blue site.

All characteristics for the proposed injection zones are discussed in the following sections. Please note, that the porosity type is highly dependent on the mineral composition of the rock and defines how much pore volume is accessible to reservoir fluids, *i.e.*, ratio of total and effective porosities. Primary intergranular porosity results from preservation of pore space after deposition and lithification of sediments. Microporosity, which is associated with clays, is present in the matrix and greatly affects the volume of effective porosity accessible to reservoir fluids.

#### **2.3.2.1 Lower Hosston Injection Zone**

##### **2.3.2.1.1 Formation Characteristics**

The Shreveport Petroleum Data Association, Inc. (SPDA) database was utilized to obtain porosity and permeability data of Hosston core throughout the modeling area of the Project Blue site in Union County, Arkansas. A total of 361 data points were analyzed from over 20 wells and depths ranged from 3,031 ft to 5,192 ft. Using a porosity cutoff of 13% to differentiate the Hosston sands from muds, the average porosity and permeability of sands is 23.8% and 438 md, respectively (Figure 2-25).

Evaluation of the Hosston sands in the East Texas Basin indicates the average porosity of all sandstones in the Hosston Formation decreases with depth from 10.6% (6,000 ft) to 4.4% (10,000 ft) (Dutton et al., 1993). Porosity reduction with depth is not a result of increased compaction, but an increase in quartz cement and decrease in secondary porosity. Dissolution of feldspar grains results in secondary porosity and as depth increases, original feldspar grains

diminish (Dutton, 1990). Large volumes of diagenetic fluids flowed through the highly porous and permeable stacked, braided-channel sandstones and resulted in extensive quartz cementation, reducing primary porosity. In the Upper Hosston (lowermost portion of the Confining Zone), impermeable mudstones surrounding discrete sandstone packages acted as barriers to diagenetic fluids. Smaller volumes of diagenetic fluids permeated through these coastal sandstones and resulted in the preservation of significant primary porosity (Dutton and Land, 1988; Dyman and Condon, 2006).

Since the main control of porosity in the sands of the Hosston is the volume of quartz cementation, the relationship between porosity and permeability is good (Dutton et al., 1993). Similar to porosity, average stressed permeability decreases with depth from 0.8 mD (at 6,000 ft) to 0.0004 mD (at 10,000 ft), in all sandstones within the Hosston Formation (as a whole). Permeability reduction with depth is a function of decreasing porosity (from quartz cementation), and increasing overburden pressure, which narrows pore throats, but does not significantly modify grain packing. Increasing overburden pressure with depth has significant impacts on permeability but has no effect on porosity (Dutton, 1990; Dyman and Condon, 2006).

At any given depth, high energy, clean, fluvial sandstones exhibit 10 times greater average permeability than lower energy, clean, coastal sandstones. Relative to fluvial sandstones, the coastal sandstones have inferior permeability due to several factors, including coastal sandstones are finer grained, contain 7% greater volume in total cement (authigenic dolomite, ankerite, illite, chlorite, and bitumen), and are dominated with secondary and microporosity networks, which are poorly connected (Dyman and Condon, 2006).

Figure 2-26 (from Dutton et al., 1993) shows a typical air-brine capillary pressure behavior for a clean, fine-grained sandstone in the Hosston Formation. The sample depth is 8,252 ft obtained from the SFE No. 2 well in east Texas. Irreducible water saturations are 27% in reservoir rock above the water table (Dutton et al., 1993).

### **2.3.2.1.2 Mineralogy and Petrophysics**

To evaluate the mineral composition of the Lower Hosston, initial testing was performed on core provided by the Texas Bureau of Economic Geology (BEG). X-ray diffraction (XRD) analysis was performed by Stratum Reservoir on five samples, 1-2H-ET (3929.20 ft), 1-4H-ET (3938.40

ft), 1-6H-ET (3945.60 ft), 1-8H-ET (3946.30 ft), 1-12H-ET (3954f ft) obtained from whole core in the Bishop No. 2 well (API: 0313903544). The average tectosilicates, phyllosilicates, and carbonates are 95%, 4%, and 1% respectively. The tectosilicate group is comprised of quartz (94.1%), k-spar (0.7%), and plagioclase (0.6%). Quartz is the dominant mineral constituent of the tectosilicate mineral group. The phyllosilicate clay group is comprised of chlorite (0.9%), kaolinite (0.9%), illite/mica (1.5%), and mixed illite/smectite (0.9%). Calcite is the primary carbonate observed in the Hosston and there are trace amounts of dolomite. The Hosston can be classified as a quartzarenite, subarkose, and sublitharenite using the Folk, 1968, sandstone classification ternary diagram (Figure 2-27).

Additionally, X-ray fluorescence (XRF) analysis was performed on samples 1-2H-ET (3929.0 ft), 1-4H-ET (3938.4 ft), 1-6H-ET (3945.6 ft), 1-8H-ET (3946.3 ft), 1-12H-ET (3954.0 ft) obtained from the Bishop No. 2 well (API: 03-139-03544). XRF elemental results are shown in Table 2-3 and are consistent with the XRD analysis. For example, the increase in quartz positively correlates with an increase in Si, Ti, and Zr detrital input proxies.

Thin section petrographic analysis was performed on five Lower Hosston samples (1-2H-ET, 1-4H-ET, 1-6H-ET, 1-8H-ET, 1-12H-ET) and indicate that the Lower Hosston is a fine-grained to very fine-grained sandstone. Grains are subangular to rounded, moderately sorted, and show low to moderate compaction. The major framework grains are very fine-medium grained detrital monocrystalline quartz, with minor amounts of polycrystalline quartz, feldspars, lithic fragments, and trace to rare amounts of muscovite, mica, and heavy minerals. Detrital clays observed are illitic and illitic/smectitic clays occurring as pore-filling, grain-coating, and pore lining. Authigenic quartz overgrowth is apparent where quartz host grains are not coated with clay minerals. The porosity ranges from 27.5% to 31.3%, and permeability ranges from 273 mD to 704 mD in the five samples analyzed by Stratum Reservoirs. Thin section petrography descriptions and images for the samples in the Lower Hosston are contained in Appendix B.

### **2.3.2.1.3 Expected Zone Capacity**

Lapis plans to inject approximately 0.5 million metric tons per year (MMt/yr) into the Lower Hosston. Total capacity estimates for the interval are 2.5 MMt of total CO<sub>2</sub> planned to be injected over a 5-year interval.

This is based upon the current understanding of porosity, permeability, thickness, and lateral extent and will be updated after collection and calibration to site specific data. Specific modeling parameters related to the relative permeability, saturation curves, and compressibility of the formation and injectate characteristics are contained in the “*Area of Review and Corrective Action Report [40 CFR 146.84(b)]*” submitted with this permit application in **Module B**.

### **2.3.2.2 Cotton Valley Injection Zone**

#### **2.3.2.2.1 Formation Characteristics**

To characterize the porosity and permeability values of the Cotton Valley Sands, core data was obtained from the SPDA database throughout the Lapis Energy modeling area in Union County, Arkansas. Six wells within the Project Blue AoR had core samples of the Cotton Valley Group interval. A total of 97 porosity and permeability measurements from these samples were obtained. At depths of 3,537.0 ft to 7,602.5 ft, porosity measurements ranged from 11.3% to 24.5%, with an average of 22.1%, and permeability measurements ranged from 0.1 mD to 2520 mD, with an average of 132.5 mD (Figure 2-28).

Several studies have evaluated the Cotton Valley Sandstones in East Texas, North Louisiana, and South Arkansas, including Swain (1943), Wilson and Hensel (1982), Dutton et al., (1993), and Dyman and Condon (2006). In East Texas, the Cotton Valley Group contains low porosities, usually less than 10%, and low permeabilities, primarily in the microdarcy range. However, some sand intervals can reach permeabilities up to 100 mD (Wilson and Hensel, 1982). There are no definitive relationships between porosity and permeability. For example, two sandstones with similar porosities may exhibit drastically different permeabilities in the East Texas Cotton Valley Group (Wilson and Hensel, 1982; Dutton et al., 1993).

In Northern Louisiana, Cotton Valley Group sandstone porosity ranges from 10 to 19 % and permeabilities can range from 1 to 280 mD (Collins, 1980; Dyman and Condon, 2006).

The Cotton Valley Group in many areas of East Texas and North Louisiana has been designated as a tight sandstone. In East Texas, the Cotton Valley Group contains very fine-fine grained sandstones that are tightly cemented and interbedded with siltstone, mudstone, and carbonate (Dutton et al., 1993). Spain et al. (2011) utilized NMR and MICP analyses to petrophysically characterize and rock type the Cotton Valley in East Texas. Based on petrophysical properties, shown in Table 2-4 (Cotton Valley petrophysical properties, Spain et al., 2011), three rock types were identified. Type I rocks are coarser grained, moderately cemented, contain clay laminations, and have larger pore sizes which are interconnected by large pore throats (radius > 0.10 microns). Type I rocks have high permeability, high effective porosity, and low irreducible water saturation. Type 2 rocks contain medium to large pore sizes, very small to large pore throats, have high total porosity, moderate effective porosity (40-85%), low permeability, and have water saturations which reflect both capillary and clay bound water. Type 3 rocks are characterized as being shaley, fine grained, contain high proportions of clay minerals and disseminated clay layers with clay bound water saturation. Type 3 rocks have small pore bodies interconnected by small pore throats < 0.05 microns in size. (Spain et al., 2011).

#### **2.3.2.2.2 Mineralogy and Petrology**

The Schuler and Bossier Formations comprise the Cotton Valley Group in Southern Arkansas. Since the Bossier Formation only extends a short distance north of the Arkansas-Louisiana state border, the Schuler Formation comprises practically the entire Cotton Valley Group in Southern Arkansas (Swain, 1943).

The Schuler Formation can be divided into two members, the upper member, named the Dorcheat, and the lower member, named the Shongaloo. The Dorcheat Member is comprised of an upper shale and sandstone unit and a lower sandstone unit. Nearshore facies are pastel varicolored shales and white sandstones with brown ankerite. These brown spheroidal ankerite pellets are present in the upper half of the Dorcheat and decrease down stratigraphic section. Volcanic ash, dark grey chert, and chloritic material, are minor constituents (Swain, 1943).

In the lower member of the Schuler (Shongaloo), nearshore facies sandstones are fine to coarse grained and have interbedded conglomerate layers. Thin sandstone layers tend to be red in color, while massive sandstone layers are white. The red color in some of the sands is due to coating of ferric oxide on the grains. Quartz grains in sandstone beds are angular to sub-angular and some contain quartz overgrowths. Conglomerates are erratically disturbed and are composed of sub-angular-rounded quartz grains and gray-white chert. The shales in the Shongaloo are mainly red and increase in red color updip. Some green shales are interbedded with sandstone and there are small amounts of varicolored shales that contain ankerite (Swain, 1943).

In 2021, McClain and Von Gonten Laboratories characterized the mineralogy of the Cotton Valley Group via x-ray diffraction (XRD) analysis on core obtained from Claiborne Parish, north Louisiana. The sandstones (sample 2) were comprised of quartz (86.3%), plagioclase (6.5%), k-spar (1.3%), and calcite (2.7%). Clay minerals consisted of illite, mica, glauconite, and chlorite and comprised 3.5% of the sandstone facies (McClain, 2021).

#### **2.3.2.2.3 *Expected Zone Capacity***

The Cotton Valley Formation has been subdivided into 3 Injection Intervals for modeling. Lapis plans to inject approximately 0.5 million metric tons per a year (MMt/yr) into each sub-divided Injection Interval. Total capacity estimates for each of the intervals is 2.5 MMt over a planned 5-years of injection for each interval. This equates to 7.5 MMt over a 15-year injection period.

This is based upon the current understanding of porosity, permeability, thickness, and lateral extent and will be updated after collection and calibration to site specific data. Specific modeling parameters related to the relative permeability, saturation curves, and compressibility of the formation and injectate characteristics are contained in the “*Area of Review and Corrective Action Report [40 CFR 146.84(b)]*” submitted with this permit application in **Module B**.

## 2.4 GEOMECHANICS AND PETROPHYSICS

This section details the mechanical rock properties and in situ fluid pressures per the 40 CFR 146.82(a)(3)(iv) standard and includes information on ductility, stress, pore pressures, and fracture gradients of the sequestration complex. Mechanical rock properties describe the behavior of the framework rock matrix and pore space under applied stresses. Mechanical rock properties are described by elastic properties (Young, Shear, and Bulk Modulus as well as Poisson's ratio) and inelastic properties (Fracture Pressure and Formation Strength).

Changes in *in-situ* stresses and strains, ground surface deformation, and potential risks, such as new caprock fracture initiation and propagation of preexisting fault opening, and slippage are crucial geomechanical aspects of large-scale and long-term CO<sub>2</sub> storage (Rutqvist, 2002). It is important to assess all the geomechanical risks before commencing the operations of CO<sub>2</sub> injection. Although all the processes involved are not always fully understood, integration of all available data, such as ground surveys, geological conditions, micro-seismicity, and ground level deformation, has led to many insights into the rock mechanical response to CO<sub>2</sub> injection (Pan et al, 2016).

Site specific data will be collected during the drilling and testing of the injection wells. Geomechanical data across the Injection Zones and the Confining Zone will be collected, along with laboratory analyses of recovered core samples. Details on the data acquisition are contained in the “*Pre-operational Testing and Logging Plan*” contained in **Module D**.

### 2.4.1 Ductility

Ductility refers to the capacity of a rock to deform to large strains without macroscopic fracturing. Ductile deformation is typically characterized by diffuse deformation (*i.e.*, lacking a discrete fault plane) and is accompanied on a stress-strain plot by a steady state sliding, compared to the sharp stress drop observed during brittle failure. In other words, when a material behaves in a ductile manner, it exhibits a linear stress vs. strain relationship past the elastic limit.

The ductility of a shale top seal is A function of compaction state. Uncompacted, low-density shales are extremely ductile and can thus accommodate large amounts of strain without

undergoing brittle failure and loss of top seal integrity. Inversely, highly compacted, dense shales are extremely brittle and may undergo brittle failure and loss of top seal integrity with very small amounts of strain. Figure 2-29 shows the relationship between ductility and density observed for 68 shales by Hoshino et al (1972).

Other parameters are expected to influence ductility, such as confining pressure and time. The mechanical behavior of rock formations is not constant but changes with various conditions, such as progressive burial as the top seal is converted from a mud to a more competent material, thus developing higher strength. Compaction decreases ductility while confining pressure increases ductility. Compaction is typically related to depth. Figure 2-30 from Hoshino et al (1972) shows density and ductility vs. brittleness against depth. Ductile samples are displayed as gray circles and brittle samples are displayed as black circles. Ductile shales did not fracture whereas brittle shales did fracture during the experiment. According to the figure, a low-density shale at a depth of 500 m is more ductile than a highly compacted shale at a depth of 5,000 m. Finally, ductility varies not only with depth of burial but also with time.

Holt et al (2020) emphasize how important it is to characterize to what extent shales may fail in a brittle or ductile manner, in both cases causing possible hole instabilities during drilling, and in the case of ductile shales, enabling permanent sealing barriers. Triaxial tests, creep tests, and other tests tailored to follow the failure envelope under simulated borehole conditions were performed on two soft shales. The more ductile shale was proved to form barriers both in the laboratory and in the field. By comparing their behavior, the authors noticed that the ductile shale exhibits normally compacted behavior while the more brittle shale is over-compacted. This points to the stress history and possibly the grain cementation as keys in determining the failure mode. Porosity, clay content, ultrasonic velocities, unconfined compressive strength, and friction angle may be used as other indicators of brittle or ductile failure behavior.

Contrary to borehole collapse during drilling, shale ductility has however proved to be useful. Successful natural shale barriers have been reported, where the annulus between casing and formation has closed after drilling, forming an efficient seal (Williams et al, 2009; Kristiansen et al, 2018). This is of large importance for plug and abandonment of oil wells but may also be considered as an alternative to cement in new wells, provided that the barrier has sufficient

thickness and is formed fast enough. Obviously, the well needs to be completed in a stable condition prior to the formation of the barrier.

On another note, ductile formations have a higher propensity to creep than brittle ones under the same loading conditions. Creep is the tendency of solid material to deform permanently under a certain load that depends on time and temperature. Typically, creep is divided into three distinct stages which are primary creep (transient elastic deformation with decreasing strain rate), secondary creep (plastic deformation with constant strain rate), and tertiary creep (plastic deformation with accelerating strain rate), as summarized in Figure 2-31 from Brendsdal (2017) (see also Fjaer et al., 2008; Hosford, 2005). Unless stresses are reduced, tertiary creep eventually leads to brittle failure.

The following factors have the potential to increase or enhance creep (Kristiansen et al, 2018):

- High clay content, especially smectite,
- High shear stresses,
- Thermal deformation from heating,
- Shale/brine interaction effects.

According to Chang and Zoback (2009), the amount of creep strain in shales is significantly larger than that in sands with less clay, which corroborates previous observations that creep strain increases with clay content. Microscopic inspections show that creep in shales appears to generate a packing of clay minerals and a progressive collapse of pore spaces. The authors observed a porosity loss and an increase of dynamic moduli in shales during creep.

Strain in uncompacted sediments is typically accommodated by creep behavior which itself may be enhanced by high clay content that induces self-sealing properties (Meckel and Trevino, 2014; Ostermeier, 2001; Hart et al., 1995). This has major implications on the suitability of confining zones because ductile deformation of mudstone seals potential leakage pathways to the surface. These include natural pathways such as faults and man-made pathways such as well boreholes (Clark, 1987).

Loizzo et al (2017) discuss how key parameters, such as the in-situ stress and creep properties, can be measured or estimated from geophysical logs, geological and geomechanical information, and active well tests. Any sedimentary formation with a clay matrix predominantly composed of smectite is a good candidate for natural barrier. Signs of sloughing shales during drilling are an excellent indicator of this phenomenon, but a series of geophysical investigations, provided by logging while drilling or wireline logging, are recommended at the initial characterization stage. Density, neutron porosity, and possibly spectral gamma ray can clarify the mineralogical composition; these logs are routinely acquired as part of a triple combo, together with sonic wave velocities. They will be included in the formation evaluation program for the Injection Wells at the Project Blue project site. The processing of the logs to identify facies, extract petrophysical and mineralogical properties, and estimate the strength of the rock will also be performed.

Defining the maximum operating pressure of the natural barrier requires the knowledge of mechanical properties and far-field stresses. The characterization of rock mechanical properties (elastic properties, anisotropy, and non-linearity) has been well documented for measurements, protocols, and practices. Young's modulus and Poisson's ratio can be estimated from the compressional and shear wave velocities and density values obtained from the offset sonic logs, using standard rock physics equations.

Finally, cement evaluation logs are very effective in identifying creeping shales. In fact, they precisely measure the ultimate effect of creep, *i.e.*, the annulus bridging by a natural barrier. One log immediately after cementing and another one approximately a week later can help distinguish between cement and creeping shale.

#### **2.4.1.1 *Ductility in Gulf Coast Examples***

The ductility of clay/shales both in the Injection Zone and in the Confining Zone, is a function of compaction state. Uncompacted, low-density shales are extremely ductile and can thus accommodate large amounts of strain without undergoing brittle failure and loss of integrity. However, highly compacted, dense, deep shales may be extremely brittle and undergo brittle failure and loss of integrity with very small amounts of strain.

Gulf Coast shales are known to exhibit viscoelastic deformational behavior that causes natural fractures to close rapidly under the action of in situ compressive stresses (Aumman, 1966; Neuzil, 1986; Bowden and Curran, 1984; Collins, 1986). Evidence of this includes rapid borehole closure often encountered while drilling and running casing in oil and gas wells along the Gulf Coast (Johnston and Knape, 1986; Clark et al., 1987). Furthermore, old abandoned (legacy) boreholes have been observed to heal across shale sections to the extent that reentering them requires drilling a new borehole (Clark et al., 1987).

This property of viscoelastic deformation behavior will cause any fractures and/or faults to close very rapidly in response to the in-situ compressive stresses, like squeezing into the fault plane from both sides. This well-known ductile (or plastic) behavior of the geologically young Gulf Coast shales is amply demonstrated by the presence of shale diapir structures and the natural closure of uncased boreholes with time (Johnston and Greene, 1979; Gray et al., 1980; Davis, 1986; Clark et al., 1987; Warner and Syed, 1986; and Warner, 1988). Jones and Haimson (1986) have found that due to the very plastic nature of Gulf Coast shales, faults will seal across shale-to-shale contacts, allowing no vertical fluid movement along the fault plane.

In 1991, a Gulf Coast borehole closure demonstration was conducted as an integral part of an EPA No-Migration Petition demonstration for DuPont Sabine River Works (now INVISTA Orange) to test the natural healing of boreholes through clay/shale sections due to clay swelling and creep and to quantify natural borehole closure (Clark et al., 2005). A test well was drilled to provide additional information on the sealing effectiveness of Miocene formations, especially the clay/shales, in a simulated abandoned borehole located on the flanks of Orange Dome (salt dome) near Orange, Texas. In the testing, a worst-case strategy was evaluated, where the mechanism of swelling and plastic creep of the clay/shales was simulated by allowing the clay/shale to heal over a week's duration and then injecting fluids into the lower test sand while monitoring pressure in the next sand vertically in the section (upper monitor sand), similar to a vertical interference test. The upper gauge in the shallow monitor sand showed no change during the testing, indicating that there was no “out of zone” movement across the 90-foot thick, healed clay/shale bed. The lack of out of zone movement was confirmed via the Schlumberger Water Flow Log® that showed no migration of fluids vertically along the walls of the borehole in the healed clay/shale section.

#### **2.4.1.2 Site Specific Ductility of the Confining Zone**

To date, there are no site-specific brittleness or ductility/creep measurements available for the confining units specific to the AoR. All assumptions have been made using the available sonic logs, the drilling reports, and as discussed in the literature above. Ductility is assessed by measuring sample strains under applied stresses at representative reservoir conditions (e.g., injection or depletion). Elastic moduli are often used as an indicator of rock creep compliance and strength, which can be related to mineral rock composition (Sone and Zoback, 2013). Site specific data will be acquired and tested on cores collected during the drilling of the Project Blue Class VI Injection Well No. 1 (Blue INJ-1) (see **Module D** for the “*Pre-Operational Testing and Logging Plan*”).

#### **2.4.2 Stresses and Rock Mechanics**

*In-situ* stress and strain are basic concepts in the geomechanics discipline. A stress is defined as a force over an area. If a force is perpendicular to a planar surface, the resulting stress is called a normal stress. If a force is applied parallel to a planar surface, it is called a shear stress. A normal stress is called either a tensile stress if the stress is pulling the material apart or a compressive stress if the stress is compressing the material. In geomechanics, compressive stresses are conventionally shown as positive. Strain is the deformation of the rock material in response to a change in the corresponding effective stress. A normal strain is defined as the change in length (caused by the change in normal effective stress) divided by its original length. A shear strain is the ratio of the change in length to its original length perpendicular to the principal stress axes of the element due to shear stress. A volume (or volumetric) strain is the ratio of the change in volume to its original volume, also called a bulk strain, when all-around change in effective confining stress is applied. These stress and strain concepts are illustrated in Figure 2-32 (Han, 2021).

The Gulf Coast Basin is generally considered as a passive margin with an extensional (normal faulting) stress regime. In a normal faulting stress regime, the vertical stress is the greatest stress (maximum principal stress) and is typically referred to as the rock overburden. Regional literature from Eaton, 1969, indicates that the overburden stress gradient for normally compacted Gulf

Coast Sediments ranges from about 0.85 psi/ft near the surface to about 1.00 psi/ft at depths of about 20,000 ft. Sedimentary rocks along the central portion of the Gulf Coastal Plain experience predominantly normal faulting, with a maximum horizontal stress oriented sub-parallel to the coastline (Lund Snee and Zoback, 2020(b)) and a minimum horizontal stress (*i.e.*, the least principal stress) oriented orthogonal to the coastline.

Published data has been used to set the orientation of the principal horizontal stresses (Meckel et al., 2017; Nicholson, 2012; Zoback and Zoback, 1980) using regional fault-strike statistics (Figure 2-33). Geomechanical assumptions for the rock properties estimated at the El Dorado site are contained in Table 2-5. The geomechanical properties of the primary Confining Zone will be further measured during the drilling and completion of the project’s injection and monitoring wells.

### **Vertical Stress: $S_v$**

The overburden stress,  $S_v$ , for normal-faulting stress regimes is assumed to have an average gradient of 1.0 psi/ft (Nicholson, 2012). This is equivalent to the lithostatic pressure exerted by rock with an average density of 2.3 g/cm<sup>3</sup> (Hovorka, 2018). Meckel, 2017, assumed a value of 1.00 psi/ft for the Lower Miocene in the Texas Gulf of Mexico.

For the El Dorado site, the  $S_v$  is calculated by integrating the composite density log obtained from the available offset well logs. The  $S_v$  gradient varies between 0.90 psi/ft and 0.92 psi/ft.

### **Minimum Horizontal Stress ( $S_{hmin}$ ):**

Minimum horizontal stress values are estimated using Eaton’s method (Eaton 1969) and analogue Biot coefficients. The Biot coefficient is the ratio of the volume of fluid change, divided by the change in bulk volume (assumption that port pressure remains constant).

The range of estimated  $S_{hmin}$  resulted in values in the range of 0.73 to 0.76 psi/ft.

$$Sh_{min} = (\nu / (1 - \nu)) * (\sigma_v - \alpha P_P) + \alpha P_P$$

Where:

$S_{hmin}$  is the minimum horizontal stress

$\nu$  is the Poisson's ratio  
 $\sigma_v$  is the vertical stress  
 $\alpha$  is the Biot coefficient, assumed to be 1  
Pp is the pore pressure.

**Maximum Horizontal Stress ( $Sh_{max}$ ):** Maximum horizontal stress values were estimated by averaging the gradients of the vertical and minimum horizontal stresses at each depth. The  $Sh_{max}$  values are estimated to be 0.82 psi/ft.

### **Shear Modulus (G):**

The Shear Modulus is a mechanical property that describes the response of a material to shear deformation and provides insight into how resistant a material is to shearing deformation (such resistance also being known as the material's "rigidity"). The Shear Modulus will be smaller than the Young's Modulus and is derived from the following basic equation:

$$G = \frac{t_{xy}}{g_{xy}}$$

Where:

$G$  = Shear Modulus (pressure units)

$t_{xy}$  = Shear stress in xy direction

$g_{xy}$  = Shear strain

The Shear Modulus was calculated in the laboratory using the available core data. Results range from  $1.10 \times 10^6$  psi to  $1.56 \times 10^6$  psi and are considered representative of the Lower Hosston and Cotton Valley Injection Zones. It should be noted that the Shear Modulus is related to the viscosity of the material; however, it is insensitive to temperature and composition of the material (Rajput et al., 2016).

### **Bulk Modulus ( $k$ ):**

The Bulk Modulus is a mechanical property that describes the ability of a material to withstand a change in volume due to compression from all directions. The Bulk's Modulus can be defined by the following equation:

$$K = -V \frac{dP}{dV},$$

Where:

$K$  = Bulk Modulus (pressure units)

$P$  = Pressure

$V$  = initial volume of a substance

The Bulk Modulus was calculated in the laboratory using the available core data. Results range from  $1.30 \times 10^6$  psi to  $2.68 \times 10^6$  psi and are considered representative for the Lower Hosston and Cotton Valley Injection Zones. It should be noted that the Bulk Modulus can also be derived if the Young's Modulus and the Poisson's Ratio are known.

### **Young's Modulus (E):**

The Young's Modulus is an inelastic property that describes the relation of tensile stress to tensile strain. The ability of a material to deform:

$$E = \frac{\sigma}{\epsilon}$$

Where:

$E$  = Young's Modulus (pressure units)

$\sigma$  = Uniaxial stress – or force per unit surface (pressure units)

$\epsilon$  = Strain, or proportional deformation (dimensionless)

The Young's modulus is calculated from density, P-wave and S-wave velocities using standard Rock Physics equations. Young's modulus impacts the calculation of the fracture gradient. The Young's Modulus range is calculated and ranges from  $1.75 \times 10^6$  psi to  $3.75 \times 10^6$  psi.

### **Poisson's Ratio ( $\nu$ ):**

The Poisson's Ratio is a constant that is used to determine the stress and deflection property of a material. It is a measure of the deformation of a material perpendicular to the load direction.

Poisson's Ratio is also calculated from density, P-wave and S-wave velocities using standard Rock Physics equations.

$$\nu = \frac{d \epsilon_{trans}}{d \epsilon_{axial}}$$

Where:

$\nu$  = Poisson Ratio (dimensionless)

$\epsilon_{trans}$  = transverse strain

$\epsilon_{axial}$  = axial strain

Poisson's Ratio is used to calculate  $Sh_{min}$  using Eaton's method (1969). It should be noted that the Poisson's Ratio of most materials will fall within a range between 0.0 and 0.5. Lower Poisson's Ratio values indicate less deformation of the material when exposed to strain, and higher values indicate greater deformation when exposed to strain. A higher Poisson's Ratio would also indicate that the subject material would be harder to fracture. Poisson's Ratio values for the site are between 0.39 and 0.40.

#### 2.4.3 Pore Pressures of the Injection Zone

In general, the Gulf Coast subsurface can be separated into three hydrologic zones. The shallowest zone, fresh to moderately saline geologic section, corresponds to fresh waters (less than 10,000 mg/l total dissolved solids) and has a typically formation pressure gradient of 0.433 psi/ft of depth (*i.e.*, a freshwater gradient). Within the shallow interval, groundwater is directed away from the areas where the Fleming Group crops out eastward towards the Gulf of Mexico (Kreitler and Richter, 1986).

Underneath the fresh to moderately saline geologic section is what Kreitler and Richter (1986) call the “Brine Hydrostatic Section”. The transition is a mixing zone where meteoric waters mix with formation waters and this exchange prevents the buildup of pressures. Formation water salinity values range from 10,000 parts per million to 50,000 parts per million total dissolved solids (Kreitler and Richter, 1986). In the lower parts of the brine hydrostatic section, formation water salinity values range from 50,000 parts per million to 150,000 parts per million, with the

bottom marked by a zone of weakly overpressured sediments (Kreitler and Richter, 1986) that transition to higher formation pressures. Kreitler and Richter (1986) propose a gradient value of 0.465 psi/ft (approximately equivalent to 9.0 pounds per gallon mud weight) to define the initial transition to overpressured sediments.

The third hydrologic zone is referred to as the overpressured zone. Overpressuring results when low permeability mudstones retard or restrict expulsion of waters from compacting mudstones (*i.e.*, mudstones are buried quicker than they can expel water). In this case, porosity of the sediments is reduced as water is expelled and a disequilibrium between increasing overburden due to sedimentation and the reduction in pore volume occurs (Zhang and Roegiers, 2010). The remaining water in the pores must support part of or all the overburden, causing the pore pressures of the trapped fluids to increase. This also allows for higher-than-expected porosities (Zhang and Roegiers, 2010). Regional overpressuring indicates a lack of communication with the shallower normally pressured brine hydrostatic section (Kreitler (1986), Zhang and Roegiers, (2011)).

From a practical standpoint, the top of overpressure represents a maximum depth for sequestration of carbon dioxide. For one, the system compression would need to overcome the elevated pore pressures in the overpressured intervals, requiring higher energy demands for operations. Secondly, as indicated above, the presence of overpressure indicates a compartmentalized system that does not allow pressure bleed-off. This is akin to storage in a tank that does not allow for pressures to escape the overpressured system. Lastly, in the overpressured zone the rate of pore pressure gradient increases faster than the fracture gradient, which reduces the allowable operating envelope as the pore pressure approaches the fracture pressure of the formations.

For the Lapis El Dorado sequestration site, the targeted injection zones are all located in the second identified zone: the “Brine Hydrostatic Section.” As such, pore pressure data have been determined from available drilling mud weights and was determined to be 0.433 psi/ft for the Lower Hosston and Cotton Valley Injection Zones.

Note: Site-specific in-situ formation pressure will be collected during the drilling of the injection wells at a future date. Details on testing and data acquisition are contained in the “*Pre-operational Testing and Logging Plan*” submitted in **Module D**.

#### 2.4.4 Calculated Fracture Gradient

The fracture gradient for Injection Intervals can be estimated using 'Eaton's Method (Eaton, 1969). For this Class VI application, the methodology follows that as presented in Moore (1974):

$$FG = \frac{(P_{ob} - P_r)e}{(1 - e)} + P_r$$

Where:

FG = Fracture Gradient  
P<sub>ob</sub> = Overburden Gradient (Figure 11-11 in Moore, -974) - depth dependent  
P<sub>r</sub> = Reservoir Pressure Gradient (original)  
e = Poisson's Ratio (Figure 11-12 in Moore, 1974) – depth dependent

Using the above equation, a fracture gradient of 0.726 psi/ft was determined for the Lower Hosston Injection Zone and ranged from 0.753 psi/ft to 0.769 psi/ft for the Cotton Valley Injection Zone. Table 2-6 contains the estimated fracture gradient and calculated (assumed) formation pressures for all injection intervals.

#### 2.5 SEISMICITY

An earthquake is a sudden shaking of the ground caused by the passage of seismic waves through the Earth after two blocks of rock material suddenly slip past one another beneath the 'Earth's surface. The plane where they slip is called the fault. The location below the Earth's surface where the earthquake starts is called the hypocenter, and the location directly above it at the surface of the Earth is called the epicenter. Seismic waves are elastic and travel at the speed of sound. These waves may be felt by humans and can produce significant damage far away from the epicenter.

The size of an earthquake can be expressed by either intensity or magnitude. Magnitude is based on an instrumental recording that is related to energy released by an earthquake, while intensity describes the felt effects of an earthquake:

**Intensity** - Number describing the severity of an earthquake evaluated from the effects observed at the 'Earth's surface on humans, structures, and natural features. Several scales

exist, but the Rossi-Forel scale (before 1931) and the Modified Mercalli scale (after 1931) are most used in the US. Intensity observations are employed to construct isoseismal maps wherein areas of equal shaking effects are contoured.

**Magnitude** - Instrumental measurement of the energy released by an earthquake recorded by seismometers or seismographs. The seismometers record the degree of ground shaking at a distance from the event and all stations should read similar values from the same seismic event. In other words, the magnitude of the earthquake does not change with distance and a single value describes the earthquake. Dr. Charles F. Richter introduced the Richter Scale which measured the scale of earthquake magnitudes. Following the Richter Scale, there have been several magnitude scale modifications based on the type of seismic wave, epicenter distance, and other factors (Leeds, 1989).

Instrumental seismology is equally as important as historic records. Instrumentation (such as seismographs) allows determination of seismic events much smaller than those which can be felt at the Earth's surface. Thus, a catalog of seismic events may contain a wide range of events that are instrumentally recorded but not felt by humans. Also, since seismic waves attenuate with distance, and because all regions cannot be adequately covered by seismographs, many small events are felt, but not always detected. Sensitive seismographs, which greatly magnify these ground motions, can detect strong earthquakes from sources anywhere in the world. The time, locations, and magnitude of an earthquake can be determined from the data recorded by seismograph stations.

The Richter Magnitude Scale was developed in 1935 by Charles F. Richter of the California Institute of Technology as a mathematical device to compare the size of earthquakes. The magnitude of an earthquake is determined from the logarithm of the amplitude of waves recorded by seismographs. Adjustments are included for the variation in the distance between the various seismographs and the epicenter of the earthquakes. On the Richter Scale, magnitude is expressed in whole numbers and decimal fractions. For example, a magnitude 5.3 might be computed for a moderate earthquake, and a strong earthquake might be rated as magnitude 6.3. Because of the logarithmic basis of the scale, each whole number increase in magnitude represents a tenfold increase in measured amplitude. As an estimate of energy, each whole number step in the

magnitude scale corresponds to the release of about 31 times more energy than the amount associated with the preceding whole number value.

At first, the Richter Scale could be applied only to the records from instruments of identical manufacture. Now, instruments are carefully calibrated with respect to each other. Thus, magnitude can be computed from the record of any calibrated seismograph.

Earthquakes with magnitude of about 2.0 or less are usually referred to as micro-earthquakes; they are not commonly felt by people and are generally recorded only on local seismographs. Events with magnitudes of about 4.5 or greater - there are several thousand such shocks annually are strong enough to be recorded by sensitive seismographs all over the world. Great earthquakes, such as the 1964 Good Friday earthquake in Alaska, have magnitudes of 8.0 or higher. On average, one earthquake of such size occurs somewhere in the world each year. The Richter Scale has no upper limit. Recently, another scale called the moment magnitude scale has been devised for more precise study of great earthquakes. The Richter Scale is not used to express damage. An earthquake in a densely populated area, which results in many deaths and considerable damage, may have the same magnitude as a shock in a remote area that does nothing more than frighten the wildlife. Large-magnitude earthquakes that occur beneath the oceans may not even be felt by humans.

The effect of an earthquake on the Earth's surface is called the intensity. The intensity scale consists of a series of certain key responses such as people awakening, movement of furniture, damage to chimneys, and finally - total destruction. Although numerous *intensity scales* have been developed over the last several hundred years to evaluate the effects of earthquakes, the one currently used in the United States is the Modified Mercalli (MM) Intensity Scale. It was developed in 1931 by the American seismologists Harry Wood and Frank Neumann. This scale, composed of 12 increasing levels of intensity that range from imperceptible shaking to catastrophic destruction, is designated by Roman numerals. It does not have a mathematical basis; instead, it is an arbitrary ranking based on observed effects.

The Modified Mercalli Intensity (Figure 2-34) value assigned to a specific site after an earthquake has a more meaningful measure of severity to the nonscientist than the magnitude, because

intensity refers to the effects experienced at that place. After the occurrence of widely felt earthquakes, the Geological Survey mails questionnaires to postmasters in the disturbed area requesting the information so that intensity values can be assigned. The results of this postal canvass and information furnished by other sources are used to assign an intensity within the felt area. The maximum observed intensity generally occurs near the epicenter.

The *lower* numbers of the intensity scale generally deal with the manner in which the earthquake is felt by people. The *higher* numbers of the scale are based on observed structural damage. Structural engineers usually contribute information for assigning intensity values of VIII or above.

### **2.5.1 Regional Seismic Activity**

Seismically, the West Gulf Coastal Plain is one of the less active regions in North America (Figure 2-35) as detailed by the seismic hazard map from the USGS. This area of Arkansas and adjacent states have a rating of V (moderate risk) for seismicity as determined via the United States Geological Survey (USGS). Natural seismicity in the West Gulf Coastal Plain is primarily from the movement along normal faults which extend to the basement. This faulting is a result of continental rifting with down to the basin extension during the opening of the Gulf of Mexico; in combination with extreme sediment loading creating down warping of previous sediments. Both extension and sediment loading remained active through the deposition of Tertiary sediments in the region. Structural features such as zones of grabens, and growth faults although capable of storing and releasing seismic energy, are weak and ineffective in generating intense ground motion.

Salt domes are the result of plastic flowage of salt that pierces or ruptures adjacent sedimentary layers or causes doming in the overlying sedimentary layers. These sediments have low density, poor cementation, and low shear strength, which results in a low shear modulus. It is doubtful that a salt dome could develop earthquakes with a magnitude greater than 3.0 on the Richter Scale. Small earthquakes may be felt locally but are unlikely to propagate damaging ground motions. Though salt domes are present in the Gulf Coast Region, there are not any located near the sequestration project in Union County.

Graben zones are the result of extensional tectonic stress, which is driven in the Gulf Coastal plain by the vertical stresses of the overlying sediment resulting in the persistent subsidence of the seafloor and resulting extension of the basin. Growth faults are the result of contemporaneous extensional faulting with sedimentation. In both grabens and growth faulting situations thicker sediments can be observed on the downthrown side of faults. Additionally, in these faulting scenarios throw tends to decrease up section and away from the origin of the fault. The sequestration site is located more than 15 miles from the nearest grabens which are associated with the Southern Arkansas Fault Zone.

The regional fault systems of Southern Arkansas are characterized by an echelon of grabens, as well as syndepositional growth faults. These faults were originally formed during the late Triassic rifting and formation of the Gulf of Mexico which began the subsidence of the Gulf Coast geosyncline. Movement and activity of these faults continued through the development of the Gulf of Mexico in response to accelerated subsidence and sedimentary deposition. An extensional stress province is associated with growth faulting from Northeastern Mexico through Arkansas. The maximum horizontal stress is subparallel to the coastline, following the strikes of the growth faults (Lund Snee and Zoback, 2016).

In Arkansas, a large majority of natural seismic activity is confined to the New Madrid Fault Zone to the north (Ausbrooks, 2011), which is located at the southern Illinois- east Missouri- northeast Arkansas-western Tennessee-western- Kentucky border (Figure 2-35). Seismicity in the state of Arkansas since 1699 through 2019 is presented in Figure 2-36, from the Arkansas Geological Survey. Note a majority of the earthquakes are located in the northeastern portion of the state.

One of the largest regional earthquakes that has occurred in the southern portion of Arkansas, is the 1911, 4.7 magnitude event at Star City (located approximately 68 miles northeast from El Dorado in Cleveland County in Figure 2-36), which does not have recorded data on the depth of occurrence or magnitude due to the age of the seismic event. In 1974, there was a 4.2 magnitude event in Gurdon, Arkansas (approximately 50 miles north-west of El Dorado in Clark County in Figure 2-36), which occurred at a relatively shallow depth of 1.0 km. Even more distant seismic regions (e.g., New Madrid Zone in Southeastern Missouri) have not developed events great

enough to cause damage at the proposed sequestration site. Details on events in Union County are discussed in the Local Seismicity section.

Liquefaction is a factor to consider when assessing seismicity in Arkansas. According to the USGS:

*“Liquefaction takes place when loosely packed, water-logged sediments at or near the ground surface lose their strength in response to strong ground shaking. Liquefaction occurring beneath buildings and other structures can cause major damage during earthquakes.”*

The eastern boundary of Arkansas is defined by the Mississippi River and contains unconsolidated to loosely consolidated material. It is particularly susceptible to liquefaction and the risk increases because of its proximity to the New Madrid Fault Zone. This northeastern portion of Arkansas has a higher risk of liquefaction, but it decreases as you move away from the Mississippi River. In Union County, the liquefaction susceptibility is low in the areas that are not along rivers and is high along rivers. The northern and eastern borders of Union County are in the high-risk zone, 4 narrow sections of high-risk zones transverse the southwest half of Union County. The sequestration site is located in the lowest-risk zone of Union County (Figure 2-37).

## 2.5.2 Seismic Risk of the Project Site

A preliminary seismic risk evaluation is conducted for the project area. The sequestration area is within Union County, which lies approximately 15 miles to the northeast of two grabens associated with the South Arkansas Fault Zone (Figure 2-38). Overall seismic risk is rated *moderate* based on:

- Site location falls on the 8-contour line of the USGS Seismic Risk Map;
- Frequency of natural earthquake events near the sequestration area;
- Low to moderate intensity of natural earthquakes felt in the sequestration area, with maximum ground motion on the surface being less than or equal to a Modified Mercalli Intensity (MMI) range of V;
- Low population density in the area limiting exposures and impacts;
- Historical economic production of oil and gas in the area; and

- No known faults within the focus of the Area of Review (AoR).

The sequestration project in Union County, Arkansas is found in an intensity level of V on the MMI (Figure 2-34). Structural features such as salt domes and growth faults, although capable of storing and releasing some seismic energy, are weak and ineffective in generating even modest ground motion. None of these associated features are located near the sequestration site.

In 1989, David J. Leeds, a certified geophysicist and engineering geologist, conducted a regional evaluation on seismicity. Leeds (1989) identified seismogenic sources, modeled a “design earthquake,” and discussed the effects of the “design” earthquake on potential Injection and Confining Zones. Applying the theories from the Leed’s study, natural seismicity is not expected to be significant issue at the project site.

Evaluations have been performed to determine the possible effects of natural events on (1) the integrity of well construction materials; and (2) the integrity of both the Injection and Confining Zones beneath the Lapis Energy sequestration site. A National Earthquake Information Center search (NEIC) (<http://earthquake.usgs.gov/contactus/golden/neic.php>) was performed in November 2022, for seismic events within a 100-mile (160 km) radius of the proposed injection site. A tabulation of the results is contained in Table 2-7. The results are presented in Figure 2-39. The search shows that since 1900, thirty earthquakes with magnitudes greater than 2.5 were recorded within 160 kilometers (~100 miles) of the El Dorado project site. Ten of these events have occurred in Union County (Figure 2-40) and are highlighted in yellow in Table 2-7.

The closest recorded earthquake occurred in December 2001, which was recorded as a 2.8 magnitude earthquake, approximately 3 km WSW of the town of El Dorado. The largest magnitude earthquake in Union County was a 3.2 magnitude event in June 1994. Six out of the ten events for Union County were recorded with magnitudes of less than 3.0.

At the project site, the likelihood of an earthquake caused by natural forces is considered remote. Additionally, the injection into the formations will be at relatively low pressures and will take place into deep, high-porosity formations, which are extensive over a broad area and that are not frequently subject to natural earthquakes. Therefore, the probability of an earthquake of sufficient intensity to damage the injection system, injection well, or the confining layer is very low.

### 2.5.3 Induced Seismicity

Seismicity related to fluid injection normally results from activity involving high pressures and large volumes, such as those associated with high-pressure water flood projects for enhanced oil recovery. This seismicity is caused by increased pore pressure, which reduces frictional resistance and allows the rock to fail. Fluid withdrawal has caused land subsidence and earthquakes due to dewatering and differential compaction of the sediments. Earthquakes of magnitude 3.4 to 4.3 on the Richter scale appear to have been caused by fluid withdrawal near some oil fields in east Texas (Davis et al., 1987), such as Sour Lake, Mexia, and Wortham Fields.

Since 2010, the occurrence of earthquakes with a magnitude greater than 3.0 have increased from 20 events per a year (1967-2000) to over 100 events per a year (2010-2013) in the central and eastern US region (Ellsworth, 2013). The increased rate of occurrence in previously inactive seismic areas has been correlated with the increased use of injection wells located near faults. Fluid injection induced earthquakes are most likely caused by the increased pore pressure from injection operations which have reduced effective stress of faults leading to failure. This mechanism has been used to explain the best-known cases of injection-induced seismicity, which was first studied in the Rocky Mountain Arsenal near Denver. New case studies have increased with the use of wastewater injection wells associated with hydraulic fracking. In many sites, smaller seismic occurrences have shown to be precursors to larger events. More data has become available since the Rocky Mountain study in the 1960's, leading to a better understanding of factors and processes associated with induced seismicity.

One of the most notable regional cases of induced seismicity associated with injection wells occurred in Youngstown, Ohio. In 2011, 12 low-magnitude seismic events occurred along a previously unknown fault line (Ohio Department of Natural Resources, 2012). These events occurred less than a mile from Class II injection well Northstar I. Previously, the area was seismically inactive, with earthquakes beginning a few months after the injection of wastewater. The injectable pressure at Northstar I was increased twice over 6 months (Ohio Department of Natural Resources, 2012) and may have reduced the effective stress on a fault. After the well was shut down by the Ohio Department of Natural Resources, the seismic activity declined. As a result

of this case, seismic monitoring prior to injection and after injection has become common in Class II sites.

A case study in the Dallas-Fort Worth (DFW) area tied small seismic events to a Class II injection well. Eleven hypocenters have been observed at a focal depth of 4.4 km and 0.5 km from a deep saltwater disposal (SWD) well (Frohlich et al., 2010). Injection at this well began eight weeks prior to the first recorded seismic event. A northeast trending fault is located approximately at the same location of the DFW focus (Frohlich et al., 2010). As a result of fluid injection into the disposal well, the stress upon the fault had been reduced and this reactivated the fault (Frohlich et al., 2010). All the seismic events associated with the DFW focus are small magnitude events (less than 3.3) and occurred very shortly after initial injection.

In Oklahoma, one of the largest earthquakes in the state's history may have been a result of wastewater injection at a Class II disposal site. In 2011, Prague, Oklahoma was the location of a 5.7 magnitude earthquake that was followed by thousands of smaller aftershocks. Wastewater had been pumped continuously into an old oil well for 17 years. As the pore spaces filled, the wellhead pressure was increased to continually inject the wastewater. This reduced the effective stress upon the Wilzetta fault located 650 meters from the well (Keranen et al., 2013). The fluid was injected into the same sedimentary strata in which 83% of the aftershocks originated (Keranen et al., 2013). In this case, the seismic event occurred years after the initial injection phase. Since the area was considered low risk seismically, there is no data on smaller earthquakes that may have proceeded the event in 2011.

In north-central Arkansas, multiple earthquakes have been triggered because of a Class II injection well. Since the operation of the disposal well in 2009, the site has experienced an increase from 2 events in 2008 to 157 events in 2011 (Horton, 2012). It was also tied to the discovery of a new vertical fault. Ninety-eight percent of earthquakes within this area occurred within 6 km of one of three waste disposal sites (Horton, 2012). The depth of the earthquake foci occurred between 6.7 and 7.6 km. Injection of fluid occurred at a depth of 2.6 km. At this disposal site, an E-W trending fault (Enders Fault) cut into the aquifer in which the fluid was injected and then acted as a conduit to the new fault at the depth of 6.7 to 7.6 km (Horton, 2012). The disposal

wells were shut down in 2011 by the Arkansas Oil and Gas Commission. The rate and size of the earthquakes steadily decreased following the shutdown of the wells (Horton, 2012).

In Texas there are at least two known examples of previously seismically inactive areas becoming seismically active after major injection programs began. One site is located in the Central Basin Platform, near Kermit, and the other is in the Midland Basin near Snyder. In both cases, large scale, high pressure, oil field related, water flooding projects were under way, and earthquakes with a magnitude of over 4.0 on the Richter scale were recorded. Historically, induced earthquakes in Texas have not exceeded 4.6 magnitudes (Frohlich et al., 2010). Factors for an induced earthquake are limited to the distance a well is located from a fault, the stress state of the fault, and a sufficient quantity of fluids from the injection well at a high enough pressure and enough time to cause movement along the fault (Ohio Department of Natural resources, 2012).

A hydraulic conduit from the injection zone to a fault may also induce earthquakes (Ellsworth, 2013). The largest injection-induced events are associated with faulting that is deeper than the Injection Zone, suggesting that the increased pressure is transmitted into the basement, which increases the potential for inducing earthquakes (Ellsworth, 2013). In all cases, faults have been reactivated at or in close proximity of Class II injection sites. In some cases, previously unknown faults have been discovered. No induced earthquakes have been known or are postulated to have been caused by Class I injection operations (Davis et al., 1987).

#### ***2.5.3.1 Induced Seismicity Analysis at the Project Site***

Assessment of the potential for induced seismicity at these locations follow the methodology outlined below, using the very conservative "zero-cohesion Mohr-Coulomb failure criterion" recommended by the U.S. Geological Survey (Wesson and Nicholson, 1987). These analyses indicate very low potential for induced seismicity caused by pressures resulting from injection activities. Nearby examples are available, such as long-term Class I injection operations at sites like Lanxess Corporation and Clean Harbors Corporation in southern Arkansas, which are regulated by the EPA.

South of the proposed site, there is a normal fault graben-horst block system known as the South Arkansas Fault Zone that was initiated due to salt mobilization from the accumulation of

overburden sediment. Brine waste disposal injection has induced movement along pre-existing strike-parallel normal fault surfaces (Cox and VanArsdale, 1991). Between 1983 and 1990, twelve earthquakes between a magnitude of 2.0 and 3.0 occurred in the El Dorado area. The two injection wells (Lanxess SWD# 7 and 13) in the El Dorado South field in closest proximity to fault surfaces at the depth of injection also lie at the center of the macroseismic area of a magnitude 2.5 earthquake of December 12, 1988 and show increases in injection rates prior to periods of seismicity (Cox and VanArsdale, 1991). However, these seismic events are well below damaging levels, are primarily located south of the site along the fault zone and would not impact the integrity of injection operations.

Since the 1990's, injection rates and volumes have been regulated and monitored because of these events. No induced seismicity events have occurred since 1990. Injection rates and the Lapis project area will be continuously monitored and always operate at 90 percent below fracture gradient and will consider the critical pressure to induce seismicity. The Lapis project is also not located along a fault system, which also lowers the risk of induced seismicity.

Additionally, the sequestration project will be injection into the Smackover, Cotton Valley, and lower Hosston Formations, which are located many thousands of feet above the Ouachita Peneplain basement complex. Injection into strata near or at the basement, with activation of pre-existing faults, has been identified as contributing to induced seismicity in those parts of the country where deep injection occurs, which will not be a factor at the project site. The 2D seismic grid which was acquired and re-processed as part of this Class VI application preparation confirms the absence of faulting near the injection site.

#### **2.5.4 Seismic Risk Models for the Project Site**

A model earthquake is used to evaluate any potential effects of natural earthquakes on subsurface geological structures associated with the sequestration project. In general, a source mechanism is required when designing a “model” earthquake. In these cases, it is usual to have a “known” active fault system with a measured strain or stress field. In more active regions of the earth, faults with strain (movement across the fault without a rupture) develop at a rate of up to 5 centimeters per year, or more (Leeds and Associates, 1989). As a meter or more of strain develops, stress

accumulates and eventually the system releases this stored strain energy in the form of elastic waves (i.e., an earthquake). The Lapis sequestration site near El Dorado is positioned in a region of seismic quiescence, the Northern Gulf Coastal Plain, which up until 1983, had no earthquakes reported in Union County. Once injection began in 1983, several earthquakes have been documented, which according to Cox and Van Arsdale (1991) are attributed to waste brine disposal along a major fault zone. Underground fluid disposal may have elevated pore pressure and reduced the normal stresses across pre-existing fault surfaces and triggered fault movement.

The South Arkansas Fault Zone is a continuation of a major structure known as the Mexia-Talco Fault Zone in East Texas and extends into southern Union County (Figure 2-38) (Cox and VanArdsdale, 1991). The Mexia and Talco Fault Zones are comprised of strike-parallel normal faults that formed narrow grabens and are connected by a zone of en echelon normal faults. The near coincidence of the Louann salt updip limit and the symmetrical graben system suggests that the highly mobile evaporite provided a weak decollement surface on which the overlying sediments slowly glided towards the center of the basin (Jackson and Wilson, 1982). The Mexia-Talco and South Arkansas Fault Zone movement is related to slow gravitational creep of salt and its sedimentary overburden rather than to movement of plate tectonics (Jackson and Wilson, 1982). It is doubtful the faults associated with a salt seismogenic source will have magnitudes greater than 3.0 and intensity MMI of IV (Leeds and Associates, 1989). Also, the normal displacement of the stresses ensure that stresses are neutralized by tensile fracture at low stresses because the tensile strength of materials is generally much lower than their compressive strength (Jackson and Wilson, 1982).

Jackson and Wilson (1982), indicate there is no geologic evidence that these faults pose a threat in the construction of hypothetical nuclear-waste facilities, which use highly conservative screening criteria for evaluating potential seismic risk. El Dorado is an area of low seismic risk where the major fault system, the South Arkansas Fault Zone, was initiated from salt mobilization due to sediment overburden. Salt sourced fault movement in the Gulf Coast area is unlikely to propagate damaging ground motions since the movement is associated with gradual creep rather than rapid breaking of brittle rock associated with large earthquakes. Brine injection into the subsurface beginning in 1983 increased pore pressure and likely reactivated pre-existing normal

faults. However, earthquakes of these magnitudes pose no danger to human welfare or property and are well below damaging levels (Cox and VanArsdale, 1991).

#### **2.5.4.1 Design Earthquake Model**

For the evaluation of the potential impact of seismicity on a Class VI Sequestration facility in Union County, a modeled seismic event with a body-wave magnitude Mb of  $4.3 \pm 0.2$  (the largest historical earthquake in Union County) can be used as a conservative working model for the design earthquake. It is presumed that the nearest seismic source would be along the South Arkansas Fault Zone, a structure initiated during the opening of the Gulf of Mexico (Cox and VanArsdale, 1991; Murray, 1961).

Another assumption is that the maximum ground motion at the surface generated by the design earthquake would be within the Modified Mercalli Intensity range of MMI of V, which equates to a horizontal surface acceleration of 0.05g (Leeds and Associates, 1989). The empirical correlation between intensity and acceleration has a wide spread of data, with recordings varying from horizontal accelerations of 0.025g to 0.150g for an MMI=V event. This is the same value used for an “Operating Basis Earthquake” (OBE) for certain Gulf Coast nuclear power plant electric generating stations. For example, the Nuclear Regulatory Commission’s estimate for the risk each year of an earthquake intense enough to cause core damage to the reactor at River Bend (north of Baton Rouge) was 1 in 40,000 according to an NRC study published in August 2010 (Hiland, 2010). Additionally, the OBE and DBE for the Arkansas Nuclear One facility (Pope County, Arkansas) are 0.10 g and 0.20 g, which are conservative estimates.

*“The Operating Basis Earthquake is that earthquake which, considering the regional and local geology and seismology and specific characteristics of local subsurface material, could reasonably be expected to affect the plant site during the operating life of the plant; it is that earthquake which produces the vibratory ground motion for which those features of the nuclear power plant necessary for continued operation without undue risk to the health and safety of the public are designed to remain functional.”*

The design earthquake in this study is based on the empirical data of normal shallow focus (<20 km) earthquakes on soft sites taken from Leeds and Associates, 1989. It is also assumed that in the Gulf coastal seismic environment, the release of energy from less competent materials than usual would result in longer surface rise times; therefore, the ground motion would be biased to longer periods (lower frequencies) than usual, and result in low accelerations, large displacements, and long durations (Leeds and Associates, 1989).

Over the years, studies of the effect of depth on seismic ground motion have all noted a clear attenuation. Observations in deep mines and boreholes have confirmed this phenomenon. Data strongly indicates dampening of amplitude with depth to an average of one-half, or less, of the ground motion. The motion may become as low as one-fifth while for small motions, where the materials remain completely elastic, the diminution of amplitude may be as small as one-tenth (Leeds and Associates, 1989). The effect of ground motion on saturated granular soils is buildup in pore water pressure. If the water table is located near the surface (within about 15 to 20 ft), if the sands are reasonably well sorted and clean (free of clay), and if accelerations exceed about 0.25g, a type of soil failure known as liquefaction can occur (Leeds and Associates, 1989). Liquefaction causes a loss of shear strength of the soil and may result in ejection of sand and water to the surface (sand boils), and collapse of the foundations of structures supported by the soil. In extreme cases, multistory buildings have rolled over (Niigata, Japan Earthquake in 1964) and buried tanks have “floated” to the surface (Leeds and Associates, 1989). There is indeed settlement and densification of the soil following liquefaction. The sequestration project area does not meet the conditions expected to trigger liquefaction since the predicted acceleration levels (0.05g) would only be about one-fifth of that required (Leeds and Associates, 1989). Note – that the Project Blue site lies in an area of low risk for liquefaction (Figure 2-37).

With depth increasing, there is less ground motion. While pore pressures could increase, the soils framework is not required to support the lithostatic sediment column. Additionally, within the short duration of shaking, there is insufficient time or room for the fluids to go to. Thus, it remains incompressible. Leeds and Associates (1989) conclude that possible interactions between sedimentary horizons due to casing penetration and cement are minimal since there are only minor differential movements as the seismic waves pass through the matrix. They conclude that there

might be only several centimeters of displacement over the wavelength of the seismic waves and that the normal elasticity of well casing and tubing is sufficient to accommodate the strain (Leeds and Associates, 1989). It is only in extreme cases, such as in 1952 in Kern County, California, where surface accelerations can reach 0.50g and there are many miles of surface rupture, that existing wells may be affected. During the 1952 event, approximately 2% of the wells in the area had some surface damage due to settlement of surficial soils (Leeds and Associates, 1989). This event caused some subsurface damage including collapsed tubing near the surface due to the sharp rise in casing pressure accompanying the shock. However, all wells returned to normal status within 2 or 3 weeks of the event (Leeds and Associates, 1989).

After reviewing data from the largest historic events of the province and modeling a “design earthquake”, the hypothetical modeling results show an event with little damage to engineered structures or facilities. Ground motion due to seismic activity is attenuated with depth. Thus, no damage to the well systems would be anticipated.

In the Gulf Coast region and Union County area, only small earthquakes have occurred in the area, such as the 2001 earthquake with a magnitude earthquake of 3.0 that occurred 2 km southeast of El Dorado, Arkansas. Larger earthquakes of  $MMI=V$  (equivalent to a 4.0-4.9 magnitude earthquake, according to Leeds, this is still classified as small) have occurred in the Gulf Coast region and did not cause damage to nearby facilities and structures. The historical seismic events in the Union County area indicate that most earthquakes near the site are approximately 3.0 magnitude and lower (including a 2.2 magnitude earthquake which occurred near the El Dorado Chemical site in 1983) and are not expected to cause damage to the Lapis sequestration structures.

#### ***2.5.4.2 Induced Seismicity Model***

For this Class VI permit application, Lapis employs conservative assumptions to the causative mechanisms of induced seismicity and the geomechanical conditions within the Union County project area of interest to conservatively constrain parameters. The potential for induced seismicity at the proposed injection site can be evaluated using the very conservative zero-cohesion Mohr-Coulomb failure criterion, recommended by the U.S. Geological Survey (Wesson

and Nicholson, 1987). This method is based on the following equation:

$$P_{crit} = \frac{S_v(3\alpha-1)}{2} \quad (1)$$

where:

$P_{crit}$  is the critical injection zone fluid pressure required to initiate slippage along faults and fractures

$S_v$  is the total overburden stress (which represents the maximum principal stress in the Gulf Coast region)

$\alpha$  is the ratio of the minimum principal stress (horizontal in the Gulf Coast region) to the maximum principal stress (overburden stress)

Inherent in Equation (1) are a number of conservative assumptions, guaranteed to produce a worst-case lower bound to the critical fluid pressure for inducing seismicity. These are:

- 1) It neglects the cohesive strength of the sediments
- 2) It assumes that a fault or fracture is oriented at the worst possible angle
- 3) It assumes a worst-case value of 0.6 for the coefficient of friction of the rock (see Figure 4 of Wesson and Nicholson, 1987)

For present purposes, Equation (1) can be expressed in a more convenient form by introducing the so-called matrix stress ratio ( $K_i$ ) (Matthews and Kelly, 1967; Eaton, 1969), which is defined as the ratio of the minimum to the maximum effective principal stresses. Effective principal stress is equal to actual principal stress minus fluid pore pressure ( $p_o$ ). Thus:

$$K_i = \frac{\alpha S_v - p_o}{S_v - p_o} \quad (2)$$

Substituting Equation (2) into Equation (1) yields:

$$\Delta P_{crit} = \left( \frac{3K_i - 1}{2} \right) (S_v - p_o) \quad (3)$$

where  $\Delta P_{crit}$  is the critical injection zone pressure build-up required to induce seismicity, with:

$$P_{crit} = p_o + \Delta P_{crit} \quad (4)$$

Equation (3) will be used to evaluate induced seismicity at the Lapis sequestration site.

The pore pressure gradient for the formations is taken from the Lanxess Class I injection wells, located southwest of the site. The pressure data using 1,684.3 psig at 3,890 ft in the Hosston provides a pore pressure gradient of 0.433 psi/ft. Based on local pressures in the Schuler Field, located approximately 10 miles southwest of the site, the pore pressure gradient for the Cotton Valley is also 0.433 psi/ft. Eaton (1969) provides a plot of the effective overburden stress ( $S_v$ ) as a function of depth for locations along the Gulf Coast. This plot indicates  $S_v$  values exceed 0.90 psi/ft for the Injection Zone reservoirs. Matthews and Kelly (1967) provide a plot of the matrix stress ratio ( $K_i$ ) for tectonically relaxed reservoir sediments along the Louisiana and Texas Gulf Coast.

The Lapis injection wells will be completed across the Lower Hosston and Cotton Valley Formations at depths ranging from 3,900 ft to 6,300 ft (approximate). The conservatively calculated critical pressure increases required to induce seismicity on a pre-existing fault for each Injection Zone formation for the Lapis sequestration site are contained in Table 2-8. These values are significantly higher than any expected and modeled pressures at the injection site. Since there are no known faults or fractures within the immediate vicinity of the determined area of review for this project, induced seismicity will not be a problem at this sequestration project.

## 2.6 HYDROGEOLOGY

The primary regulatory focus of the USEPA injection well program is protection of human health and environment, including protection of potential underground sources of drinking water (USDWs). A USDW is defined by the EPA as an aquifer which supplies any public water system and contains fewer than 10,000 mg/L total dissolved solids (TDS). The following sections detail the regional and local hydrogeology and hydrostratigraphy in accordance with the 40 CFR 146.82(a)(3)(vi) and 146.82(a)(5) standards.

### 2.6.1 Regional Hydrogeology

The major aquifers of Arkansas are represented in Figure 2-41. The state of Arkansas is divided into two major regional aquifer systems, which are separated by a fall line along the northwestern

boundary of the Mississippi Embayment. To the north of the fall line is the Interior Highlands Aquifer System comprised of 5 primary aquifers across north and northwestern Arkansas. This regional system includes the Arkansas and White River drainage basins and consists of highly folded and fractured Paleozoic rocks of the Ouachita mountains and Quaternary Alluvial deposits from the major rivers within the system.

To the south and east of the fall line is the Coastal Plain Aquifer System which is comprised of multiple aquifers and stretches from the Texas / Arkansas border through to the Mississippi river alluvial plain. The Coastal Plain aquifer system is a much greater source of water than the Interior Highlands, in part because it contains more extensive and thicker sedimentary packages. Cretaceous and younger formations contain usable quality water (*i.e.*, <3,000 milligrams per liter (mg/L) TDS) and potentially usable quality water (*i.e.* <10,000 mg/L TDS), which defines the base of the lowermost USDW. The coastal plain aquifer system regionally outcrops along the fall line designated by the western margins of the Mississippi Embayment and the units dip and thicken towards the south and east of the Gulf Coast plain. Kresse (2014) describes the 11 aquifers that comprise the Coastal Plain Aquifer System in Arkansas and one additional confining unit. In ascending order, from deepest to the shallowest, the 12 hydrogeologic units are:

- The Trinity Aquifer
- The Tokio Aquifer
- The Ozan Aquifer
- The Nacatoch Aquifer
- The Midway Group
- The Wilcox Aquifer
- The Carrizo Aquifer
- The Cane River Formation
- The Sparta Aquifer
- The Jackson Group
- Quaternary Alluvial Aquifers.

Figure 2-42 contains a stratigraphic column of geohydrologic units in the Coastal Plain of the State of Arkansas, which encompasses the Lapis Project Blue sequestration site. This column

denotes the aquifer units for the southern and eastern regions of the state. Not all aquifers are present throughout the area of interest due to erosional periods.

Groundwater moves through aquifer systems from areas of high hydraulic head to areas of lower hydraulic head. Regional uses from industrial and public water systems can impact the groundwater movement and divert the direction of water flow, usually towards and area of high population. Where available, published potentiometric maps for the regional aquifers are provided and discussed in their hydro-stratigraphic section.

Water quality is highly variable. In general, the water quality in southern Arkansas is considered good near outcrops but quality decreases downdip, and deeper into the subsurface, with increases in levels of sulfate, chloride, sodium, and in some localities, arsenic concentrations. Localized high salinity driven by intrusion from underlying formations, evapotranspiration processes in areas of low recharge, and inadequate flushing in downgradient areas of residual salinity from deposition in marine environments, can affect water quality (Kresse et. al, 2014). Significant quantities of groundwater occur in the Coastal Plain Aquifer System, however some of it is unusable due to moderate to high salinity, iron, and arsenic concentrations. Groundwater is generally fresh in most of the outcrop/recharge areas but demonstrates geochemical changes along flow paths toward the gulf coast.

Due to the similarity in the geochemical changes observed amongst many of the Cretaceous and Tertiary aquifers in the Coastal Plain system, Kresse et al (2014) developed a groundwater evolution model from outcrop to subsurface. This model has three main phases of groundwater evolution: 1) Early Stage: carbonate mineral dissolution along flow paths, resulting in calcium-bicarbonate, 2) Middle Stage: sodium-bicarbonate water with increased cation exchange capacity (in presence of sulfates dedolomitization this can lead to calcite precipitation), and 3) Final Stage: mixing with high chloride concentrations from original formation water (Kresse et al, 2014).

In the Coastal Plain Aquifer System groundwater is characterized by its variability in quality across the state, water quality is dependent on multiple factors such as distance from outcrop, depth, lithology, and groundwater evolution along flow path. In Arkansas groundwater is generally poor in quality compared to surface water, therefore over 66% of the public water

supply in the state comes from surface water (Holland, 2007). Locally there are aquifers which meet drinking water standards and serve as important public supply sources, however 72% of the water from the aquifers of the Coastal Plain system is used for irrigation, electricity generation, and industrial purposes.

The groundwater in the vicinity of the project area is considered fresh (water quality suitable for public consumption) in the unit's equivalent to the Sparta and shallower, and to be saline to brine in the units deeper than the Cane River Formation. Due to the water quality the deeper aquifers have primarily been used as injection and disposal intervals (Broom et al, 1984). It is also worth noting that due to the extensive use of the Sparta aquifer in Union County significant drawdown was observed. In 1996 the state of Arkansas declared El Dorado as a critical area and began a conservation program for water use from the Sparta in the county (Kresse et al, 2014). As part of this program a pumping facility was installed on the Ouachita River to supplement water supply. As a result of these conservation measures the water level in the Sparta aquifer has been rising since 2003.

The following subsections detail the hydrostratigraphy of the Coastal Plain Aquifer System for the southwestern Arkansas region in ascending order.

#### ***2.6.1.1 Trinity Aquifer***

The Trinity Aquifer is a hydrostratigraphic unit of Cretaceous sands that can be a significant source of water in southwestern Arkansas. The Trinity aquifer occurs within the Trinity Group of the Lower Cretaceous and overlies the Cotton Valley Formation. The Trinity Aquifer depth ranges from 4,000 ft - 5,000 ft in central Union County and is saline. The Trinity aquifer is composed of 6 units; 3 of which can be significant water bearing intervals. The significant water bearing zones of the Trinity aquifer are the Pike gravel, Ultima Thule gravel and Paluxy sand (Kresse et al, 2014).

The Pike and Ultima Thule are characterized by pebbles and cobbles with interbedded sand and clay; with the main difference being that the Ultima Thule gravel is finer in nature than the Pike gravel. The Paluxy is the principal water bearing unit of the Trinity aquifer and is a well sorted, fine white sand interbedded with clay and limestone and (Kresse et al, 2014). The Trinity aquifer

can supply freshwater in an area confined within a few miles of the outcrop; however due to facies changes and common clay rich sediments downdip use as an aquifer is restricted to Columbia and Sevier Counties (Kresse et al, 2014). In the project area it is not considered a potential USDW.

#### ***2.6.1.2 Tokio Aquifer***

The Tokio aquifer is an Upper Cretaceous unit that is a locally important source of water in southwestern Arkansas. It is however completely saline in the project area. Due to uplift that occurred during the Middle Cretaceous, which was followed by erosion, the Tokio aquifer can range from unconformably being in contact with Pennsylvanian aged sediments in the northeastern part of the state, to contacting the Glen Rose Group (Cretaceous) in the center of the Mississippi Embayment. In central Union County the Tokio group occurs at a depth around 3,000 ft and is characterized by discontinuous interbedded gray clay and poorly sorted cross bedded sands with lignite and scattered carbonaceous material (Kresse et al, 2014). Typically, the Tokio is only a significant source of water within 5 miles of the outcrop due to an increase in salinity with depth along the flow path to the southeast. Where present as an aquifer in Hempstead, Howard, Miller and Sevier Counties it is recognized as 3 distinct sand bodies, which are separated by clay and marl. The Tokio is not considered a groundwater source in the study area due to salinity.

#### ***2.6.1.3 Ozan Aquifer***

The Ozan aquifer consists of discontinuous sand beds with varying proportions of clay and limey material that demonstrate variable thickness. It is present as an aquifer in an extremely narrow band extending from western Little River County to northeastern Clark County and contains some of the poorest quality water of any of the aquifers in the Coastal Plain (Kresse et al, 2014). There has been no reported use after 1965 and the Ozan is not considered a source of potential groundwater or an USDW in the project area.

#### ***2.6.1.4 Nacatoch Aquifer***

The Nacatoch aquifer is characterized by interbedded unconsolidated sands with lenses and beds of fossiliferous sandy limestone. As seen with many Cretaceous sands throughout Arkansas the

variability in lithology and continuity are a result of the nearshore depositional environment and cyclic eustatic changes during this time (Kresse et al, 2014). As observed with other Cretaceous sands, the extent where the Nacatoch is a productive aquifer is confined to areas very close to the outcrop, which coincide with the shoreline during depositional times. Where the Nacatoch is used as a source of groundwater it can be divided into 3 distinct units: 1) a lower interbedded clay-rich marl, 2) a middle fossiliferous glauconitic sand, 3) and an upper unconsolidated cross bedded fine grained quartz sand (Kresse et al, 2014). The upper unit is the principal water producer of the Nacatoch aquifer. In the regional study area, the Nacatoch is not considered a source of groundwater and has been producing oil in El Dorado since discovery in 1920 (Broom et al, 1984).

Aside from oil production there was a significant amount of brine production which resulted in the decline in the hydraulic head of the Nacatoch, which led operators to reinject brine into the formation to repressurize. Broom (1984) conducted a study to see if the deep Cretaceous sands were a source of potential contamination of the shallow aquifers and concluded that the thick marine shales of the Midway group, which separate the Tertiary and Cretaceous sediments, are sufficient to prevent communication and contamination. This is confirmed by pressure differences in the subsurface across the Cretaceous and Tertiary sediments in Union County.

#### ***2.6.1.5 Midway Aquitard***

The Midway Group is the first Tertiary deposit in the Gulf of Mexico and is characterized by a package of marine clays and shales. The Midway ranges in thickness from a few hundred to thousands of feet and is believed to have highly effective confining properties which limit the capacity of the formation to accept, transmit, and discharge fluids (Broom et al, 1984). The geochemical characteristics and hydraulic head differences of units above and below the Midway group support that the Midway acts as a confining unit in the Coastal Plain aquifer system.

#### ***2.6.1.6 Wilcox Aquifer***

The Wilcox aquifer is the lowermost of the Tertiary units that produces groundwater in the Coastal Plain aquifer system. The Wilcox is predominately a source of groundwater along the margins of the Mississippi Embayment, as observed with many of the Cretaceous sands in the Coastal Plain aquifer system. In Arkansas, the Wilcox is divided into two distinct lithologic units:

1) the lower Wilcox which consists of interbedded lignitic sands and clays, and 2) the upper Wilcox which consists of interbedded layers of shale with irregular and discontinuous sand bodies (Kresse et al, 2014). In northern Arkansas, the Wilcox contains many more thick sands, which are a significant source of public, domestic and industrial water supply. However due to facies changes the Wilcox does not demonstrate good water quality in the regional study area and is not used for public supply.

In Union County the Wilcox depth ranges from 700 ft to 1,500 ft from the northwest to southeast. Testing completed by the Arkansas Oil and Gas Commission, Arkansas Geological Commission, USGS, Tennyson Oil Company, and Walter Alderson of an abandoned oil well Lacy B-1 showed that the TDS of the water from the Wilcox in the El Dorado field was 4,900 mg/L (Broom et al, 1984). In the project area, the Wilcox has been solely used as a disposal zone for brine.

#### ***2.6.1.7 Carrizo Aquifer***

The Carrizo aquifer is the lowermost unit of the Claiborne group and the first of the Eocene aquifers in the Coastal Plain system. The Carrizo is a minor aquifer in Arkansas and is predominately used for domestic supply in the southwestern portion of the state (Kresse et al, 2014). The Carrizo is found in northernly elongated sinuous bands that are discontinuous and highly variable in thickness. The Carrizo is deposited as valley and channel fill sediments on an irregular erosion surface on top of the Wilcox formation and represents an ancient fluvial plain (Kresse et al, 2014). The depositional nature of the Carrizo limits the aerial extent to which it is a viable aquifer in southwestern Arkansas. The lithology is characterized by fine to coarse micaceous massively bedded quartz sands with minor interbedded clays and occasional lenses of lignite. In the regional study area, the Carrizo can be less than 30 ft thick where present (Kresse et al, 2014). Near the outcrop the Carrizo has water of sufficient quality for domestic supply, but quality rapidly degrades downgradient due to elevated chloride concentrations. (Hosman, 1996).

#### ***2.6.1.8 Cane River Aquitard***

The Cane River formation is characterized by a sequence of marine clays and shales with thin discontinuous marine sands and has historically been listed as a part of the regional Claiborne confining unit (Kresse et al, 2014). Due to the lithology and depositional nature of the Cane River

it is sparsely a source of groundwater from a regional perspective and has been considered a “perfect” confining unit with practically no capacity for intake, transmission, or release of fluids (Broom et al, 1984). However, there are localities along the margins of the Mississippi Embayment within 5 miles of outcrop that contain up to 40 percent sand content and serve as a source of groundwater for public supply to small communities (Kresse et al, 2014). Cane River water quality is classified as a soft sodium-bicarbonate and located at the very near surface. In Union County, the Cane River is not a source of ground water and serves as a confining unit due to the high clay content. Downgradient, chloride concentrations as high as 1,410 mg/L are observed, which exceed the Federal secondary drinking-water regulation of 250 mg/L (Kresse et al, 2014).

#### ***2.6.1.9 Sparta Aquifer***

The Sparta aquifer is the source of the second highest volume of groundwater supply in the state and is recognized as the thickest sand in the Mississippi Embayment. In some locations the thickness is nearly 700 ft. The widespread thickness and sand content of the Sparta makes it a productive source of groundwater throughout almost the entire Coastal Plain aquifer system. The Sparta has three distinct lithologic units, which comprise two individual hydrogeologic units. The lower Sparta is characterized by thick bedded sands, which range from coarse to fine and can be up to 300 ft thick. The middle Sparta consists of clay and silt. The upper Sparta is termed the Greensand and contains thin bedded very fine to fine grained sandy clay with significant glauconite content (Kresse et al, 2014).

Differing potentiometric surfaces from the lower Sparta and the Greensand unit confirm that the middle unit acts as a confining layer, which isolates the other hydrogeologic units of the Sparta (Kresse et al, 2014). Though it is a significant source of water there are two predominate locations in Jefferson and Union Counties where it serves as the primary source of groundwater for both public supply and industrial use and therefore has undergone extensive depletion. Due to this extensive use in 1996 the Sparta aquifer was declared a critical area. A conservation program was implemented, which is still in force, and has resulted in rising water levels within the aquifer (Kresse et al, 2014).

### ***2.6.1.10 Cockfield Aquifer***

The Cockfield aquifer is also a significant aquifer in the southern and eastern portions of Arkansas. In some locations yields are high enough to support public and industrial use (Kresse et al, 2014). It is characterized as a fine to medium grained sand that grades into a silty clay with lignite and carbonaceous material. There is considerable variability in thickness throughout the region indicating that these non-marine sands were deposited because of longshore currents and deltaic channels in a nearshore environment (Kresse et al, 2014). As a result of the depositional environment, lithology, and variability in thickness it is possible that sands within the Cockfield may not be hydraulically connected. In the regional study area, the Cockfield is an USDW and contains water with 100 – 200 mg/L TDS (Broom et al, 1984). In Union County, the Cockfield can be found in outcrop throughout most of the county except where it is overlain by Quaternary Alluvium in river bottoms. The thickness of the Cockfield in Union County is on average around 200 ft and individual sands range from 50 ft to 75 ft but can be up to 100 ft thick (Broom et al, 1984). Prior to 1920, when the development of the El Dorado oil field commenced, Cockfield was the source of all groundwater in Union County. Following the 1940's, with the decline in local oil production, the Cockfield aquifer has predominately been used for domestic supply (Kresse et al, 2014).

### ***2.6.1.11 Jackson Group***

The Jackson Group comprises a Late Eocene sequence of largely unconsolidated clays with rare, interbedded siltstone and sandstone units. Because of the predominance of fine-grained sediments and overall low hydraulic conductivity it is designated as a regional confining unit (Kresse et al, 2014). There are locations in southeastern Arkansas where the Jackson Group did serve as a source of domestic and small farm supply, as the region did not yet have ample public supply for small towns. The area where groundwater was used from the Jackson is confined to exposed deposits south of the Arkansas River (Kresse et al, 2014). The groundwater from the Jackson group is recognized as some of the poorest quality in the state; it displays especially elevated sulfate concentrations upward of 3,080 mg/L (Kresse et al, 2014). The Jackson Group is not present in the project area.

### ***2.6.1.12 Quaternary Alluvium Aquifer***

The Quaternary Alluvial aquifers are one of the most valuable natural resources in the state of Arkansas, of which there are three hydrogeologic units. These units are in order of increasing significance and volume of supply: 1) Red River Alluvial aquifer (RRAA), 2) Ouachita – Saline Rivers Alluvial aquifer (OSRAA), and 3) the Mississippi River Valley Alluvial aquifer (MRVAA). The MRVAA is limited to the eastern one third of Arkansas (see inset of Figure 2-41). In the southwestern portions of the state are the smaller less aerially expansive and productive RRAA and OSRAA that provide sources of groundwater. The Quaternary Alluvium sediments of the Coastal Plain aquifer system are the result of erosion and deposition (Kresse et al, 2014). The smaller scale nature of the Red River and Ouachita River drainage basins is reflected in the nature of the thinner and less aerially extensive alluvium than seen on the eastern side of the state in the Mississippi River drainage basin.

The RRAA is present in southwestern Arkansas over an area of about 540 mi<sup>2</sup> with a maximum thickness of 90 ft (Kresse et al, 2014). It is comprised of a coarsening downward sequence of clay, silt, sand, and gravel and is confined to the drainage and tributaries of the Red River. Irrigation is the dominant use of water from the RRAA, accounting for 83 percent of water pumped from the aquifer, the remaining is used for duck hunting ponds. Due to water quality issues from elevated chloride concentrations of up to 46,250 mg/L reported in Miller County and due to seepage from oil-field associated brine storage pits the RRAA was no longer used for public supply after the 1950's (Kresse et al, 2014).

The OSRAA is also present in southwestern Arkansas and is comprised of silt and beds of fine to very fine-grained sand with some clay (Kresse et al, 2014). The OSRAA is unconfined and in regions where the sand is coarse enough it may be in connection with rivers and can display a wide variability in aquifer properties. The deposits of the OSRAA are thin and restricted in aerial extent and can be found incising older Pleistocene terrace deposits of the Mississippi River (Kresse et al, 2014). Groundwater wells from the OSRAA are mostly shallow domestic wells with depths of less than 30 ft and therefore there is not as much water quality data as other aquifers which are more extensively used across the state. From the samples collected the TDS were generally less than 250 mg/L but there were nitrate concentrations above 10 mg/L, possibly

because of the depth of the wells and influence of septic systems and nearby farm acreage (Kresse et al, 2014).

The most prominent of the Quaternary Alluvium deposits is the MRVAA which not only has the largest aerial extent but is the most significant hydrogeologic unit in the state; in 2010 the MRVAA accounted for 94 percent of all groundwater use and 62% of the total combined water use in the state (Kresse et al, 2014). It is characterized by proximal river unconsolidated sands, gravels, and silts. Due to the consistent sediment supply of the Mississippi, low relief of the region and wandering nature of streams shifting position during evolution there is a consistent and widespread regional geology to this aquifer (Kresse et al, 2014). The MRVAA is split into two distinct units: 1) a lower unit which is the primary aquifer consisting of sands and gravels, and 2) the upper unit which consists of fine sands, silt, and clay. The lower unit was most likely developed by discharge streams carrying glacial outwash from meltwater resulting in the grain size and composition of the deposit. The primary use of the water from the MRVAA is for agriculture and irrigation, this is dominated by rice farming. As of 2010 Arkansas was the leading rice producer in the United States (Kresse et al, 2014). Secondary uses for the MRVAA are aquaculture (duck hunting) and public supply. Due to the significant use of the MRVAA, water levels in the aquifer experienced significant declines and the aquifer eventually reached unconfined conditions. In 1998 the Arkansas Natural Resources Commission designated the MRVAA to be in a critical groundwater area and began a remediation and conservation program. Surface water diversions from the White River and Arkansas River were planned to supplement usage from the MRVAA. The USGS along with state and local governments continue to monitor the use of the MRVAA, due to its significance as a natural resource to the state. The water quality from the MRVAA is generally good compared to the EPA primary drinking-water standards (U.S. Environmental Protection Agency, 2009). However, in deeper parts it can have elevated concentrations of arsenic, as well as high salinity from upwelling (Kresse et al, 2014). The MRVAA is not present in Union County near the project site. According to Broom et al (1984) Quaternary alluvium is present in the bottomlands of most streams and rarely exceeds 25 ft thick.

## 2.6.2 Local Hydrogeology

The Lapis – Project Blue site is located near the town of El Dorado in central Union County in southern Arkansas. Hydro-stratigraphic units of importance range in age from the Tertiary to recent-aged strata and include in ascending order: (1) Wilcox (2) Sparta Sand (which is subdivided into the El Dorado and the Greensand), and the (3) Cockfield formations.

Within the Mississippi Embayment, the Sparta Aquifer is formed from the Sparta Sands, which are comprised of unconsolidated sands, silt, and clay of Eocene age and mimics the ancestral Mississippi River (Figure 2-43). The Sparta Sands are also referred to as the Memphis Sands in other states, however, both sands represent stratigraphic equivalents (Sowby, 2013). In Union County, the primary source of groundwater is from the Sparta-Memphis, with much lesser contributions from the Cockfield Formation and other aquifers such as Quaternary and Alluvial deposits, based upon a 2015 Arkansas Groundwater Protection and Management Report.

Surface water from the Ouachita River is also supplied to three of the largest industrial users in El Dorado, which include Lanxess, El Dorado Chemical Plant, and Lion Oil. Prior to 2004, these large industrial users, along with all of Union County, solely relied on the Sparta Aquifer for groundwater, which resulted in a significant water level reduction. These industrial users converted their water supply from the Sparta Aquifer to the Ouachita River, which helped to reduce the Sparta Aquifer groundwater withdrawal by 6.0 MGD (800,000 ft<sup>3</sup>/d) in 2007 and 10.7 MGD (1,430,000 ft<sup>3</sup>/d) in 2012 (Sowby, 2013). Groundwater reduction efforts since 2005 have resulted in the Sparta Aquifer water level rising within central Union County, near El Dorado. A potentiometric map for the Sparta is provided in Figure 2-44 note the large drawdown towards the city of El Dorado.

The horizontal hydraulic conductivity of the Sparta Aquifer ranges from 2.5 to 48 ft/d, with the higher values being typical of confined areas, and the lower values being typical of unconfined areas (Sowby, 2013). The Sparta Sands range in thickness from 100 to 1,000 ft in southern Arkansas and is confined by the overlying Cook Mountain Formation and the underlying Cane River Formations (Sowby, 2013). The Sparta Aquifer is deep and confined but outcrops on both sides of the Mississippi River, to the west and east. In the western Sparta Sand outcrop area,

infiltration of precipitation is the main groundwater recharge process, though stream leakage, irrigation seepage, and flow from adjacent aquifers can provide significant recharge volumes too. The groundwater pumped in Union County is derived from these water infiltration processes that occur in the narrow outcrop area to the west (Sowby, 2013).

### **2.6.3 Determination of the Base of the Lowermost USDW**

The most accurate method for determining formation fluid properties is through the analysis of formation fluid samples. In the absence of formation fluid sample analyses, data from open-hole geophysical well logs can be used to calculate formation fluid salinity by determining the resistivity of the formation fluid ( $R_w$ ) and converting that resistivity value to a salinity value. The two primary methods to derive formation fluid resistivity from geophysical logs are the “Spontaneous Potential Method” and the “Resistivity Method”. The Spontaneous Potential Method derives the formation fluid resistivity from the resistivity of the mud filtrate and the magnitude of the deflection of the formation spontaneous potential (SP) response (*i.e.*, the electrical potential produced by the interaction of the formation water, drilling fluid, and mudstone content of the formation). The Resistivity Method determines the formation fluid resistivity from the resistivity of the formation ( $R_t$ ) and its resistivity factor ( $F$ ), which is related to the formation porosity and a cementation factor (Schlumberger, 1987).

#### ***2.6.3.1 Spontaneous Potential Method***

The spontaneous potential curve from an open-hole geophysical well log records the electrical potential (voltage) produced by the interaction of the connate formation water, conductive drilling fluid, and certain ion selective rocks (mudstones). Opposite mudstone beds, the spontaneous potential curve usually defines a straight line (called the mudstone baseline) while opposite permeable formations, the spontaneous potential curve shows excursions (deflections) away from the mudstone baseline. The deflection may be to the left (negative) or to the right (positive), depending primarily on the relative salinities of the formation water and drilling mud filtrate. When formation salinities are greater than the drilling mud filtrate salinity, the deflection is to the left. For the reverse salinity contrast, the deflection is to the right. When salinities of the formation fluid and drilling mud filtrate are similar, no spontaneous potential deflection will occur.

The deflection of the spontaneous potential curve away from the mudstone baseline in a clean sand is related to the equivalent resistivities of the formation water ( $r_{we}$ ) and the drilling mud filtrate ( $r_{mf}$ ) by the following formula (Schlumberger, 1987):

$$SP = -K \log \left( \frac{r_{mf}}{r_{we}} \right)$$

For NaCl solutions,  $K = 71$  at  $77^{\circ}\text{F}$  and varies in direct proportion to the temperature ( $T$ ) by the following relationship (Schlumberger, 1987):

$$K = 61 + 0.133 T$$

From the above equations, by knowing the formation temperature, the resistivity of the mud filtrate, and the spontaneous potential deflection away from the mudstone baseline, the resistivity of the formation water can be determined (Figure 2-45). From the formation water resistivity and the formation temperature, the salinity of the formation water can be calculated (Figure 2-46).

### 2.6.3.2 Resistivity Method

The Resistivity Method determines the formation fluid resistivity from the formation resistivity ( $R_t$ ) and the formation resistivity factor ( $F$ ), which is related to the formation porosity and a cementation factor (Schlumberger, 1987). The resistivity of the formation (in ohm.meters) is a function of 1) resistivity of the formation water, 2) amount and type of fluid present, and 3) pore structure geometry. The rock matrix generally has zero conductivity (infinitely high resistivity) except for some clay minerals, and therefore does not have any effect in the resistivity log response.

Induction geophysical logging determines the formation resistivity  $R_t$  by inducing an electrical current into the formation and measuring the conductivity (reciprocal of the resistivity). The induction logging device investigates deeply into the formation and is focused to minimize effects of the borehole, surrounding formations, and invaded zones (Schlumberger, 1987). The induction log measures the true resistivity of the formation (Schlumberger, 1987). The conductivity measured in the induction log is the most accurate resistivity measurement under 2 ohm.m. Electrical conduction in sedimentary rocks almost always results from the transport of ions in the

pore-filled formation water and is affected by the amount and type of fluid present and pore structure geometry (Schlumberger, 1988).

In general, high-porosity sediments with open, well-connected pores have lower resistivity, and low-porosity sediments with sinuous and constricted pore systems have higher resistivity. It has been established experimentally that the resistivity of a clean, water-bearing formation (*i.e.*, one containing no appreciable clay or hydrocarbon) is proportional to the resistivity of the saline formation water (Schlumberger, 1988). The constant of proportionality is called the formation resistivity factor (F), where:

$$F = \frac{R_t}{R_w}$$

For a given porosity, the formation resistivity factor (F) remains nearly constant for all values of  $R_w$  below 1.0 ohm.m. For fresher, more resistive waters, F may decrease as  $R_w$  increases (Schlumberger, 1987). It has been found that for a given formation water, the greater the porosity of a formation, the lower the resistivity of the formation and the lower the formation factor. Therefore, the formation factor is inversely related to the formation porosity. In 1942, G.E. Archie proposed the following relationship (commonly known as Archie's Law) between the formation factor and porosity based on experimental data:

$$F = \frac{a}{\phi^m}$$

Where:

$\phi$  = porosity

a = an empirical constant

m = a cementation factor or exponent.

In sandstones, the cementation factor is assumed to be 2, but can vary from 1.2 to 2.2 (Stolper, 1994). In the shallower sandstones, as sorting, cementation, and compaction decrease, the cementation factor can also decrease (Stolper, 1994). Experience over the years has shown that the following form of Archie's Law generally holds for sands in the Gulf Coast and is known as the Humble Relationship (Schlumberger, 1987):

$$F = \frac{0.81}{\phi^m}$$

Combining the equations for the Humble relationship and the definition of the formation factor, the resistivity of the formation water ( $R_{we}$ ) is related to the formation resistivity ( $R_t$ ) by the following expression:

$$R_t = \frac{R_{we} \times 0.81}{\phi^m}$$

#### **2.6.3.3 Methodology used in the Site Evaluation**

To determine the formation water resistivity, and therefore salinity, in a particular zone, the resistivity of a sand containing 10,000 mg/l TDS formation waters must be determined. The value can then be used to calculate the equivalent deep reading formation resistivity  $R_t$ . For central Union County, the USDW is projected to be at or below 1,400 ft, therefore, a moderately cool subsurface temperature applies. At a depth of 1,400 ft, the calculated subsurface temperature is expected to be 84.8° F. The Schlumberger Gen-9 chart (Resistivity of NaCl Solutions – Figure 2-46) is scaled in units of parts per million. However, at the dilute end the equivalence of 10,000 mg/l TDS and 10,000 ppm TDS is quite close (*i.e.*, 10,000 mg/l = 10,011.4 ppm). The formation water resistivity for a 10,000 ppm NaCl solution at a temperature of 84.8° F is 0.52 ohm.m. An Archie-type equation can be used to calculate the deep reading resistivity that would be observed in a sand with a formation water with a resistivity of 0.52 ohm.m. Using an average porosity value of 36 percent for the unconsolidated Wilcox sands (per offset analogue well data), the formation resistivity  $R_t$  cut-off can be calculated from the basic Archie equation, such as:

$$R_t = \frac{0.52 \text{ ohm.m} \times 0.81}{0.35^2} = 3.4 \text{ ohm.m}$$

Therefore, a conservative conclusion would be to consider that sands with a formation resistivity greater than 3.4 ohm.m are likely to be USDW's in the area. This methodology is then employed to review shallow well logs in central Union County. To be conservative, the base of the lowermost USDW across the evaluated logs is placed at the deep resistivity of 3.0 ohm.m.

## 2.6.4 Base of the Lowermost USDW

As an example, for identification of the base of the lowermost USDW, the J. D. Reynolds Company Byrd #1 well was drilled in 1961 to a total depth of 3,367 ft. The well was logged with Spontaneous Potential, Shallow and Deep Induction, and Deep Conductivity curves from the surface casing point at 100 ft to total depth (Figure 2-47). In the figure, a vertical red dashed line is placed along the 3 ohm.m scale for reference. The open hole geophysical well log shows the sands of the Wilcox Group with deep resistivities between 3.0 and 5.0 ohm.m. Below the Wilcox at a depth of 1,416 ft-KB is the Midway Shale, where deep resistivities are 2.0 ohm.m or less. Within the Midway group there are a few “spikes” in the deep resistivity that exceed the 3 ohm.m value but there is no spontaneous potential development and based upon the regional lithology of the Midway these spikes are presumably not sands. At a depth from 2,134 to 2,160 ft the Nacatoch sand is seen with a resistivity at 1 ohm.m or less, indicating saline conditions (approximately 18,000 ppm NaCl).

The base of the Lowermost USDW is then placed at the top of the Midway Shale / base of the Wilcox in the project area. A.5 in Appendix A presents the base of the Lowermost USDW at contours intervals of 100 ft and is consistent across the delineated AoR.

## 2.6.5 Water Well Data Sets

Water well data was gathered from a combination of private wells from El Dorado Chemical Company (LSB Industries Inc), the ADEQ Water Quality Monitoring Data Search, and the Water Well Construction Report Database of the Arkansas Department of Agriculture. A water well search was performed using a search radius of 5 miles extending from the Lapis Energy acreage in the Water Well Construction Report Database. A tabulation of all water/monitoring wells within the delineated AoR is contained in Table 2-9, with a total of 61 wells. Note that the wells which shared the same well identification number and latitude and longitude across all databases, were considered duplicates and filtered out of the dataset. The data set contains 15 surficial monitoring points such as streams and rivers, 25 wells used for monitoring and less than 100 ft deep. The remaining 20 wells extended from a depth of 90 ft to 841 ft and are used for Public

Supply, Irrigation, Industrial, and commercial purposes. No wells are completed deeper than within the Sparta Formation. Data from Table 2-9 is presented in Figure 2-48.

Note that there are no Class I or Class II injection well operations within the Lapis site or the Lapis project 1-mile AOR boundary. The closest active brine production and brine injection occurs in the Smackover and is approximately 3.8 miles south-southwest of the Lapis site. Additionally, USEPA and Arkansas State databases were searched to identify current or historical subsurface cleanup sites. No sites were identified within the delineated AoR or immediate vicinity of the LSB Industries Chemical Facility.

## 2.6.6 Local Water Usage

In Union County, which has a population of approximately 38,340 people (U.S. Census Bureau, 2020), the main source of municipal and industrial groundwater is the Sparta-Memphis Aquifer. The city of El Dorado is the county seat and the largest city. As of 2012, Union County is supplied from 62 registered wells and withdraws 10.55 Mgal/d of groundwater from the Sparta-Memphis. Large subsurface water withdrawal from Sparta-Memphis for industrial and municipal use, is causing a cone of depression surrounding El Dorado as shown in the pink box of Figure 2-44 (Schrader, 2014).

In Union County, all aquifers deeper than the Sparta yield waters exceeding 3,000 milligrams per liter (mg/L) TDS (Broom et al, 1984). This exceeds standards set forth by the National Secondary Drinking Water Regulations of 500 mg/L. The Tertiary aquifers that are present in Union County both have waters with TDS below 500 mg/L, with the Sparta being the largest contributor to the groundwater use in the county.

The Arkansas Natural Resources Commission (ANRC) pursuant to the Arkansas Ground Water Protection and Management Act of 1991, produced an Arkansas Groundwater Protection and Management Report for 2015. The report provides information regarding water-level monitoring, water usage, and well construction data from 2014 to 2015 (Arkansas Natural Resource Commission, 2016). In 2012, there were a total of 55 registered wells, which withdrew 10.31 Mgal/d from the Sparta-Memphis Aquifer in Union County, Arkansas. Of these 55 wells, 20 wells withdrew 5.3 Mgal/day of groundwater for industrial use and 35 wells withdrew 5.01 Mgal/d of

groundwater for public supply. The Cockfield Formation accounted for 0.18 Mgal/d of withdrawal from 2 wells in Union County. One of these wells withdrew 0.18 Mgal/day for industrial purposes and the other well was for public supply but did not withdraw any groundwater. Quaternary, alluvial, and terrace deposit aquifers withdrew 0.05 Mgal/d of groundwater from 1 well for public supply usage. All other aquifers withdrew 0.01 Mgal/d of groundwater from 4 wells for public supply use. Cumulatively, there were a total of 62 wells (41 public supply and 21 industrial) which withdrew 10.55 Mgal/d (5.07 public supply and 5.48 industrial) of groundwater from 4 sources (Sparta-Memphis Aquifer, Cockfield Formation, Quaternary alluvial aquifers, and other aquifers), the Sparta-Memphis Aquifer being the dominant source (Arkansas Natural Resource Commission, 2016).

Prior to 2004, Union County's only source of groundwater for industrial and municipal use was the Sparta Aquifer. In efforts to prevent additional water level reduction in the Sparta, Union County initiated groundwater reuse and began using alternative water sources, such as surface water, to supply the three largest industry users. In 2004, a pipeline and pumping station were created, which pulled 4.8 Mgal/d of surface water from the Ouachita River to supply the 3 largest industrial users, who previously relied exclusively on the Sparta Aquifer for water. These industrial users include Lanxess (formerly named Great Lakes and Chemtura), El Dorado Chemical Company, and Lion Oil. The conversion of these three industrial users to Ouachita River surface water, in combination with groundwater conservation efforts, reduced Union County's groundwater withdrawal by roughly 7.5 Mgal/d in 2005 (USGS, 2008). From 2005 to 2011, groundwater levels have risen on average 5 ft or more annually in central Union County as a result of the groundwater to Ouachita River surface water conversion (Figure 2-49) (Schrader, 2014).

## **2.6.7 Injection Depth Waiver**

The targeted injection zones for the Lapis – Project Blue site, are deeper than the base of the lowermost USDW by more than 2,000 ft. Therefore, this section is not applicable.

## 2.7 GEOCHEMISTRY

The proposed data collection program (submitted in “**Module D – Pre-Operational Testing**”) has been designed and implemented to determine the mineralogy of the Injection, Containment and Confining Zones, as well as characterize the interstitial fluids in each one of these zones.

Below the base of the lowermost USDW and throughout the entire interval of interest, all rock formations contain saline brines. Open hole log analysis techniques, such as wireline spontaneous potential and resistivity logging measurements and interpretation, can be used to define the vertical distribution of salt concentrations. For more accuracy, fluid samples will be collected in-situ and brought to the surface to be analyzed in the lab (as outlined in Module D). These different sources of data will be integrated and compared to existing data available in the region through literature papers and agency databases.

To the south and southwest of the Project Blue site, lithium and bromine are produced in commercial volumes. The production of these commodities is not expected to be impacted by the injection wells and is addressed in further detail in Section 2.8 - Economic Geology.

The formation brine composition used in this permit application came from both publicly available data from wells drilled in the area and private driller files/reports from local wells. The public data samples, used as proxies for site specific data, from the USGS Produced Water Database, were taken when the wells were initially drilled.

Much of the sample data is decades old and the procedures may not have been the same for each of the tests. Exact methodologies are not comprehensively detailed, but we have performed quality assurance on the data that we have. The sampling and testing of the wells, core, and brine were not done as a part of a group research program and occurred at different times over several decades and were performed by different companies, and sometimes tested different parameters.

As such, having the wide range of variation in the data was useful in establishing confidence in the data. Generally, the data suggests trends in behavior that would be expected of each of the individual parameters. However, any egregious outliers were removed, and we worked in medians

and averages to limit miscalculations due to poor quality data, if needed. Overall, the data used for this permit application is reliable and prolific.

Analysis was performed on each zone separately and combined as appropriate for analysis. The parameters that rely on depth (*i.e.* gradients) were analyzed as a combined set and the formation brine properties were grouped by each confining/injection zone or interval, as appropriate.

Data from 139 wells was used for the geochemical section of this permit application. There was slight variation in sample types, ranges, dates, and locations, but the major chemical components were represented across the data set and the wells were mostly all from Union and Columbia Counties in southern Arkansas. Occasionally, samples from adjacent counties were included, when appropriate. Determination and correlation of formation and testing parameter nomenclature was done. Extreme outliers were removed from the data set and the sample data was correlated to well logs and literature, when available. All samples and analysis were grouped by known meaningful correlations, specific to the respective confining/injection zone, interval, or formation.

### **2.7.1 Formation Brine Properties**

No wells have been drilled specifically for this permit, however logs, water data, and core records and analyses were obtained from an onsite well, from other wells associated with the facility and from regional offset wells to use as analogues in lieu of site-specific data at this initial stage. The subsurface data is supported by peer reviewed studies in the literature and is used to make an evaluation of the expected properties of the native formation fluid. Because Union County has been drilled for hydrocarbons since 1937 and has been researched extensively over the last decade, it is well represented in the literature, in academic theses, and in industry studies. The sample data used in this permit application was obtained from multiple sources, including the USGS, which provided fluid sample records. The core measurements and core data that are used as analogues in this permit application, to help make evaluations for the expected properties of the solid-phase geochemistry, came from both the literature and from facility records.

Because the sampling and testing of the wells, core, and brine used to characterize the geochemistry for Project Blue were not done as a part of a group research program and came from

multiple sources, there are some limitations and uncertainties regarding the quality of the pre-existing data. Sampling occurred at different times over a period of several decades and was performed by different companies. Sometimes different parameters were tested. Testing procedures were not all well documented and may not have been exactly the same for each of the tests. However, quality assurance was performed on the pre-existing data.

Formation fluid samples will be collected from the Project Blue Injection Wells from the targeted Injection Zones as presented in the “*Pre-Operational Testing and Logging Plan*” submitted in **Module D**.

#### **2.7.1.1 Temperature**

The borehole radius and fluid invasion (mud filtrate) both influence the temperature measured at the borehole and attenuates over time (Poulsen et al., 2012). These temperatures are affected by the time duration from the end of circulation and the time the logging tool takes to reach the bottom of the well. Because the mud column has not had sufficient time to reach temperature equilibrium (Harrison et al., 1983) in situ bottom hole temperature measurements recorded at the time of drilling represent cooler than actual formation temperatures. The Harrison Correction Equation can be applied to bottomhole temperature (BHT) values to account for the deviation between formation temperatures and driller BHT measurements (Harrison et al., 1983).

The highest formation temperature encountered when drilling the onsite Schuler Drilling Company EDC No. 1 well was 159° F, as recorded on the well header of the drilling well log. For this permit, bottom hole temperatures from the well log recorded temperatures of 139 offset wells are fitted to a linear depth trend. The origin point at depth is zero represents the mean annual surface temperature in El Dorado, Arkansas of 64.2° F. This trend line indicates an uncorrected temperature gradient of 1.52° F/100 ft beneath the proposed injection site.

The Arkansas Geological Survey produced a publication on the thermal properties of the Smackover in 2013, in which they applied the Harrison Correction Equation to BHT from wells in Columbia and Union counties in southern Arkansas. This published data accounts for wells with similar depths and wells with greater depths than the wells included in our original gradient

calculation. Integrating this published corrected temperature data with our gradient shifts the geothermal gradient to 1.76° F/100 ft (3.29° C/100 m) for the region (Nordorf, 2013).

Using the calculated geothermal gradient of 1.76° F/100 ft, the estimated subsurface temperature for each zone can be calculated as follows (Table 2-10) and is presented in Figure 2-50.

### **2.7.1.2 *Salinity***

The USGS produced water database has reported measured values of TDS, of the formations in the proposed Injection Zones, the Lower Hosston and the Cotton Valley. The values are summarized in Table 2-10.

Compared to seawater, the Lower Hosston and Cotton Valley formation fluids have higher concentrations of dissolved solids and have higher salinities, which both increase with depth. The highest of the dissolved solids are Chlorides, Sodium, Calcium, and Magnesium. A baseline of seawater TDS is 36,000 (TDS mg/L). It increases to 166,000 (TDS mg/L) in the Lower Hosston and to 189,000 (TDS mg/L) in the Cotton Valley.

### **2.7.1.3 *Viscosity***

Viscosity is the tendency of a fluid to resist flow. These initial viscosity values are based upon no site-specific data and assumptions made for the site-specific salinity and temperature. The approximate formation brine viscosity at reservoir conditions is determined using a Microsoft EXCEL spreadsheet correlation as a function of pressure, temperature, and NaCl content developed by Douglas M Boone in 1993. Each of the Injection Zones produce waters with higher-than-average chloride values. To determine NaCl we used the following equation:

$$\text{NaCl (mg/L)(ppm)} = \text{Cl (chloride)} \times 1.65 \text{ Na (sodium)}$$

To calculate NaCl from measured chloride values, then plotted the calculated NaCl values on the nomograph correlation chart (Figure 2-51). Using this methodology at the assumed formation conditions, the injection interval viscosities expected are presented in Table 2-10.

Generally, viscosity decreases as a function of increasing depth due to increasing temperatures. In zones with brines that have very high concentrations of TDS, the effect of temperature on

viscosity decreases. USGS data and site-specific data were used for the viscosity calculations in this permit application. Because the calculation of viscosity is performed with a conversion calculator, it may introduce some uncertainty. However, the graphical and tabular analysis of the data confirm that salinity values increase with depth, as expected. As part of the drilling program, the formation fluids for the injector well will be evaluated at the time of drilling. The site-specific data on the formation fluid will be used to refine the static and dynamic simulation model, as well as refine the geochemical modeling.

## **2.7.2 Compatibility of the CO<sub>2</sub> with Subsurface Fluids and Minerals**

Interactions between carbon dioxide and the formation brine and matrix materials in the subsurface can be categorized as those that occur during the period of injection or immediately following injection, and those that occur over the long term of carbon dioxide storage. While interactions occurring during injection and in the early phase of carbon dioxide sequestration can be directly studied and evaluated, the longer-term interactions over tens to hundreds of years can only be evaluated through modeling and other forms of prediction. In general, geologic materials are not overly reactive, or very slowly reactive, with acids such as carbonic acid. Carbonic acid (H<sub>2</sub>CO<sub>3</sub>) is a weak acid that dissociates into a proton (H<sup>+</sup> cation) and a bicarbonate ion (HCO<sub>3</sub><sup>-</sup> anion).

Because the permeability of the confining and containment zones (shales) is expected to be several orders of magnitude lower than the permeability of the injection zones (sands), in a practical sense, the carbon dioxide sequestered in the Injection Zones has a much higher potential to contact and react with the rocks and fluids in these intervals. Additionally, because of the low permeability of the aquiclude shales, only reactions near or at the shale/sand interface are likely to occur. Injection operations elevate pressure within the injection interval both during injection and for a period of time afterwards (during pressure recovery). This elevated pressure provides the driving force for vertical permeation of injected fluids and formation brines into the overlying aquitards. Buoyance of the sequestered carbon dioxide also provides an additive driving force. Permeation is the greatest immediately adjacent to the wellbore where the pressure buildup is large and involves primarily the injected fluids. Further from the injection wells, the vertical

permeation drops off significantly and may only affect either the original formation brine or the injected fluids, depending on the location of the carbon dioxide plume.

Occasionally, fluids may move into the base of the overlying aquitard from the injection interval below and compress some of the native brines immediately above it. This compression raises the pressure within the lower portion of the aquitard and expands the pores immediately above the interface. Aquitard materials, such as clay/shales, are known to exhibit significant pore expansion (Neuzil, 1986). The combined effects of native brine compression and aquitard pore expansion provide the necessary space to store the entering fluids. This process does not occur uniformly throughout the thickness of the aquitard. It is rather confined to a narrow region very close to the lower aquitard boundary. Throughout the remainder of the aquitard, there is virtually no indication that any changes have taken place. This narrow region near the base of the aquitard is referred to as the “compression boundary layer”. It contains new fluids that have entered since the beginning of the injection, as well as original formation brines that have been pushed upward into the expanded pores and compressed by the entering fluids. The vast majority of the fluids within this layer are typically the original formation brines.

With continued injection, the compression boundary layer increases in thickness and may eventually encompass the entire aquitard thickness. Native fluids originally present at the top of the aquitard may then begin seeping out into the next overlying permeable layer. The time for this to occur is proportional to the square of the aquitard thickness and inversely proportional to the “hydraulic diffusivity” of the aquitard material (Bredehoeft and Pinder, 1970). Because the hydraulic diffusivity of many aquitard materials (such as shales) is very low (Neuzil, 1986; Neuman and Witherspoon, 1969a and 1969b; and Hantush, 1964), the time is in the order of decades (Chen-Charpentier and Herrera, 1982) which is comparable to the operational lifetime of many underground sequestration facilities. Thus, compressive storage effects in the aquitard layers are important when modeling injection-induced permeation into an aquitard during injection and shortly after operation of the waste facility. When injection is discontinued, some of the waste may seep back into the injection interval from the aquitard. This reverse permeation phenomenon always occurs when the pressure in the injection interval decreases.

The vertical permeation distance reaches an absolute maximum either during injection (typically at the end of the injection period) or after an infinite time has passed since injection operations have stopped. The time necessary to attain the maximum distance depends on the compressive storage properties of the aquitard. For aquitards with high compressive storage capabilities, the maximum permeation distance occurs at the end of the injection period. For aquitards with low storage capabilities, the maximum will occur at an infinite time.

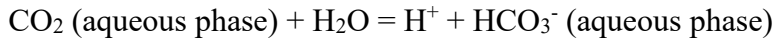
Long after injection operations have stopped, the driving force for vertical permeation usually dissipates, along with the compressive storage of fluids in the aquitard. The pressure-driven rate of fluid movement into the overlying aquitard decreases to zero, leaving only the residual buoyance force. Before the carbonic acid from the sequestered carbon dioxide can react with the clay/shales of the aquitard, it must first migrate from the injection interval strata into the base of the overlying aquitard. During the movement within the injection interval, the acid can be partially or totally neutralized by the carbonates, clays, and other silicates (e.g., feldspars) in the formation. This neutralization halts any further dissolution of carbonate minerals, so that the fraction of dissolved carbonates (relative to pre-injection carbonate mineral amount) is extremely small.

The modeling of strong acids injected into Class I wells presented by DuPont indicates that:

- During injection, injected acids react with at most 2 inches per year of the shale in the overlying arresting aquiclude layer. This rate drops to less than 0.1 inch per year if the waste is injected at least 5 ft below the base of the arresting shale.
- After injection ceases, injected acids react with at most an additional 2 ft of the overlying arresting aquiclude layer for all eternity.
- In the unlikely event that the overlying arresting aquiclude shale layer contains a vertical streak of highly reactive material, such as calcite, the acid could at most migrate 26 inches into this streak: 16 inches during a 60-year period of injection and an additional 10 inches for all eternity post-closure.
- Permeation through the arresting shale due to pressure buildup during injection is more important than shale-acid reactions in determining how far injected fluids can migrate into the overlying arresting aquiclude shale.

Therefore, interactions of the sequestered carbon dioxide and the formation fluids and materials are the most critical within the injection interval.

At the pressure and temperature conditions typical of carbon sequestration projects, carbon dioxide is soluble to a limited degree. The dissolved carbon dioxide transforms the native formation brine into a carbonic acid, such as:



The carbonic acid can react with and dissolve minerals in the matrix, which acts to neutralize the lower pH. The sequestration process includes both short- and long-term geochemical impacts. Short-term CO<sub>2</sub>-water-rock interactions can affect injection over the operational time period (tens of years), such as dry-out and salt precipitation in the near-wellbore area from formation fluid evaporation. In addition, at first contact with CO<sub>2</sub> (*i.e.*, at the front of the CO<sub>2</sub> plume), carbonic acid is formed via CO<sub>2</sub> dissolution in the native formation brine. This triggers dissolution of carbonate minerals. This is not a reason for concern, because in the same process the carbonic acid is quickly neutralized, meaning that a new equilibrium is rapidly established between the elevated CO<sub>2</sub> concentration and the carbonate minerals. The new equilibrium is already established after only a small amount of carbonate dissolution, so that porosity and permeability changes are negligible. Behind the CO<sub>2</sub> plume front (where the formation brine is already neutralized) no further carbonate dissolution takes place. Long-term impacts and reactions can affect permanence of trapping of the carbon dioxide via mineral trapping. The long-term geochemical processes consist of a combination of slow dissolution and precipitation reactions. Significant long-term dissolution without simultaneous co-precipitation is impossible because it would lead to unrealistic supersaturation levels in the formation brine. In most systems, precipitation dominates over dissolution resulting in a gradual decrease of porosity and permeability, and a gradual mineral trapping of CO<sub>2</sub>.

The extent of secondary trapping mechanisms within the injection interval is highly site-specific and depends on the geology, structure, and hydrology of each reservoir. For instance, increasing pore fluid salinity decreases carbon dioxide solubility (Gunter et al., 1993). The purity of the injected carbon dioxide also affects the storage capacity of the reservoir (Talman, 2015). In such

sedimentary settings, the injected carbon dioxide may remain mobile for centuries and trapping relies primarily on the impermeability of the overlying caprock and sealing faults. Large and extensive saline aquifers are essentially hydrodynamic traps, where the injected carbon dioxide is expected to move rapidly through the pore space, interacting with a larger volume of the reservoir. This interaction increases the extent of all secondary mechanisms (National Academies of Sciences Engineering Medicine, 2019).

The carbonic acid can readily react with calcium carbonate and hydroxide minerals, which also reduces the acidity of the formation brine. In addition to the precipitation of carbonates, a host of other fluid-rock reactions can take place within the injection zone. Silicate minerals in arkoses and shales display textures in experiments indicating that these minerals are reacting with carbonic acid (Kaszuba et al., 2002). Acid reacts with feldspars in a manner similar to its reaction with clays. However, the overall rate is slower with feldspars than with clays because in typical rock matrix, the feldspar is present as large particles, so the surface area available for feldspar to react is much smaller than for clay particles.

With silica, the silica can be solubilized by an acid as follows:



The rate of dissolution of silica is generally quite slow but becomes faster as the hydroxyl concentration increases. Note also that the rate is 10,000 times faster at a pH of 8.5 than at a pH of 3 (Iler, 1979).

Mineral compatibility, from CO<sub>2</sub>-brine-rock interaction experiments conducted in support of basin characterization projects under the Department of Energy, suggests that feldspars (plagioclase and albite-K-spar system) are destabilized by the drop in pH associated with carbon dioxide dissolution in the formation brine water, favoring the formation of minerals such as kaolinite, muscovite, and paragonite (LBNL, 2014).

The principal effect of acid on clays is to leach metal ions from the clay lattice sites, leaving behind a silica framework. In experiments which monitored the x-ray diffraction pattern of the clays as the metal ions were leached out by acid, the pattern remained very similar to the original

clay x-ray pattern even when 50% of the aluminum had been extracted from the mineral (Matthews et al., 1955). There are two types of sites in clays where metal ions can be located. The largest fraction of metal ions is located within the octahedral sites of the clay structure. These are part of the alumina sheet in the mineral structure and are coordinated to six oxygens. A smaller fraction of the metal ions occupies the tetrahedral sites. These are part of the silica sheet and are coordinated to four oxygens. Octahedrally coordinated aluminum is leached out at a faster rate than tetrahedrally coordinated aluminum (Turner, 1964).

At the Frio Brine Pilot Test (in the Texas Gulf Coast Region), following carbon dioxide breakthrough, samples from the monitoring well showed sharp drops in pH, pronounced increases in alkalinity and iron content, and significant shifts in the isotopic compositions of formation waters, dissolved inorganic carbon, and methane (Kharaka et al., 2006). Geochemical modeling of the Frio Brine Pilot indicates that brine pH would have dropped lower but was buffered by dissolution of carbonate and iron oxyhydroxides (Kharaka et al., 2006). The dissolution of minerals, especially iron oxyhydroxides and leaching of clays could mobilize metals and organic compounds in formations containing residual hydrocarbons or other organics (Kharaka et al., 2006).

The experimental and modeling analyses suggest that mineral precipitation and dissolution reactions (within the target formation) are not expected to lead to significant changes to the underground hydrologic system over time frames (approximately 30 years) typically relevant for injection operations.

### **2.7.3 Site Specific Geochemical Modeling**

Further evaluation of the geochemical database, especially related to redox reactions and H<sub>2</sub>S, is required to reduce model prediction uncertainties. A site-specific follow-up study using composition from of the source, along with the formation data (mineralogical and formation fluid compositions) will be performed after the drilling, testing, and completion of the Project Blue Injection Wells. Such follow-up work should include a 1D and/or 2D modelling study to assess the reactive transport effects of CO<sub>2</sub>, the uncertainty quantifications (impact of physiochemical model input parameter uncertainties like mineral dissolution/precipitation kinetic rates), and the

impact of contaminants in the reaction stream. The future geochemical modeling will also evaluate potential clogging of the near-well area, hence injectivity loss, due to water evaporation (dry-out) in the injected CO<sub>2</sub> and salt precipitation. Salt accumulation can be enhanced because of capillary backflow of brine from the aquifer to the dry-out area.

The sampling program for the injection wells has been designed to include fundamental testing to evaluate key geochemical parameters. Secondary trapping mechanisms include solubility trapping by dissolution of the injected carbon dioxide into the in-situ formation brine, residual gas trapping by capillary forces, and mineralization by chemical interactions between the injected carbon dioxide, formation fluids, and the rock matrix.

The sampling program, which will be implemented during well construction, has been designed to include the sampling of relevant formation fluids and formation materials so that tests on both the Injection Zone and caprock can be made (see Data Acquisition Plan in Module D – Pre-Operational Testing). The interactions between carbon dioxide, formation brines, and formation minerals will be analyzed using geochemical and reactive transport models to evaluate changes in formation water chemistry, mineral precipitation and dissolution reactions, and any potential resulting effects on formation porosity and/or permeability.

## 2.8 ECONOMIC GEOLOGY OF THE AREA

When oil was first produced from the Smackover Formation in southern Arkansas, formation brine was not economical and considered a waste byproduct associated with oil production. During the 1950's, elevated concentrations of bromine and lithium were measured in the Smackover brine and commercial extraction of the bromine and lithium became an economic staple of Arkansas. Note: that all sequestration operations will be isolated from the deeper production of the Smackover Formation.

### 2.8.1 Lithium

Lithium, a light, metallic mineral, is a critical mineral, which is defined by the Energy Act of 2020 and the USGS as a “non-fuel mineral or mineral material essential to the economic or national security of the USA and which has a supply chain vulnerable to disruption” and is

characterized as “serving an essential function in the manufacturing of a product, the absence of which would have significant consequences for the economy or national security” (Burton, 2022). The Arkansas Geological Survey identifies eighteen critical minerals in Arkansas, including lithium. Figure 2-52 shows the significance of lithium in Union County, Arkansas.

Lithium is a critical element because of its importance in green technology and its many uses in decreasing percentage of world consumption. These uses include ceramics and glass, rechargeable batteries, lubricating greases, continuous casting mold flux powders, air treatment, polymer production, primary batteries, primary aluminum production, and other uses (Merriman, 2014; Schulz et al., 2017).

Figure 2-53 portrays a projection of the worldwide lithium demand from 2019 to 2030. In 2019, the demand for lithium carbonate equivalent was 263,000 metric tons and is expected to grow to 2,114,000 metric tons in 2030. This increase demand in lithium within the next decade is due to the battery demand for electric vehicles (Garside, 2022).

In Arkansas, lithium is found in the minerals cookeite, taeniolite, and lithophorite, which are associated with the hydrothermal quartz veins and alkaline igneous rocks of the Ouachita Mountains and the Magnet Cove Igneous Complex, and in formation brines produced from the Smackover Formation in Union, Columbia, Miller, Lafayette, and Ouachita Counties. The USGS estimates that there are 500 million tons of lithium in the brines of south Arkansas and that the concentration of lithium in Smackover brine can reach 445 parts per million (AGS, 2022a).

The Arkansas Geological Survey indicates that most lithium production occurs from two companies. One company has a brine production rate of 20 tons of lithium carbonate per year and another company is in the process of building a pilot plant to test their extraction techniques (AGS, 2022a).

The Lanxess Smackover Project by Standard Lithium Ltd. is one of the lithium carbonate production companies in southern Arkansas and estimates a final lithium carbonate production of 20,900 tonnes per year at the completion of the project (Worley and Standard Lithium LTD, 2019). The Lanxess property, located in Union County, Arkansas, is the closest brine production facility to the Project Blue site. Figure 2-54 shows the location of the Lanxess property relative

to the Lapis Energy – Project Blue site, and the concentration of lithium in brine producing wells. Higher lithium concentrations primarily occur in Columbia County and within the Lanxess property in Union County. Bromine

Bromine is classified as an industrial mineral, which is defined by the Arkansas Geological Survey as " a non-metallic rock, mineral, or sediment of economic value – exclusive of metal ores, fossil fuels, and gemstones" and can "include many common materials, such as rock (limestone, dolostone, and sandstone), gravel, sand, several varieties of clay, and uncommon materials, such as bromine brine, diamond, gypsum, novaculite, syenite, and tripoli". These are materials that can sometimes be salvaged and reused for other purposes but cannot be recycled profitably and continuously need new sources.

Bromine is a corrosive halogen and compounds can be found in lakes, ocean water, and formation brines. One of the world's most enriched sources of bromine is from the formation brines produced from the Smackover Formation in southern Arkansas. At 4,000 to 4,600 ppm, bromine concentrations in the Smackover are up to 70 times greater than ocean water (AGS, 2022b). The two active bromine producers in southern Arkansas are Albemarle Corporation and Lanxess (formerly named Great Lakes and Chemtura). Albemarle operates production and extraction plants in Columbia County, Arkansas and Lanxess operates extraction and production facilities in Union County, Arkansas (AGS, 2022b). Figure 2-55, created by the Arkansas Geological Society and the USGS, shows the locations of industrial minerals throughout Arkansas.

In 2022 Arkansas was the leading producer of bromine in the world, followed by China, Israel, and Jordan. In 2013, 28% of the global bromine production (225,000 tonnes) was from Arkansas making the USA the second largest bromine producer in the world (AGS, 2022b). Based on USA's price of bromine in 2013 (\$3.50 to \$3.90 per kg), this would have roughly been worth \$800 million in bromine production from Arkansas (AGS, 2022b).

## 2.8.2 Proximity to the Lapis Energy – Project Blue Site

The Lanxess property is in closest proximity to the Lapis Energy – Project Blue site, at 2.6 miles southwest of the Lapis study area (Figure 2-54). All of Lanxess' wells and pipelines are contained within the Lanxess property boundary, which is outlined in red. Like hydrocarbon migration, CO<sub>2</sub>

plumes will move updip over time due to buoyancy (Jordan and Doughty, 2009; Fawad and Mondol, 2021). The CO<sub>2</sub> plume pathway model for Project Blue indicates that the plume will migrate updip toward the north-northeast. The sequestration operations at the Project Blue site are modeled into the Cotton Valley and Lower Hosston Formations, which are not expected to interfere with nearby bromine or lithium operations.

### 2.8.3 Oil Fields

Hydrocarbon production in southern Arkansas is most prolific in Union, Lafayette, Columbia, and Miller Counties. Hydrocarbons were generated in the Dense Brown Member of the Lower Smackover Formation and migrated into overlying Jurassic and Cretaceous formations. The oil fields in closest proximity to the Project Blue site are the Lisbon and Agnes Road Field, approximately 1.3 miles southwest, and the El Dorado East Field, approximately 4 miles southeast with production from the Nacatoch, Graves, Tokio, Blossom, Hosston, and the Cotton Valley Formations. Modeling for this project indicates the CO<sub>2</sub> plume migration will be toward the north-northwest, which is away from the El Dorado East Field. For these reasons, Class VI well injection into the Cotton Valley and Lower Hosston Formations, is not expected to interfere with active oil field production in the region.

## 2.9 SITE SUITABILITY SUMMARY

The Lapis El Dorado project site is suitable for injection of CO<sub>2</sub> as per 40 CFR 146.83 standards for the Confining and Injection Zones. The key factors driving site suitability are summarized below:

- In general, and compared to other portions of the county, a minimum of artificial penetrations (legacy wells) penetrates the Lower Cretaceous Sequence Boundary (LSCB) Confining Zone in the delineated AoR, thus reducing associated CO<sub>2</sub> leakage risk.
- Storage reservoir depths are at approximately 4,000-6,000 ft TVDSS, which is favourable for supercritical CO<sub>2</sub> injection and increases site efficiency (injecting denser supercritical CO<sub>2</sub> means more can be stored in equivalent pore space).
- The Project Site is located within a structurally quiescent area and no faulting is observed within the delineated AoR.

- Structural dips are approximately 1 to 1.5 degrees, which is low and generally favorable for migration assisted CCS in a saline aquifer.
- There are two stacked injection zones in the storage complex, the Lower Hosston and the Cotton Valley Formation, thus improving site capacity.

The Lower Hosston and Cotton Valley Injection Zones are siliciclastic dominated packages. The heterogeneity and distribution of the sand and shale facies, as well as correlative internal shales and potential barriers, provide substantial local immobilization and containment of the proposed volumes of CO<sub>2</sub> to be injected. Along with the local trapping and immobilization of CO<sub>2</sub> by small and larger scale structural heterogeneity, substantial volumes of CO<sub>2</sub> can be trapped in the pore spaces by capillary forces and dissolution in the *in-situ* brine.

The low structural dips at the site result in lower rates of lateral migration. Any mobile CO<sub>2</sub> that moves to the top of the injection zone and along the base of the confining zone will travel more slowly, and thus allow for more time to be dissolved in the brine, trapped in the capillary pore spaces, or mineralized and thus reduce containment risk.

The mineralogy of the storage complex (geologic matrix) and formation water is not expected to be reactive with the injected CO<sub>2</sub> stream, which will be confirmed with data collected at the site during site appraisal. Injection and monitoring well materials, that will be subject to the injected CO<sub>2</sub> stream, have been chosen for their corrosion resistance. The chosen well designs thus further reduce the containment risk.

The Injection Wells have been sited at a general location just south of the main EDCC facility on LSB property, to account for the plume movement updip and to make optimal use of the pore space available on LSB's property. The rates of injection of CO<sub>2</sub> have been optimized to reduce the risk of a potential loss of containment of the mobile CO<sub>2</sub>, as well as loss of containment of the *in-situ* injection zone formation fluids, by avoiding pressure build-up above defined threshold values.

Project Blue has been designed to utilize one Injection Interval at any given time. 4 injection intervals have been identified, 3 in the Cotton Valley Injection Zone and 1 in the Hosston Injection Zone. The aim is to inject 5 years in each interval to control the size and drift of the plume.

Modeling in the “Area of Review and Corrective Action Plan” submitted in Module B, has been designed using conservative assumptions (when data is unknown). The geology underneath the EDCC facility site will be able to accommodate all or most of the CO<sub>2</sub> injected during the 20-year project life of Project Blue.

### **3.0 AOR AND CORRECTIVE ACTION PLAN**

Lapis has uploaded the “*AOR and Corrective Action Plan*” technical report [40 CFR 146.82(a) and 146.84(b)] via the EPA GSDT portal.

The report contains the details of the computational modeling [40 CFR 146.84(c)], which includes pressure and plume maps at 5-year intervals for the simulated 20-year operation period. The data used in the model is derived from regional data and from wells proximal to the project site. Until information is obtained from the site specific well, this data is used as a basis for predicting the critical pressure and plume extent.

The Lapis-Project Blue site has been simulated using two injection zones (with subzones), with each zone modeled for 5-year periods independently, and not concurrently. The order of modeled injection operations is as follows (in ascending order):

- 1) Cotton Valley Injection Zone – Injection Interval 1–(CV1) - Modeled from 2025 to 2030
- 2) Cotton Valley Injection Zone – Injection Interval 2–(CV2) - Modeled from 2030 to 2035
- 3) Cotton Valley Injection Zone – Injection Interval 3–(CV3) - Modeled from 2035 to 2040
- 4) Lower Hosston Injection Zone - Modeled from 2040 to 2045

Total time of simulation modeled for the project is 20-years (5-years per zone). AoR delineation has been determined for the site using geological characterization data and computational modeling data showing the projected lateral and vertical migration of the CO<sub>2</sub> plumes (for each interval).

The technical report also includes a tabulation of all wells within the delineated AoR [per 40 CFR 146.82(a)(4)]. A total of 45 wells are contained within the AoR, however, only 12 wells extend deep enough to penetrate the Injection Zones. A thorough evaluation of each of these wells, using well records, scout tickets, and logs was performed. Other than Artificial Penetration No. 1 (Shuler Drilling Inc., EDC No. 1 well), no improperly constructed or improperly plugged wells fail the conservative modeling screening evaluation. Therefore, the corrective action program is limited to just Artificial Penetration No. 1 (Shuler Drilling Inc., EDC No. 1 well), as all other

artificial penetrations are either properly constructed, plugged and abandoned (e.g., for CO<sub>2</sub> and brine vertical movement), or have sufficient resistant borehole material as to prevent the movement of brine into or between USDWs. Artificial Penetration No. 1 (Shuler Drilling Inc., EDC No. 1 well) will be replugged prior to initiation of carbon dioxide injection.

A reevaluation schedule for AoR delineation is set at 5-year intervals during injection operations. This plan will be updated as the project is developed to be consistent with the data derived from the injection wells, as well as collected through the operation and testing of the wells over the life of the project.

The technical report, tabulation of wells within the delineated AoR, and computation modeling

#### **AoR and Corrective Action GSDT Submissions**

**GSDT Module:** AoR and Corrective Action

**Tab(s):** All applicable tabs

Please use the checkbox(es) to verify the following information was submitted to the GSDT:

- Tabulation of all wells within AoR that penetrate confining zone **[40 CFR 146.82(a)(4)]**
- AoR and Corrective Action Plan **[40 CFR 146.82(a)(13) and 146.84(b)]**
- Computational modeling details **[40 CFR 146.84(c)]**

details have been uploaded in **Module B** – AoR and Corrective Action identified below.

## **4.0 FINANCIAL RESPONSIBILITY**

Lapis has submitted a Financial Responsibility Demonstration (FRD) in accordance with 40 CFR 146.82(a) and 146.85. The submittal covers activities identified in the corrective action plan, injection plugging plan, post-injection site care and closure, and the emergency and remedial response plan. Additionally, it covers the monitoring and reporting activities during injection and closure operations.

Cost estimates for the activities were provided by independent third-party contractors and /or by knowledge of industry standards and practices per 40 CFR 146.85(c). The cost estimates include project management, administrative costs, overhead, and contingency and are presented in Table 4-1.

Cost estimates with supporting documentation have been uploaded on the “Cost Estimates” Tab in Module C of the GS DT portal for this initial submittal of a permit application. Actual values may change due to inflation of costs or additional changes to the final project. If the cost estimate changes, Lapis will adjust the value of the FRD, and it will be submitted to the authorized regulatory body for review and approval on an “as needed” basis. Detailed information and supporting documents have been submitted through the GS DT through “***Module C – Financial Responsibility Demonstration.***”

### **Financial Responsibility GS DT Submissions**

**GS DT Module:** Financial Responsibility Demonstration

**Tab(s):** Cost Estimate tab and all applicable financial instrument tabs

Please use the checkbox(es) to verify the following information was submitted to the GS DT:

Demonstration of financial responsibility ***[40 CFR 146.82(a)(14) and 146.85]***

## **5.0 INJECTION WELL CONSTRUCTION**

On behalf of LSB Industries, Lapis Energy is requesting a permit for two Class VI carbon dioxide (CO<sub>2</sub>) sequestration wells.

The first Injection Well (Project Blue Class VI Injection Well No. 1) will be completed in the Cotton Valley Formation Injection Zone. The second Injection Well (Project Blue Class VI Injection Well No. 2) will be completed into the Lower Hosston Injection Zone. The wells will be constructed in accordance with 40 CFR 146.86(b) standards for Class VI Injection Wells. Note: unless specified, all depths in this section are relative to the ground level.

The following sections address the procedures to drill, sample, complete, operate, and test the proposed wells, as well as specifications of the construction materials. Additionally, procedures for plugging and abandoning the wells are also provided. Specification of maximum instantaneous rate of injection; average rate of injection; and the total monthly and annual volumes requested are also included. All construction data meets the requirements for a Class VI well under 40 CFR 146.82(a)(9), (11), and (12).

All phases of well construction will be supervised by qualified individuals acting under the responsible charge of a licensed professional engineer who is knowledgeable and experienced in practical drilling engineering and who is familiar with the special conditions and requirements of Class VI CO<sub>2</sub> injection well construction.

### **5.1 PROPOSED STIMULATION PROGRAM**

A detailed stimulation plan will be developed for the Project Blue site, which will be initially employed after the drilling and completion of the Injection Wells. The stimulation program will consist of an acidization and wellbore flowback (utilizing coiled tubing) to remove formation skin damage due to invasion of solids during drilling and any perforation damage. The acid treatment will most likely consist of the following acids, with acid treatment chemicals and actual volumes to be determined based on core analysis, evaluation of open hole logs, and footage of interval to be treated at the time of placement:

- 15% Hydrochloric Acid (HCl)
- 7.5% HCl + 1.5% Hydrofluoric (HF) Acid

Best practices for recommended volumes for acid stimulations generally range from 25 to 100 gallons per foot of completion, depending on the severity of the suspected near wellbore formation damage. Chemicals will be added to the acid blends to limit clay swelling, reduce emulsions, and inhibit reaction to the completion equipment. The type and quantity of these chemicals will be determined based on formation characteristics determined from core and wireline log evaluation. For all stimulation fluids that could be used it will be verified that there is no adverse reaction with confinement of the reservoir [per 40 CFR 146.82 (A)(9)]. Additional acids and the use of diverter fluids may be considered at the time of placement. The acid fluids will be displaced from the wellbore using non-hazardous treating water or brine.

Additional stimulation treatment may be necessary if the injection performance of the well remains unacceptable following treatment. Procedures will be submitted for approval by the UIC Program Director prior to any additional stimulation work.

## 5.2 CONSTRUCTION DESIGN

The proposed completion schematics for Project Blue Injection Wells are included as Figure 5-1 (Project Blue Class VI Injection Well No. 1) and Figure 5-2 (Project Blue Class VI Injection Well No. 2). The Injection Wells will be planned and constructed to the same specifications down to setting of the Intermediate Casing at +/-3,010 ft, with appropriate correlative depth shifts depending on geographic placement. The deeper portions of the Injection Wells will be specific to each well, as detailed below. The schematics include well casing specifications and setting depths, cementing data, and completion details. Note that the continuous recording equipment and automatic shutoff devices will be illustrated on a future schematic once the surface facilities and pipeline design have been completed. The proposed Wellhead Schematics for the wells are included as Figure 5-3.

### 5.2.1 Casing String Details

Casing specifications for the proposed Injection Wells are detailed in Tables 5-1. Stress

calculations for all well casings are included in Appendix C. All components of the surface and protection casings will be manufactured to API standards and are designed for the proposed life of the well, based on the materials of construction and the environment of use. The casing strings will consist of both carbon steel (non-CO<sub>2</sub> contact) and 25Cr-80 (for CO<sub>2</sub> contact usage) to ensure the longevity of the wellbore: A mixed string of carbon steel above approximately 3,450 ft and 25Cr-80 below approximately 3,450 ft will be used for the protection casing. Additionally, all casing strings will be fully cemented to surface, which will provide additional isolation of the casing string from external formation fluids along the borehole path.

Prior to running the casing in the hole, each string will be visually inspected and drifted to ensure that no defects are present. The connections will be cleaned, and the manufacturer's recommended thread compound will be applied to the pin of each connection before make-up.

### **5.2.2 Centralizers**

Each casing string will have bow type centralizer attached to the casing at intervals along the entire well path. The centralizers will be placed to maximize the casing standoff from the well bore to enhance the cementing of the wells. The centralizers will be placed as follows:

- 1 Centralizer 8 ft above the float shoe, straddling a stop collar;
- 1 Centralizer 8 ft above the float collar, straddling a stop collar;
- 1 Centralizer every other joint, to surface on the surface casing.
- 1 Centralizer every other joint to the stage collar at approximately 3,450 ft on the protection casing;
- 1 centralizer above and below any stage collar, straddling a stop collar;
- 1 Centralizer every third joint, up to the surface on the protection casing; and
- 1 Centralizer approximately 10 ft below ground level.

Actual placement of centralizers will be determined once the drilling of each well section is completed, and logs have been reviewed. Additional centralizers may be used as needed to provide the highest quality cementing job as possible.

### **5.2.3 Annular Fluid**

The annular fluid designed for the well is 9.0 lb/gal (1.08 Sp. Gr.) sodium chloride brine with corrosion inhibitor and oxygen scavenger. An annulus monitoring and pressurization system will maintain the annulus at least 100 psi pressure greater than the injection tubing pressure at all times.

### **5.2.4 Cementing Details**

The cement program has been designed using cement types and additives which will be compatible with the CO<sub>2</sub> stream and formation fluids over the lifetime of the project [per 40 CFR 146.86 (b)(5)]. The Injection Wells will use both standard cement and a CO<sub>2</sub> resistant cement to ensure the longevity of the wellbore. All casing strings will be cemented to surface, which will provide additional isolation of the casing string from external formation fluids along the borehole path. A two-stage cement job is planned for the surface casing in the well, with a 9-5/8-inch DV tool installed at approximately 1,900 ft. A two-stage cement job is planned for the protection casing string with 7-inch carbon steel cementing stage tool installed at approximately 2,965 ft. Expected downhole temperature at total depth is 175° F at 6,350 ft, which is not considered detrimental to the cement. The cement will increase in hardness over time and reach a value close to its maximum compressive strength soon after setting.

### **5.2.5 Tubing and Packer Details**

Tubing specifications for the proposed Injection Wells are detailed in Table 5-2. Tubular stress calculations for all well casing and tubing are included in Appendix C. The wells will be completed with L-80 or better injection tubing to provide resistance to corrosion from dry CO<sub>2</sub> injection. The tubing will extend from the surface to the injection packer, with a slip-and-seal assembly installed to provide engagement with the surface wellhead.

The proposed injection packer will be set in the protection casing in each well above the top-most perforation in the well. For Project Blue Class VI Injection Well No. 1, the initial completion in the Cotton Valley Injection Zone 1 is at a depth of approximately 5,920 ft. The proposed packer will be constructed with 25CR steel or better for all the parts that will be in contact with the

injection stream (“wetted parts”). The packer assembly will include a Polished Bore Receptacle (PBR) of sufficient length to account for potential tubing movement during well operation.

Prior to running the tubing in the hole, each string will be visually inspected and drifted to ensure that no defects are present. The connections will be cleaned, and the manufacturer’s recommended thread compound will be applied to the pin of each connection before make-up. Each connection of the injection tubing will be externally pressure tested to ensure no leaks exist upon makeup.

The injection packer will also be visually inspected to ensure no defects are present. A pressure test of the annulus will be conducted during installation of the packer to confirm proper setting and absence of leaks.

### **5.3 PROPOSED DRILLING PROGRAM – INJECTION WELLS**

Normal plant and area safety rules and regulations will be in force during installation of the wells. Prior to well construction, the ground surface will be graded to level. An all-weather location will be installed, with additional reinforcement placed under the rig substructure area. The rig contractor will provide power for the rig and associated equipment. The construction site will be barricaded to prevent entry by unauthorized personnel. Normal handling of the wellbore solids and fluids is anticipated during the drilling phases of the work and completion phases of the work.

All phases of well construction will be supervised by qualified individuals acting under the responsible charge of a licensed professional engineer who is knowledgeable and experienced in practical drilling engineering and who is familiar with the special conditions and requirements of Class VI CO<sub>2</sub> injection well construction.

### 5.3.1 Injection Well Drilling Procedures – Project Blue Class VI Injection Well No. 1 (INJ-1)

#### 5.3.1.1 Proposed Drilling Procedure – Project Blue Class VI Injection Well No. 1 (INJ-1)

The drilling program for the Project Blue Class VI Injection Well No. 1 (INJ-1) at the EDCC El Dorado Facility contains a conductor hole, water string, surface hole, and protection hole. All depths in the outlined procedure are referenced to the kelly bushing (KB), which is estimated at 20.0 ft above ground level.

##### Conductor Hole

1. Prepare surface location and mobilize drilling rig. Drill mousehole and rathole.
2. Pick up casing hammer and drive 26-inch conductor pipe to approximately 90 ft or until 100 blows per foot penetration rate is reached. (Alternate is to auger the conductor hole *and grout the casing.*)

##### Water String

1. Drill 17-1/2-inch hole to 900 ft (+/-) using drilling fluid as detailed in the Drilling Fluids section of this procedure. Take deviation surveys every 250 ft. Maximum deviation from vertical should be no more than 3 degrees, and maximum deviation between surveys will be targeted at no more than 1 degree.
2. Run open hole electric logs as listed in Module D – Pre-Operational Testing.
3. Run 13-3/8-inch surface casing to 900 ft (+/-). Refer to Section 5.2.1 – Casing String Details for a detailed description of the casing.
4. Cement the casing in place using the stab-in method. Refer to Section 5.3.5 – Proposed Cementing Program.
5. If no cement returns are observed at surface, a temperature or similar diagnostic survey will be run to determine the top of cement. Grout the un-cemented annular space to the surface if necessary.

6. After waiting on cement for a minimum of 12 hours or until compressive strength has reached 500 psi, whichever is longer, cut off water string casing and conductor pipe and install 13-3/8-inch x 3,000 psi SOW casing head and pressure test.
7. Nipple up 13-5/8-inch 3M Blowout Preventers (BOP), choke manifold, and ancillary equipment and pressure test to a low pressure of 250 psig and a maximum pressure of 3,000 psig.
8. Run cased hole logs listed in Module D – Pre-Operational Testing.

### **Surface Hole**

1. Drill 12-1/4-inch surface hole to 3,010 ft (+/-) using drilling fluid as detailed in the Drilling Fluids section of this procedure. Take deviation surveys every 500 ft. Maximum deviation from vertical should be no more than 3 degrees, and maximum deviation between surveys will be targeted at no more than 1 degree.
2. Run open hole electric logs as listed in Module D – Pre-Operational Testing.
3. Run 9-5/8-inch surface casing to 3,010 ft (+/-). Refer to Section 5.2.1 – Casing String Details for a detailed description of the casing.
4. Cement the casing in place using the stab-in method. Refer to Section 5.3.5 – Proposed Cementing Program.
5. If no cement returns are observed at surface, a temperature or similar diagnostic survey will be run to determine the top of cement. Grout the un-cemented annular space to the surface if necessary.
6. After waiting on cement for a minimum of 12 hours or until compressive strength has reached 500 psi, whichever is longer, cut off the water and conductor pipe and install an 11-inch 3,000 psi x 9-5/8-inch SOW casing head and pressure test.
7. Nipple up 11-inch 3M Blowout Preventers (BOP), choke manifold, and ancillary equipment and pressure test to a low pressure of 250 psig and a maximum pressure of 3,000 psig.
8. Run cased hole logs listed in Module D – Pre-Operational Testing.

### **Protection Hole**

1. Pick up a 8-3/4-inch drilling assembly and trip into the wellbore. Pressure test the surface casing to 1,600 psi for 30 minutes.
2. Displace the fresh water from cementing with a water-based drilling fluid to improve hole cleaning and stability. Drill out casing float equipment.
3. Drill an 8-3/4-inch protection hole from surface casing point to 6,475 ft (+/-) into the Cotton Valley Formation. The actual total depth of the well will be contingent on the subsurface depth of the base of the Cotton Valley. Take inclination surveys every 500 ft to monitor well path.
4. Attempt to collect conventional whole cores at selected geologic intervals within the Confining Zone and Lower Hosston and Cotton Valley Injection Zones in the injection well. Refer to Module D – Pre-Operational Testing for details on the coring program.
5. Run electric wireline logs and collect rotary sidewall core samples (if needed) over the open hole interval. Refer to Module D – Pre-Operational Testing for details.
6. Run 7-inch casing (mixed string) to the planned casing point (6,475 ft). Refer to Section 5.2.1 – Casing String Details for a detailed description of the casing.

*Note: Lapis Energy is evaluating “smart well” completion technologies to monitor Differential Temperature, Acoustic, and Bottomhole Pressure. Lapis may elect to add “smart well” monitoring to the completion.*

7. Rig up cementing equipment and cement the protection casing in place. Cement will be placed in two stages with the lower cements being CO<sub>2</sub> resistant cements and the upper cement being a lightweight cement blend. A 7-inch carbon steel cementing stage tool plus an optional 7-inch external casing packer will be installed at approximately 2,965 ft for the two-stage cementing. Refer to Section 5.3.5 – Proposed Cementing Program.

8. In the event cement returns are not observed at the surface, a temperature or similar diagnostic survey will be run to determine the top of cement. After the cement top is located, a procedure to grout in the un-cemented annular space will be provided.
9. After finishing the cementing, land the 7-inch casing by installing the casing hanger in the C-22 bowl of the 11-inch 3M casing head flange. The BOP stack will be picked up and a rough cut will be made on the 7-inch casing above the casing hanger. The 7-inch cut joint will be removed and measured, and the 11-inch BOP stack will nipple down and be removed.
10. Cut and dress the 7-inch casing above the casing hanger for the required length for the secondary seal. Install and nipple up a 7-1/16-inch 5M x 11-inch 3M tubing spool with a secondary seal in the 11-inch bottom flange for the 7-inch casing. Test the seals and confirm the mechanical integrity between the 11-inch flanges, casing hanger primary seal, and casing hanger secondary seal.
11. Install a 7-1/16-inch 5M dry hole tree on the 7-1/16-inch flange on the casing spool to protect the well.
12. Rig down and release the drilling rig and drilling equipment.
13. Clean up the location in preparation for the completion operations.

#### **5.3.1.2 Drilling Contingency Plans**

If unforeseen events occur during drilling operations, detailed plans to remedy the specific problem will be implemented using best engineering practices and judgment based on facts. The following are general contingency plans to address specific problems.

##### **Borehole Drilling Lost Circulation Plan**

If circulation is lost (moderate probability) while drilling either the surface or protection casing borehole, lost circulation material pills will be pumped to re-establish circulation. Depending upon the severity of lost circulation encountered, lost circulation material may need to be blended with the drilling fluid in concentrations dictated by hole conditions to maintain circulation to the surface casing point. Should lost circulation occur while drilling from the base of conductor to

the surface casing point, paper, cottonseed hulls, or other forms of standard lost circulation material may be used to remedy the loss condition. A cement truck may be mobbed to location and placed on “standby” to minimize “wait time” if severe loss of circulation is encountered.

### **Borehole Drilling Overpressured Zone**

If an overpressure zone is encountered (not expected) while drilling the surface or protection hole, the drilling fluid pump rate down the drill pipe will be increased while the drill fluid density is increased. The increased pumping rate will continue until the well stops flowing. If a drilling influx is encountered while drilling any other hole section, the blow out preventer (BOP) will be closed-in, and the well will be secured. The influx will be circulated out of the well while maintaining constant bottom hole pressure using the choke to prevent additional influx. Finally, the mud weight will be increased to a density sufficient to 142verbalancee the well while circulating through the choke to maintain constant bottom hole pressure throughout the circulation. Once kill weight mud has been circulated around and the well is confirmed to not be flowing, drilling will recommence.

### **Borehole Deviation Issues**

Take inclination surveys at a minimum every 500 ft, or as required by state regulations, and at the TD for the hole size to monitor the well path. A target maximum deviation from vertical is 3 degrees and target maximum dogleg severity is 2.5 degrees per 100 ft. If the maximum recommended deviation is exceeded, an evaluation will be made to determine whether remedial action is necessary.

#### **5.3.1.3 Proposed Completion Procedures – Project Blue Class VI Injection Well No. 1 (INJ-1)**

The completion procedure has been developed to utilize the Cotton Valley Injection Zone 1 (lower most Cotton Valley interval) for sequestration of the injected CO<sub>2</sub> as the initial reservoir for sequestration. It is anticipated that the full interval in the Cotton Valley Injection Zone 1 will be utilized and will be perforated based on results from the open hole logging program. The following is a proposed completion procedure for the EDCC facility.

1. Move in workover rig and equipment required for the completion operations.
2. Nipple up 7-1/16-inch 5M BOPs on the well and pressure test the BOPs.
3. Pick up a 6-1/8-inch bit and drilling assembly below the workstring casing scraper for 7-inch and trip into the wellbore.
4. Drill out the cementing stage equipment at  $\pm 2,965$  ft and circulate the well clean. Continue lowering the bit and drilling assembly in the well to the cement in the casing to  $\pm 10$  ft above the float collar. If excess cement is present, drill out the cement, circulate the well clean, and remove the workstring from the well.
5. Pick up a 6-1/8-inch bit and casing scraper for 7-inch casing and trip into the well to the plugged back total depth (PBTD) of  $\pm 6,430$  ft. Circulate the well clean and remove the workstring from the well. Wait on temperature stabilization for a minimum of 36 hours.
6. Rig up and run differential temperature survey, radial cement bond, and casing evaluation logs as detailed in the Module D – Pre-Operational Testing.
7. Pressure-test the casing string to 1,500 psi for 30 minutes.
8. Displace the drilling fluid in the wellbore with completion fluid.
9. Rig up wireline unit and perforate 7-inch casing with a minimum of 4 shots per foot with 90 degree or 6 shots per foot with 60-degree phasing. The plan is to have three completions in the Cotton Valley Injection Interval. The first completion is planned for the CV1 Interval in the following table and the well will be perforated in the CV1 Interval. The actual perforation will be selected from the open hole logs.

Cotton Valley Inj Zones	Perforation Interval	Formation/Lithology
CV3	± 4,880 to 5,300 ft	Cotton Valley/Sandstone
CV2	± 5,320 to 5,920 ft	Cotton Valley/Sandstone
CV1	± 5,940 to 6,285 ft	Cotton Valley/Sandstone

*(Note: Perforating depths are approximate and will be determined after review of open hole logs & oriented perforating will be required if DTS/DAS cable is run on casing if this optional design is selected at a future date)*

10. Lower the workstring into the wellbore to the bottom of the protection casing and circulate solids from the wellbore.

Note: Formation stimulation and an injection test may be added at this point before the installation of the injection packer and injection tubing.

11. Pick up 7-inch x 4-1/2-inch injection packer (packer constructed using CO<sub>2</sub> resistant 25CR materials) with a polished bore receptacle (PBR) on workstring or wireline and lower into wellbore.
12. Set injection packer at approximately 5,920 ft. Conduct preliminary pressure test to verify pressure integrity of the well annulus.
13. Conduct an injection test to assess the performance of the injection interval.
14. Retrieve the workstring from the wellbore while laying it down.
15. Pick up the seal assembly on 4-1/2-inch L-80 injection tubing and lower into the wellbore. Externally pressure test each connection to 2,500 psi.
16. Circulate inhibitive packer fluid through the tubing-casing annulus until completion brine is fully displaced.
17. Space out the tubing to position the seal assembly in the PBR and land the land the tubing hanger in the tubing spool. A preliminary annulus pressure test will be conducted to verify pressure integrity.
18. Nipple down well control equipment and install 7-1/16-5M x 4-1/16-inch 5M tubing head adapter with 4-1/16-inch 5M tree section with FF trim or better and pressure test the 7-1/16-inch 5M flanged connection between the tubing spool and tubing head adapter.

19. Rig down the workover rig and demobilize from site.
20. Rig up coiled tubing and nitrogen equipment. Conduct formation backflow with nitrogen to develop well and collect native formation brine samples. An acid stimulation treatment may also be required and may be followed by either a wellbore flowback to remove drilling/completion solids from near-wellbore interval or displacement of the acid into the formation.
21. Conduct mechanical integrity test and ambient pressure test per Module D – Pre-Operational Testing.
22. Return well to site for installation and connection of surface equipment and piping.

**General Notes:**

- *All depths referenced are approximate and are based on the expected log depth.*
- *Actual depths may vary based on lithology of local formations.*

**5.3.1.4 Proposed Drilling Fluids Program**

Lost circulation material (LCM) will be on location to treat for fluid losses in top hole sands above the potential injection intervals. The fluid system will be pre-treated with LCM before encountering any known or suspected loss zones. High-viscosity sweeps will be used to assist hole cleaning. Sodium chloride (NaCl) is planned for use as the completion fluid. The fluid weight (density) will be maintained to contain reservoir pressures without inducing flow to the wellbore. Table 5-3 is provided to show the proposed well fluids per hole.

**5.3.1.5 Proposed Cementing Program**

The water, surface, and protection casing strings will be cemented using model cementing technology and practices to meet the standards of 40 CFR 146.86(b). All casing strings will be fully cemented to surface, which will provide additional isolation of the casing string from external formation fluids along the borehole path. For the protection casing strings, the CO<sub>2</sub> resistant cement will be brought above the Confining Zone in each well. Cementing standards and materials as described in Section 5.2.4 will be used during the construction of the wells.

## **Water String**

The following cementing program (Table 5-4) is proposed for installation of the water string:

- 13-3/8-inch in 17-1/2-inch borehole at  $\pm 900$  ft
- Stab-in Float shoe;
- Cement to surface;
- Cement volumes are estimated 75% excess over bit size in open hole interval;
- Actual volume to be calculated from caliper log plus 20% excess; and,

In the event the hole diameter exceeds the scale of a 2-dimensional caliper, a minimum of 150% of the annular space between the casing and the maximum caliper reading will be used for calculating cement volume for that section of the wellbore. The plan will be to circulate cement until cement returns are observed on surface unless extreme lost circulation is encountered during the cementing.

## **Surface Casing**

The following cementing program (Table 5-5) is proposed for installation of the surface casing string:

- 9-5/8-inch in 12-1/4-inch borehole at  $\pm 3,010$  ft
- Two Stage cement job with cement to surface. Verified with cement returns at surface;
- Cement volumes are estimated 30% excess over bit size in open hole interval;
- Actual volume to be calculated from caliper log plus 20% excess; and,
- In the event the hole diameter exceeds the scale of a 2-dimensional caliper, a minimum of 150% of the annular space between the casing and the maximum caliper reading will be used for calculating cement volume for that section of the wellbore.

## **Protection Casing**

The following cementing program (Table 5-6) is proposed for installation of the protection casing string:

- 7-inch in 8-3/4-inch borehole at  $\pm 6,475$  ft
- Two Stage cement job with cement to surface. Verified with cement returns at surface;
- Cement volumes are estimated 30% excess over bit size in open hole interval and 10% excess in casing;
- Actual volume to be calculated from caliper log plus 20% excess; and,
- In the event the hole diameter exceeds the scale of a 2-dimensional caliper, a minimum of 50% of the annular space between the casing and the maximum caliper reading will be used for calculating cement volume for that section of the wellbore.

### **5.3.1.6 Proposed Casing Equipment and Jewelry**

#### **Water Casing**

13-3/8-inch Float Equipment and Jewelry

1. Stab-in float shoe on the bottom of the first joint
2. Approximately two hinged bow spring centralizers and three limit clamps:
  - 1 Centralizer 8 ft above the float shoe, 1 centralizer 8 ft below the float collar, one centralizer 8 ft above the float collar;
  - 1 Centralizer straddling the collar between the second and third joints of casing; and

1 Centralizer every other collar, up to the surface

#### **Surface Casing**

9-5/8-inch Float Equipment and Jewelry

1. Float shoe on the bottom of the first joint

2. Float collar between the first and second joints
3. Multistage Tool at ~1,900 ft plus an optional external casing packer
4. 1 bottom wiper plug (optional)
5. 1 top wiper plug
6. Approximately 13 hinged bow spring centralizers and three limit clamps:
  - 1 Centralizer 8 ft above the float shoe, 1 centralizer 8 ft below the float collar, one centralizer 8 ft above the float collar;
  - 1 Centralizer straddling the collar between the second and third joints of casing; and
  - 1 Centralizer every other collar, up to the surface.

### **Protection Casing**

#### 7-inch Float Equipment and Jewelry

1. Float shoe
2. Float collar, 1 joint above the float shoe
3. Multistage Tool at ~2,965 ft plus an optional external casing packer
4. 1 bottom wiper plug (optional)
5. 1 top wiper plug
6. Approximately 73 hinged bow spring centralizers:
  - 1 Centralizer 8 ft above the float shoe, straddling a stop collar;
  - 1 Centralizer 8 ft above the float collar, straddling a stop collar;
  - 1 Centralizer every other joint, to 3,000 ft;
  - 1 Centralizer every third joint, from 3,000 ft to the surface; and
  - 1 Centralizer approximately 10 ft below ground level.

### **5.3.1.7 Well Logging, Coring, and Testing Program**

Details on the proposed logging program are contained in the “Pre-Operational Testing and Logging Plan” submitted in Module D. All tools will be run on a wireline and will be compatible with open hole and cased hole diameters, allowing for successful testing runs.

## **5.3.2 Injection Well Drilling Procedures – Project Blue Class VI Injection Well No. 2 (INJ-2)**

### ***5.3.2.1 Proposed Drilling Procedure – Project Blue Class VI Injection Well No. 2 (INJ-2)***

The drilling program for the Project Blue Class VI Injection Well No. 2 (INJ-2) at the EDCC El Dorado Facility contain a conductor hole, water string, surface hole, and protection hole. All depths in the outlined procedure are referenced to the kelly bushing (KB), which is estimated at 20.0 ft above ground level.

#### **Conductor Hole**

1. Prepare surface location and mobilize drilling rig. Drill mousehole and rathole.
2. Pick up casing hammer and drive 26-inch conductor pipe to approximately 100 ft or until 100 blows per foot penetration rate is reached. (Alternate is to auger the conductor hole *and grout the casing.*)

#### **Water String**

1. Drill 17-1/2-inch hole to 900 ft (+/-) using drilling fluid as detailed in the Drilling Fluids section of this procedure. Take deviation surveys every 250 ft. Maximum deviation from vertical should be no more than 3 degrees, and maximum deviation between surveys will be targeted at no more than 1 degree.
2. Run open hole electric logs as listed in Module D – Pre-Operational Testing.
3. Run 13-3/8-inch surface casing to 900 ft (+/-). Refer to Section 5.2.1 – Casing String Details for a detailed description of the casing.
4. Cement the casing in place using the stab-in method. Refer to Section 5.3.5 – Proposed Cementing Program.

5. If no cement returns are observed at surface, a temperature or similar diagnostic survey will be run to determine the top of cement. Grout the un-cemented annular space to the surface if necessary.
6. After waiting on cement for a minimum of 12 hours or until compressive strength has reached 500 psi, whichever is longer, cut off water string casing and conductor pipe and install 13-3/8-inch x 3,000 psi SOW casing head and pressure test.
7. Nipple up 13-5/8-inch 3M Blowout Preventers (BOP), choke manifold, and ancillary equipment and pressure test to a low pressure of 250 psig and a maximum pressure of 3,000 psig.
8. Run cased hole logs listed in Module D – Pre-Operational Testing.

### **Surface Hole**

1. Drill 12-1/2-inch surface hole to 3,010 ft (+/-) using drilling fluid as detailed in the Drilling Fluids section of this procedure. Take deviation surveys every 500 ft. Maximum deviation from vertical should be no more than 3 degrees, and maximum deviation between surveys will be targeted at no more than 1 degree.
2. Run open hole electric logs as listed in Module D – Pre-Operational Testing.
3. Run 9-5/8-inch surface casing to 3,010 ft (+/-). Refer to Section 5.2.1 – Casing String Details for a detailed description of the casing.
4. Cement the casing in place using the stab-in method. Refer to Section 5.3.5 – Proposed Cementing Program.
5. If no cement returns are observed at surface, a temperature or similar diagnostic survey will be run to determine the top of cement. Grout the un-cemented annular space to the surface if necessary.
6. After waiting on cement for a minimum of 12 hours or until compressive strength has reached 500 psi, whichever is longer, cut off the water and conductor pipe and install an 11-inch 3,000 psi x 9-5/8-inch SOW casing head and pressure test.

7. Nipple up 11-inch 3M Blowout Preventers (BOP), choke manifold, and ancillary equipment and pressure test to a low pressure of 250 psig and a maximum pressure of 3,000 psig.
8. Run cased hole logs listed in Module D – Pre-Operational Testing.

### **Protection Hole**

1. Pick up a 8-3/4-inch drilling assembly and trip into the wellbore. Pressure test the surface casing to 1,600 psi for 30 minutes.
2. Displace the fresh water from cementing with a water-based drilling fluid to improve hole cleaning and stability. Drill out casing float equipment.
3. Drill an 8-3/4-inch protection hole from surface casing point to 4,700 ft (+/-) into the top of the Cotton Valley Formation. The actual total depth of the well will be contingent on the subsurface depth of the base of the Hosston. Take inclination surveys every 500 ft to monitor well path.
4. Run electric wireline logs and collect rotary sidewall core samples (if needed) over the open hole interval. Refer to Module D – Pre-Operational Testing for details.
5. Run 7-inch casing (mixed string) to the planned casing point (4,700 ft). Refer to Section 5.2.1 – Casing String Details for a detailed description of the casing.

*Note: Lapis Energy is evaluating “smart well” completion technologies to monitor Differential Temperature, Acoustic, and Bottomhole Pressure. Lapis may elect to add “smart well” monitoring to the completion.*

6. Rig up cementing equipment and cement the protection casing in place. Cement will be placed in two stages with the lower cement being CO<sub>2</sub> resistant cement and the upper being a lightweight cement blend. A 7-inch carbon steel cementing stage tool will be set at+/-2,965 ft for the two-stage cementing. Refer to Section 5.3.5 – Proposed Cementing Program.

7. In the event cement returns are not observed at the surface, a temperature or similar diagnostic survey will be run to determine the top of cement. After the cement top is located, a procedure to grout in the un-cemented annular space will be provided.
8. After finishing the cementing, land the 7-inch casing by installing the casing hanger in the C-22 bowl of the 11-inch 3M casing head flange. The BOP stack will be picked up and a rough cut will be made on the 7-inch casing above the casing hanger. The 7-inch cut joint will be removed and measured, and the 11-inch BOP stack will nipple down and be removed.
9. Cut and dress the 7-inch casing above the casing hanger for the required length for the secondary seal. Install and nipple up a 7-1/16-inch 5M x 11-inch 3M tubing spool with a secondary seal in the 11-inch bottom flange for the 7-inch casing. Test the seals and confirm the mechanical integrity between the 11-inch flanges, casing hanger primary seal, and casing hanger secondary seal.
10. Install a 7-1/16-inch 5M dry hole tree on the 7-1/16-inch flange on the casing spool to protect the well.
11. Rig down and release the drilling rig and drilling equipment.
12. Clean up the location in preparation for the completion operations.

### ***5.3.2.2 Drilling Contingency Plans***

If unforeseen events occur during drilling operations, detailed plans to remedy the specific problem will be implemented using best engineering practices and judgment based on facts. The following are general contingency plans to address specific problems.

#### **Borehole Drilling Lost Circulation Plan**

If circulation is lost (moderate probability) while drilling either the surface or protection casing borehole, lost circulation material pills will be pumped to re-establish circulation. Depending upon the severity of lost circulation encountered, lost circulation material may need to be blended with the drilling fluid in concentrations dictated by hole conditions to maintain circulation to the surface casing point. Should lost circulation occur while drilling from the base of conductor to

the surface casing point, paper, cottonseed hulls, or other forms of standard lost circulation material may be used to remedy the loss condition. A cement truck may be mobbed to location and placed on “standby” to minimize “wait time” if severe loss of circulation is encountered.

### **Borehole Drilling Overpressured Zone**

If an overpressure zone is encountered (not expected) while drilling the surface or protection hole, the drilling fluid pump rate down the drill pipe will be increased while the drill fluid density is increased. The increased pumping rate will continue until the well stops flowing. If a drilling influx is encountered while drilling any other hole section, the blow out preventer (BOP) will be closed-in, and the well will be secured. The influx will be circulated out of the well while maintaining constant bottom hole pressure using the choke to prevent additional influx. Finally, the mud weight will be increased to a density sufficient to overbalance the well while circulating through the choke to maintain constant bottom hole pressure throughout the circulation. Once kill weight mud has been circulated around and the well is confirmed to not be flowing, drilling will recommence.

### **Borehole Deviation Issues**

Take inclination surveys at a minimum every 500 ft, or as required by state regulations, and at the TD for the hole size to monitor the well path. A target maximum deviation from vertical is 3 degrees and target maximum dogleg severity is 2.5 degrees per 100 ft. If the maximum recommended deviation is exceeded, an evaluation will be made to determine whether remedial action is necessary.

#### **5.3.2.3 Proposed Completion Procedures – Project Blue Class VI Injection Well 2 (INV-2)**

The completion procedure has been developed to utilize the Lower Hosston Injection Zone for sequestration of the injected CO<sub>2</sub> as the initial reservoir for sequestration. It is anticipated that the full interval in the Lower Hosston Injection Zone will be utilized and will be perforated based on results from the open hole logging program. The following is a proposed completion procedure for the EDCC facility:

1. Move in workover rig and equipment required for the completion operations.
2. Nipple up 7-1/16-inch 5M BOPs on the well and pressure test the BOPs.
3. Pick up a 6-1/8-inch bit and drilling assembly below the workstring casing scraper for 7-inch and trip into the wellbore.
4. Drill out the cementing stage equipment and circulate the well clean. Continue lowering the bit and drilling assembly in the well to the cement in the casing to 10 ft above the float collar. If excess cement is present, drill out the cement and circulate the well clean, and remove the workstring from the well.
5. Pick up a 6-1/8-inch bit and casing scraper for 7-inch casing and trip into the well to the plugged back total depth (PBTD). Circulate the well clean and remove the workstring from the well. Wait on temperature stabilization for a minimum of 36 hours.
6. Rig up and run differential temperature survey, radial cement bond, and casing evaluation logs as detailed in the Module D – Pre-Operational Testing.
7. Pressure-test the casing string to 1,500 psi for 30 minutes.
8. Displace the drilling fluid in the wellbore with completion fluid.
9. Rig up wireline unit and perforate 7-inch casing with a minimum of 4 shots per foot with 90 degree or 60-degree phasing as detailed in the following table:

Perforation Interval	Formation/Lithology
± 3,910 to 3,930 ft	Hosston/Sandstone
± 4,030 to 4,080 ft	Hosston/Sandstone
± 4,110 to 4,130 ft	Hosston/Sandstone
± 4,155 to 4,290 ft	Hosston/Sandstone
± 4,315 to 4,350 ft	Hosston/Sandstone
± 4,375 to 4,420 ft	Hosston/Sandstone

*(Note: Perforating depths are approximate and will be determined after review of open hole logs & oriented perforating will be required if DTS/DAS cable run on casing if this optional design is selected at a future date)*

10. Lower the workstring into the wellbore to the bottom of the protection casing and circulate solids from the wellbore.

Note: Formation stimulation and an injection test may be added at this point before the installation of the injection packer and injection tubing.

11. Pick up 7-inch x 4-1/2-inch injection packer (packer constructed using CO2 resistant 25CR materials) with a polished bore receptacle (PBR) on workstring or wireline and lower into wellbore.
12. Set injection packer at approximately 3,800 ft. Conduct preliminary pressure test to verify pressure integrity of the well annulus.
13. Conduct an injection test to assess the performance of the injection interval.
14. Retrieve the workstring from the wellbore while laying it down.
15. Pick up the seal assembly on 4-1/2-inch L-80 injection tubing and lower into the wellbore. Externally pressure test each connection to 2,500 psi.
16. Circulate inhibitive packer fluid through the tubing-casing annulus until completion brine is fully displaced.
17. Space out the tubing to position the seal assembly in the PBR and land the land the tubing hanger in the tubing spool. A preliminary annulus pressure test will be conducted to verify pressure integrity.
18. Nipple down well control equipment and install 7-1/16-5M x 4-1/16-inch 5M tubing head adapter with 4-1/16-inch 5M tree section with FF trim or better and pressure test the 7-1/16-inch 5M flanged connection between the tubing spool and tubing head adapter.
19. Rig down the workover rig and demobilize from site.
20. Rig up coiled tubing and nitrogen equipment. Conduct formation backflow with nitrogen to develop well and collect native formation brine samples. An acid stimulation treatment may also be required and may be followed by either a wellbore flowback to remove drilling/completion solids from near-wellbore interval or displacement of the acid into the formation.
21. Conduct mechanical integrity test and ambient pressure test per Module D – Pre-Operational Testing.

22. Return well to site for installation and connection of surface equipment and piping.

**General Notes:**

- *All depths referenced are approximate and are based on the expected log depth.*
- *Actual depths may vary based on lithology of local formations.*

***5.3.2.4 Proposed Drilling Fluids Program***

Lost circulation material (LCM) will be on location to treat for fluid losses in top hole sands above the potential injection intervals. The fluid system will be pre-treated with LCM before encountering any known or suspected loss zones. High-viscosity sweeps will be used to assist hole cleaning. Sodium chloride (NaCl) is planned for use as the completion fluid. The fluid weight (density) will be maintained to contain reservoir pressures without inducing flow to the wellbore. Table 5-3 is provided to show the proposed well fluids per hole.

***5.3.2.5 Proposed Cementing Program***

The surface and protection casing strings will be cemented using model cementing technology and practices to meet the standards of 40 CFR 146.86(b). All casing strings will be fully cemented to surface, which will provide additional isolation of the casing string from external formation fluids along the borehole path. For the protection casing strings, the CO<sub>2</sub> resistant cement will be brought to the Confining Zone. Cementing standards and materials as described in Section 5.2.4 will be used during the construction of the wells.

**Water String**

The following cementing program (Table 5-4) is proposed for installation of the water string:

- 13-3/8-inch in 17-1/2-inch borehole at ±900 ft
- Stab-in Float shoe;
- Cement to surface;
- Cement volumes are estimated 75% excess over bit size in open hole interval;
- Actual volume to be calculated from caliper log plus 20% excess; and,

In the event the hole diameter exceeds the scale of a 2-dimensional caliper, a minimum of 150% of the annular space between the casing and the maximum caliper reading will be used for calculating cement volume for that section of the wellbore. The plan will be to circulate cement until cement returns are observed on surface unless extreme lost circulation is encountered during the cementing.

### **Surface Casing**

The following cementing program (Table 5-5) is proposed for installation of the surface casing string:

- 9-5/8-inch in 12-1/4-inch borehole at  $\pm 3,010$  ft
- Two Stage cement job with cement to surface. Verified with cement returns at surface;
- Cement volumes are estimated 30% excess over bit size in open hole interval;
- Actual volume to be calculated from caliper log plus 20% excess; and,
- In the event the hole diameter exceeds the scale of a 2-dimensional caliper, a minimum of 150% of the annular space between the casing and the maximum caliper reading will be used for calculating cement volume for that section of the wellbore.

### **Protection Casing**

The following cementing program (Table 5-6) is proposed for installation of the protection casing string:

- 7-inch in 9-7/8-inch borehole at  $\pm 4,700$  ft
- Two Stage cement job with cement to surface. Verified with cement returns at surface;
- Cement volumes are estimated 25% excess over bit size in open hole interval;
- Actual volume to be calculated from caliper log plus 20% excess; and,
- In the event the hole diameter exceeds the scale of a 2-dimensional caliper, a minimum of 50 percent of the annular space between the casing and the maximum caliper reading will be used for calculating cement volume for that section of the wellbore.

### ***5.3.2.6 Proposed Casing Equipment and Jewelry***

#### **Water Casing**

##### **13-3/8-inch Float Equipment and Jewelry**

1. Stab-in float shoe on the bottom of the first joint
2. Approximately two hinged bow spring centralizers and three limit clamps:
  - 1 Centralizer 8 ft above the float shoe, 1 centralizer 8 ft below the float collar, one centralizer 8 ft above the float collar;
  - 1 Centralizer straddling the collar between the second and third joints of casing; and

1 Centralizer every other collar, up to the surface

#### **Surface Casing**

##### **10-3/4-inch Float Equipment and Jewelry**

1. Float shoe on the bottom of the first joint
2. Float collar between the first and second joints
3. Multistage Tool at ~1,900 ft plus an optional external casing packer
4. 1 bottom wiper plug (optional)
5. 1 top wiper plug
6. Approximately 13 hinged bow spring centralizers and three limit clamps:
  - 1 Centralizer 8 ft above the float shoe, 1 centralizer 8 ft below the float collar, one centralizer 8 ft above the float collar;
  - 1 Centralizer straddling the collar between the second and third joints of casing; and
  - 1 Centralizer every other collar, up to the surface.

#### **Protection Casing**

##### **7-inch Float Equipment and Jewelry**

1. Float shoe

2. Float collar, 1 joint above the float shoe
3. Multistage Tool at ~2,965 ft plus an optional external casing packer
4. 1 bottom wiper plug (optional)
5. 1 top wiper plug
6. Approximately 55 hinged bow spring centralizers:
  - 1 Centralizer 8 ft above the float shoe, straddling a stop collar;
  - 1 Centralizer 8 ft above the float collar, straddling a stop collar;
  - 1 Centralizer every other joint, to 3,000 ft;
  - 1 Centralizer every third joint, from 3,000 ft to the surface; and
  - 1 Centralizer approximately 10 ft below ground level.

#### **5.3.2.7 Well Logging, Coring, and Testing Program**

Details on the proposed logging program are contained in the “Pre-Operational Testing and Logging Plan” submitted in Module D. All tools will be run on a wireline and will be compatible with open hole and cased hole diameters, allowing for successful testing runs.

## **6.0 PRE-OPERATIONAL LOGGING AND TESTING**

Lapis has designed the sequestration project with the injection wells to be completed into one or more of the project Injection Zones described above. The injection wells will follow the 40 CFR §146.87(a), (b), (c), and (d) and standards for logging and testing requirements. Coring will be adaptive and based on drilling parameters, wellbore conditions, overall core recovery, and core quality as each project well is drilled. All wells will demonstrate mechanical integrity prior to receiving authorization to inject.

The data obtained in this plan will be used to validate and update, if necessary, the “*Area of Review and Corrective Action Plan*” (submitted in **Module B**), to define and reduce uncertainties with the site characterization, revise the “*E.1-Testing and Monitoring Plan*” (submitted in **Module E**), and determine final operational procedures and limits.

This plan has been uploaded in **Module D**:

“*D. Pre-Operations Testing and Logging Plan (Rev. 0 – January 2023)*”

### **Pre-Operational Logging and Testing GSDT Submissions**

**GSDT Module:** Pre-Operational Testing

**Tab(s):** Welcome tab

Please use the checkbox(es) to verify the following information was submitted to the GSDT:

Proposed pre-operational testing program [**40 CFR 146.82(a)(8) and 146.87**]

## **7.0 WELL OPERATION**

Lapis will operate the injection wells on the property of the EDCC per the operating requirements in accordance with 40 CFR 146.82(a)(7) and (10). No injection operations will occur between the outermost casing and the USDW per 40 CFR 146.88 (a). Operating the well in this fashion will prevent the movement of fluids that could result in the pollution of a USDW and will prevent leaks from the subject injection well into unauthorized zones.

During injection operations, continuous measurements will be taken at the wellhead for injection pressure, rate, volume, and temperature of the CO<sub>2</sub> stream [40 CFR 146.88(e)(1)]. The maximum injection pressure is governed by the fracture gradient. Operating injection pressures are set at 90 percent below the calculated values. Site specific *in-situ* fracture gradients will be determined during the drilling and testing of the Class VI Injection Wells for each Injection Zone.

If there are major changes to the operational stream (density changes, composition, etc.) or a new source, Lapis may reevaluate and adjust the operating pressures with approval from the UIC Program Director. Under routine operations, injection pressures that approach the limits shown below will trigger reduced injection or a full system shutdown. Well conditions will then be monitored to decide on steps to return to full rate injection. In cases where return to full injection is not possible, additional troubleshooting steps may be required. Values in Tables 7-1 to 7-4 will be updated after drilling the injection well in the column “updated Value”. Table 7-1, 7-2, 7-3 and 7-4 state the operation procedures for each of the injection intervals starting with the first and deepest zone, the Cotton Valley Injection Interval CV1 and ending with the shallowest zone the Hosston Injection Interval.

Lapis will provide an analysis of the chemical and physical characteristics of the CO<sub>2</sub> stream prior to injection operations [40 CFR 146.82(a)(7)(iv)]. The source(s) of the final stream will also be provided in accordance with 40 CFR 146.82(a)(7)(iii).

During operations, Lapis will analyze the composite carbon dioxide stream to yield data representative of its chemical and physical characteristics and to meet the requirements of 40 CFR §146.90(a) as presented in the “*E.1 - Testing and Monitoring Plan*”, submitted in **Module E**.

## **8.0 TESTING AND MONITORING**

In accordance with USEPA 40 CFR §146.90, Lapis has developed a testing and monitoring plan for the lifetime of injection operations. In addition to demonstrating that the injection wells will be operating as expected, that the carbon dioxide plume and pressure front are moving as predicted, and there is no endangerment to USDWs, the monitoring data will be used to validate and guide any required adjustments to the geologic and dynamic models used to predict the distribution of carbon dioxide within the storage complex, supporting AoR evaluations and a non-endangerment demonstration. Additionally, the testing and monitoring components include a leak detection plan to monitor and account for any movement of the carbon dioxide outside of the storage complex.

Direct in-zone monitoring at the injection wells will confirm that the wells are performing as intended; delivering the carbon dioxide to the subsurface storage intervals only (Injection Zones), do not exceed safe injection pressures, and measure the pressure response in the reservoir intervals (a key model match parameter). Downhole pressure gauges and injection logging in the constructed injection wells will be used for data collection.

Additionally, a new in-zone well (Project Blue In Zone Monitor Well (Blue DM-2)) will be drilled in the up-dip direction near the northeastern property boundary, which will validate the indirect monitoring method(s) and the dynamic model, calibrating both the growth of sequestered carbon dioxide plume and pressure front over time. A contingent second in-zone well (Project Blue In Zone Monitor Well (Blue DM-1)) could be drilled in the south part of the plant (relative to the injection wells), if indirect monitoring methods do not provide sufficient information on plume growth over time. Downhole pressure gauges and injection logging in the constructed in-zone monitoring well(s) will be used to collect real-time, continuous data. The in-zone monitor well(s) will be located initially outside of the carbon dioxide plume and will primarily monitor the pressure changes due to the developing pressure front.

The TMP has been uploaded in **Module E** – Project Plan Submission as Report:

*“E.1 – Testing and Monitoring Plan (Rev. 0 – January 2023)”*

A Quality Assurance and Surveillance Plan (QASP) for all testing and monitoring activities, required pursuant to §146.90(k), is provided in Appendix 1 – Quality Assurance and Surveillance Plan (QASP) to the TMP.

#### Testing and Monitoring GSDT Submissions

**GSDT Module:** Project Plan Submissions

**Tab(s):** Testing and Monitoring tab

Please use the checkbox(es) to verify the following information was submitted to the GSDT:

Testing and Monitoring Plan [**40 CFR 146.82(a)(15) and 146.90**]

## **9.0 INJECTION WELL PLUGGING**

The Injection Well Plugging Plan has been developed using the GSĐT Template and meets the requirements under 40 CFR 146.92(b). It contains testing prior to closure, detailed plugging plans, and plugging schematics for the Project Blue injection wells in this application. It has been uploaded in **Module E** – Project Plan Submission as Report:

*“E.2 – Injection Well Plugging Plan (Rev. 0 – January 2023)”*

This plan will be updated as the project is developed to be consistent with the Injection Wells “as built” after construction.

### ***Injection Well Plugging GSĐT Submissions***

**GSĐT Module:** Project Plan Submissions

**Tab(s):** Injection Well Plugging tab

Please use the checkbox(es) to verify the following information was submitted to the GSĐT:

Injection Well Plugging Plan [**40 CFR 146.82(a)(16) and 146.92(b)**]

## **10.0 POST INJECTION SITE CARE (PISC) AND SITE CLOSURE**

The Post Injection Site Care (PISC) and Site Closure Plan has been developed using the GSĐT Template and meets the requirements under 40 CFR 146.9. It has been uploaded in **Module E** – Project Plan Submission as Report:

*“E.3 – Post Injection Site Care and Closure Plan (Rev. 0 – January 2023)”*

Lapis plans to implement a PISC over a 50-year timeframe to demonstrate conformance and containment. Data will be gathered to track the position of the CO<sub>2</sub> plume, declining pressure front and to demonstrate that the USDW is not endangered, using an adaptive, sustainable, risk-based monitoring approach. Figures representing the pressure differentials in each injection zone, as well as figures projecting the plume extent, both at the end of the 50-year observation period are included.

Depending on project performance during the project life cycle, Lapis may request an alternative PISC timeframe based upon modeling results and AoR reevaluations. Prior to authorization for site closure, Lapis will demonstrate that no additional monitoring is needed to ensure that the geologic sequestration project does not pose an endangerment to USDWs as per 40 CFR 146.93(b)(3).

### **PISC and Site Closure GSĐT Submissions**

**GSĐT Module:** Project Plan Submissions

**Tab(s):** PISC and Site Closure tab

Please use the checkbox(es) to verify the following information was submitted to the GSĐT:

PISC and Site Closure Plan **[40 CFR 146.82(a)(17) and 146.93(a)]**

## **11.0 EMERGENCY AND REMEDIAL RESPONSE**

The Emergency and Remedial Response Plan (ERRP) has been developed using the GSĐT Template and meets the requirements under 40 CFR 146.94(a). It has been uploaded in **Module E** – Project Plan Submission as Report:

*“E.4 – Emergency and Remedial Response Plan (Rev. 0 – January 2023)”*

The EERRP Plan will be updated and further developed to meet the project's needs throughout three phases of development: 1) Construction; 2) Operation; and 3) Post-Injection Site Closure. Revisions will be drafted and notated with date of submittal. Detailed information is contained in the Emergency and Remedial Response Plan [40 CFR 146.94(a)] submitted within **Module E** – Project Plan Submission through the GSĐT Tool.

### **Emergency and Remedial Response GSĐT Submissions**

**GSĐT Module:** Project Plan Submissions

**Tab(s):** Emergency and Remedial Response tab

Please use the checkbox(es) to verify the following information was submitted to the GSĐT:

Emergency and Remedial Response Plan **[40 CFR 146.82(a)(19) and 146.94(a)]**

## **12.0 INJECTION DEPTH WAIVER AND AQUIFER EXEMPTION**

### **EXPANSION**

Lapis is not requesting an Injection Depth Waiver or an Aquifer Exemption Expansion. Therefore, this section is not applicable.

## **13.0 OPTIONAL ADDITIONAL PROJECT INFORMATION**

Lapis has not identified any current Federal laws that may impact injection at the El Dorado site.

## **14.0 OTHER RELEVANT INFORMATION**

No additional information or documents have been requested by the UIC Program Director to date for this Class VI Permit Application at the Project Blue site in El Dorado, Arkansas.

However, Lapis has performed an initial assessment using the Environmental Justice Screening and Mapping Tool (EJSscreen Tool) in February 2023. Reports applicable to the project are contained in **Appendix D** to this Project Narrative.

## **REFERENCES**

Adams, R. L., 2009, Basement tectonics and origin of the Sabine Uplift: Gulf Coast Association of Geological Societies Transactions, v. 59, p. 3-19.

Archie, G. E., 1942, The electrical resistivity log as an aid in determining some reservoir characteristics, Petroleum Transactions of the AIME, v. 146, p. 54-62.

Arkansas Geological Survey (AGS), 2022a, Arkansas Critical Mineral Fact Sheet, <https://www.geology.arkansas.gov/minerals/critical-minerals.html>, accessed 10 October 2022.

Arkansas Geological Survey (AGS), 2022b, Brine (Bromine) in Arkansas, <https://www.geology.arkansas.gov/energy/brine-in-arkansas.html>, accessed 10 October 2022.

Arkansas Natural Resources Commission, 2016, Arkansas groundwater protection and management report for 2015, p. 81.

Aronow, S. and Wesselman, J. B., 1971, Groundwater Resources of Chambers and Jefferson Counties, Texas: Texas Water Development Board Report No. 133.

Aumman, H. H., 1966, Experimental study of the effect of stress on the creep in shales: Exxon Production Research Report, (private communication to R. E. Collins, DuPont consultant)

Bartberger, C.E., Condon, S.M., Dyman, T.S., 2002: Is There a Basin-Centered Gas Accumulation in Cotton Valley Group Sandstones, Gulf Coast Basin, U.S.A., U.S. Geologic Survey Bulletin 2184-D.

Bentley, C. B., 1983, Preliminary Report of the Geohydrology Near Cypress Creek and Richton Salt Domes, Perry County, Mississippi: Water-Resources Investigations Report 83-4169, U. S. G. S., Jackson, MS.

Bethke, C. M., Harrison, W. J., Upson, C. and Altaner, S. P., 1988, Supercomputer analysis of sedimentary basins: *Science*, v. 239, Washington, D. C.

Bishop W.F., 1973, Late Jurassic Contemporaneous Faults in North Louisiana and South Arkansas: *The American Association of Petroleum Geologists Bulletin*. V. 57, No. 5. P 858 – 977.

Bowden, R. K., and Curran J. H., 1984, Time dependent behavior of joints in shale: *Proc. 25th Symposium of Rock Mechanics*, Northwestern University, Evanston, Illinois, published by American Institute of Mechanical Engineers, New York, New York, pp. 320328

Bredehoeft, J.D., and Pinder, G.F., 1970, Digital Analysis of Areal Flow in Multiaquifer Groundwater Systems: A Quasi Three-Dimensional Model. *Water Resources Research*, 6, 883-888.

Brendsdal, A.O.E., 2017, The capacity of creeping shale to form an annular barrier, Master Thesis, Norwegian University of Science and Technology, Department of Geoscience and Petroleum.

Broom, M.E., Bush, W.V., Kraemer, T.F., 1984, A reconnaissance Study of Saltwater Contamination in the El Dorado Aquifer, Union County, Arkansas: *Water Resources Circular 14*, Arkansas Geological Commission and U.S. Geological Survey

Burton, J., 2022, U.S. Geological Survey releases 2022 list of critical minerals: USGS, February 22, 2022, <https://www.usgs.gov/news/national-news-release/us-geological-survey-releases-2022-list-critical-minerals>, accessed 10 October 2022.

Byerly, G. R., 1991, Igneous activity, in Salvador, A., *The Gulf of Mexico Basin*: Boulder,

Caughey, C. A., 1977, Depositional systems of the Paluxy Formation, *The University of Texas at Austin, Bureau of Economic Geology Geological Circular 77-8*.

Chang, C. and Zoback, M.D., 2009, Viscous creep in room-dried unconsolidated Gulf of Mexico shale (I): Experimental results. *Journal of Petroleum Science and Engineering*, 69, 239-246

Chen-Charpentier, B. and Herrera I.R., 1982, Numerical Treatment of Leaky Aquifers in the Short Time Range. *Water Resources Research*. 18. 557-562

Clark, J. E., 1987, Groundwater flow in deep saline aquifers: Special Session on the Hydrologic and Geochemical Processes Involved in Deep Injection of Liquid Wastes, Groundwater Committee of the American Geophysical Union and the International Association of Hydrogeologists, Baltimore, Maryland.

Clark, J. E., 1988, Groundwater flow in deep saline aquifers: Special Session on the Hydrologic and Geochemical Processes Involved in Deep Injection of Liquid Wastes, Groundwater Committee of the American Geophysical Union and the International Association of Hydrogeologists, Baltimore, Maryland.

Clark, J. E., Howard, M. R., and Sparks, D. K., 1987, Factors that can Cause Abandoned Wells to Leak as Verified by Case Histories from Class II injection, Texas Railroad Commission files: International Symposium on Subsurface Injection of Oilfield Brines, Underground Injection Practices Council, New Orleans, LA., p. 166-223.

Clark J. E., Bonura, D. K., Papadeas, P. W., McGowen, R., 2005, Gulf Coast Borehole-Closure-Test Well Near Orange, Texas: *Developments in Water Science*, v. 52, p. 157-166.

Clifford, H. J., 1973, Hydrodynamics of the Mt. Simon Sandstone, Ohio, and Adjacent Areas: in *Underground Waste Management and Artificial Recharge* Vol. 1, American Association of Petroleum Geologists, Tulsa, OK.

Clifford, H. J., 1975, Subsurface Liquid Waste Injection in Ohio: *Ohio Geological Survey Information Circ.*, n. 43.

Collins, S. E., 1980, Jurassic Cotton Valley and Smackover reservoir trends, east Texas, north Louisiana, and south Arkansas: American Association of Petroleum Geologists Bulletin, v. 64, no. 7, p. 1004–1013.

Collins, R. E., 1986, Potential Breaches in the Confining Layer Near Injections Wells on the Gulf Coastal Plain. Report to E.I. du Pont de Nemours & Co. Inc.

Cox, R. T. and Van Arsdale, R. B., 2002, The Mississippi Embayment, North America: a first order continental structure generated by Cretaceous superplume event: Journal of Geodynamics, v. 34, p. 163-176

Dane C.H., 1929: Upper Cretaceous Formations of Southwestern Arkansas, Arkansas Geological Survey Bulletin 1. P 1 – 249.

Davis, K. E., 1986, Factors Effecting the Area of Review for Hazardous Waste Disposal Wells: Proceedings of the International Symposium on Subsurface Injection of Liquid Wastes, New Orleans, National Water Well Association, Dublin, OH, p. 148-194.

Davis, S. D., Pennington, W. D., and Carlson, S. M., 1987, A compendium of earthquake activity in Texas: Bureau of Economic Geology Circular, The University of Texas at Austin, Austin, Texas, in press.

Dennen, K. O., and Hackley, P. C., 2012, Definition of greater Gulf Basin Lower Cretaceous Shale gas assessment unit, United States Gulf of Mexico Basin onshore and state waters: Search and Discovery Article # 10429.

Devery, D. M., 1982, Subsurface Cretaceous strata of Mississippi: Mississippi Department of Natural Resources, Bureau of Geology and Energy Resources Information Series, v. 82, no. 1, p. 1–24

Dickinson, K. A., 1968b, Petrology of the Buckner Formation in adjacent parts of Texas, Louisiana, and Arkansas: Journal of Sedimentary Petrology, v. 38, no. 2, p. 555-567.

Dutton, S. P., Clift, S. J., Hamilton, D. S., Hamlin, H. S., Hentz, T. F., Howard, W. E., Akter, M. S., and Laubach, S.E., 1993, Major low-permeability sandstone gas reservoirs in the continental United States: Austin, Tex., University of Texas, Bureau of Economic Geology, Report of Investigations No. 211, p. 221.

Dyman, T.S., Condon, S.M., 2006, Assessment of undiscovered conventional oil and gas resources – Upper Jurassic-Lower Cretaceous Cotton Valley Group, Jurassic Smackover Interior Salt Basins Total Petroleum System, in the East Texas Basin and Louisiana-Mississippi Salt Basins Provinces: U.S. Geological Survey Digital Data Series DDS-69-E, Chapter 2, 48 p.

Eaton, B. A., 1969, Fracture Gradient Prediction And its Application In Oilfield Operations, Journal of Petroleum Technology, October 1353 – 1360.

Ellsworth, W.L., 2013, Injection-induced earthquakes: Science, v.341, p. 6142-6148

Enomoto, C. B., Scott, K. R., Valentine, B., Hackley, P. C., Dennen, K., and Lohr, C., 2012, Preliminary evaluation of the shale gas prospectivity of the Lower Cretaceous Pearsall Formation in the onshore Gulf Coast region, United States: Transactions – Gulf Coast Association of Geological Societies, v. 62, p. 63-115.

Ewing, T. E. and Galloway, W. E., 2019, Evolution of the Northern Gulf of Mexico Sedimentary Basin, in Miall, A. D., ed., Sedimentary Basins of the United States and Canada, Second Edition: The Netherlands, Elsevier, p. 627-694

Ewing, T. E., 2009, The Ups and Downs of the Sabine Uplift and Northern Gulf of Mexico Basin; Jurassic Basement Blocks, Cretaceous Therman Upfits and Cenozoic Flexure: Gulf Coast Association of Geological Societies Transactions, v. 59, p. 253-269

Fjær, E., Holt, R. M., Raaen, A., 2008, Petroleum related rock mechanics, 2nd edition. Elsevier, Amsterdam Fjær E, Stenebråten, J. F., Bakheim S, 2018, Laboratory test for studies on shale barrier formation. In: 52nd U. S. Rock mechanics/ geomechanics symposium proceedings. American Rock Mechanics Association

Fawad, M., and Mondol, N. H., 2021, Monitoring geological storage of CO<sub>2</sub>: a new approach: *Scientific Reports* 11, 5942 (2011), p. 1-9.

Fogg, G. E. and Kreitler, C. W., 1982, Groundwater hydraulics and hydrochemical facies in Eocene aquifers of the East Texas Basin: University of Texas at Austin, Bureau of Economic Geology Report of Investigations No. 127, 75 p.

Fogg, G. E., Seni, S. J. and Kreitler, C. W., 1983, Three-dimensional ground-water modeling in depositional systems, Wilcox Group, Oakwood Salt Dome area, East Texas: Texas Bureau of Economic Geology Report of Investigations 133, Austin, 55 p.

Foot, R.Q., 1984, Open-File Report Vol. 1984 (84-339), Summary report on the regional geology, petroleum potential, environmental consideration for development, and estimates of undiscovered recoverable oil and gas resources of the United States Gulf of Mexico Continental Margin in the area of proposed oil and gas lease sales nos. 81 and 84. US Geological Survey Open-File Report 84-339, p. 1-193.

Forgotson, J. M., 1963, Depositional history and paleotectonic framework of Comanchean Cretaceous Trinity stage, Gulf Coast area: *AAPG Bulletin*, v. 47, no. 1, p. 69-103.

Frohlich, C., Potter, E., Hayward, C., and Stump, B., 2010, Dallas-Fort Worth earthquakes coincident with activity associated with natural gas production: *The Leading Edge*, v. 29, p. 270-275.

Galloway, W. E., 2008, Depositional evolution of the Gulf of Mexico sedimentary basin, in Hsü, K. J., ed., *Sedimentary basins of the world, Volume 5, The sedimentary basins of the United States and Canada*, Miall, A. D., ed.: The Netherlands, Elsevier, p. 505–549.

Galloway, W. E., Hobday, D. K. and Magara, K., 1982(a), Frio Formation of the Texas Gulf of Mexico Basin-depositional systems, structural framework and hydrocarbon origin, migration, distribution, and exploration potential: Bureau of Economic Geology, Report of Investigations No. 122, The University of Texas at Austin, Austin, Texas, p. 78.

Galloway, W. E., Hobday, D. K., and Magara, K., 1982a, Frio Formation of the Texas Gulf of

Mexico Basin-depositional systems, structural framework, and hydrocarbon origin, migration, distribution, and exploration potential: Bureau of Economic Geology, Report of Investigations No. 122, The University of Texas at Austin, Austin, Texas, p. 78.

Galloway, W. E., Ganey-Curry, P. E., Li, X. and Buffler, R. T., 2000, Cenozoic depositional history of the Gulf of Mexico basin: AAPG Bulletin, v. 84, no. 11, p. 1743-1774.

Galloway, W. E., Whiteaker, T. L. and Ganey-Curry, P., 2011, History if Cenozoic North American Drainage basin evolution, sediment yield and accumulation in the Gulf of Mexico Basin, Geosphere, August 211; v. 7; no. 4; p. 938-973

Garside, M., 2022, Projection of worldwide lithium demand from 2019 to 2030, <https://www.statista.com/statistics/452025/projected-total-demand-for-lithium-globally/>, accessed 10 October 2022

Granata, W.H., 1963, Cretaceous stratigraphy and structural development of the Sabine Uplift Area, Texas and Louisiana: Reference Report of the Shreveport Geological Society, v. 5, p. 50-96.

Gray, G. R., H. C. H. Darley, and W. F. Rodgers, 1980, Composition and Properties of Oil Well Drilling Fluids: Gulf Publishing Company, Houston, Texas.

Grunau, H. R., 1987, A worldwide look at the cap-rock problem: Journal of Petroleum Geology, v. 103, p. 245-266.

Gunter, W., Perkins, E. and McCann, T., 1993, Aquifer disposal of CO<sub>2</sub>-rich gases: Reaction design for added capacity: Energy Conversion and Management. 34, p. 941-948.

Hackley, P. C., 2012, Geological and geochemical characterization of the Lower Cretaceous Pearsall Formation, Maverick Basin, south Texas: A future shale gas resource: AAPG Bulletin, v. 96, no. 8, p. 1449-1482.

Hackley, P., Valentine, B.J., Enomoto, C.B., Lohr, C.D., Scott, K.R., Dulong, F.T., and Fanning, A.M., 2014, Aptian ‘Shale Gas’ Prospectively in the Downdip Mississippi Interior Salt Basin, Gulf coast USA, Unconventional Resources Technology Conference

Han, H. X., 2021, Effects of transient borehole deformation on rock stress and rock properties analysis: University of Waterloo Doctoral Thesis

Hantush, M. S., 1964, Hydraulics of Wells: Advances in Hydroscience,” Vol. 1, Ed.: V. T. Chow, Academic Press, New York, pp. 281–432.

Harris, P. M., and Dodman, C. A., 1987, Jurassic evaporites of the U. S. Gulf Coast: The Smackover-Buckner contact: The Society of Economic Paleontologists and Mineralogists (SEPM) Depositional and Diagenetic Spectra of Evaporites, p. 174-192.

Hart, B. S., Flemings, P. B., and Deshpande, A., 1995, Porosity and pressure: Role of compaction disequilibrium in the development of geopressures in a Gulf Coast Pleistocene basin. *Geology*, 23(1), 45-48.

Hiland, P., 2010, Generic Issue 199 GI-199, Implications of updated probabilistic seismic hazard estimates in central and eastern United States on existing plants, Safety Risk Assessment: Nuclear Regulatory Commission

Holland, T.W, 2007, Water Use in Arkansas, 2005: U.S Geological Survey Scientific Investigations Report 2007-5241, 32p.

Holt, R.M., Larsen, I., Fjær, E. and Stenebraten, J.F., 2020, Comparing mechanical and ultrasonic behaviour of a brittle and a ductile shale: Relevance to prediction of borehole stability and verification of shale barriers, *J. of Petroleum Science and Engineering*, 187, 106746.

Horton, S., 2012, Disposal of hydrofracking waste fluid by injection into subsurface aquifers triggers earthquake swarm in central Arkansas with potential for damaging earthquake: *Seismological Research Letters*, v. 83, no. 2, p. 250-260.

Hosford, W. F., 2005, Mechanical Behaviour of Materials, Cambridge: Cambridge University Press, The Edinburgh building.

Hosman, R. L., 1996, Regional Stratigraphy and subsurface geology of Cenozoic deposits. Gulf Coastal Plain, South-Central United States: U. S. Geological Survey professional paper; 1416-G

Hovorka, S.D., Tutton, P., and Trevino, R.H., 2018, Feasibility study of CO<sub>2</sub> storage in saline formations in the region of the planned Lake Charles Methanol Plant", Final Report, Gulf Coast Carbon Center, Bureau of Economic Geology, Jackson School of Geosciences, The University of Texas at Austin, July 30, 2018

Iler, R. K., 1979, The chemistry of silica: New York, Wiley, p. 866.

Imlay R.W., 1949, Lower Cretaceous and Jurassic Formations of Southern Arkansas and Their Oil and Gas Possibilities, State of Arkansas Division of Geology: Information Circular 12.

Jackson, M. P. A. and Galloway, W. E., 1984, Structural and depositional styles of Gulf Coast Tertiary continental margins: Application to hydrocarbon exploration: Am. Assoc. Petroleum Geologists, Continuing Education Course Note Series No. 25, p. 226.

Jackson, M. P. A, and Wilson, B. D., 1982, Fault tectonics of the East Texas Basin: Geological Circular 82-4, p. 31.

Johnston, O. C. and Greene, C. J., 1979, Investigation of Artificial Penetrations in the Vicinity of Subsurface Disposal Wells: Texas Department of Water Resources.

Johnston, O. C., and Knape, 1986, Pressure effects of the static mud column in abandoned wells: Texas Water Commission LP 86-06, 106 p.

Jones, T. A. and Haimson, J. S., 1986, Demonstration of Confinement: An Assessment of Class 1 Wells in the Great Lakes and Gulf Coast Regions: Journal of the Underground Injection Practices Council, Number 1, pp. 279-317.

Jordan, P., and Doughty, C., 2009, Sensitivity of CO<sub>2</sub> migration estimation on reservoir temperature and pressure uncertainty, *Energy Procedia*, v. 1, p. 2825-2832.

Kaszuba, J.P., Janecky, D.R. and Snow, M., 2002, October. Experimental evaluation of mixed fluid reactions between supercritical carbon dioxide and a NaCl brine: relevance to geologic aquifer carbon sequestration. In *2002 Geological Society of America annual meeting, session* (Vol. 135, No. 3, pp. 27-30).

Keranen, K.M., Savage, H.M., Abers, G.A., and Cochran, E.S., 2013, Potentially induced earthquakes in Oklahoma, USA: Links between wastewater injection and the 2011 M 5.7 earthquake sequence: *Geology*, v. 41, p. 699-702.

Kharaka Y.K., Cole D.R., Hovorka S.D., Gunter W.D., Knauss K.G., Freifeld B.M. (2006) Gas–water–rock interactions in Frio Formation following CO<sub>2</sub> injection: implications for the storage of greenhouse gases in sedimentary basins. *Geology* 34(7):577–580

Kirkland, B. L., 1988, Petrographic and graphic analysis of shelf-edge porosity in the Lower Cretaceous Sligo Formation South Texas: *Transactions – Gulf Coast Association of Geological Societies*, v. 38, p. 590

Kose, S. G., 2013, Crustal Architecture, Cretaceous Rise and Igneous Activity of Sabine, Monroe and Jackson Uplifts, Northern Gulf of Mexico Basin, Master's Thesis, University of Houston

Kresse, T.M, Hays, P.D., Merricman, K.R., Gillip, J.A., Fugitt, D.T., Spellman, J.L., Nottmeier, A.M., Westerman, D.A., Blakcstock, J.M., and Battreal, J.L., 2014 Aquifers of Arkansas – Protection, management, and hydrologic and geochemical characteristics of groundwater resources in Arkansas: U.S. Geological Survey Scientific Investigations Report 2014-5149, 334p.

Kristiansen, T.G., Dyngeland, T., Kinn, S., Flatebø, R. and Aarseth, N.A., 2018, Activating shale to form well barriers: Theory and field examples, SPE-191607-MS.

Kreitler, C. W., 1986, Hydrogeology of sedimentary basins as it relates to deep-well injection of chemical wastes, Proceedings of the International Symposium on Subsurface Injection of Liquid Wastes, New Orleans, National Water Well Assoc., Dublin, Ohio, pp. 398-416.

Kreitler, C. W. and Richter, B.C. 1986, Hydrochemical Characterization of Saline Aquifers of the Texas Gulf Coast Used for the Disposal of industrial Waste: The University of Texas at Austin. Bureau of Economic Geology. contract report to the U.S. Environmental Protection Agency. Contract No. R-812785-01-0. 164 p.

Kreitler, C. W., Akhter, M. S., Donnelly, A. C. A. and Wood, W. T., 1988, Hydrogeology of formations used for deep-well injection, Texas Gulf Coast: Prepared for the U. S. Environmental Protection Agency under Cooperative Agreement ID No. CR812786-01-0, The University of Texas at Austin, Bureau of Economic Geology Austin, Texas, 215 p.

LBNL, 2014, Final report on experimental and numerical modeling activities for the Newark Basin: Lawrence Berkeley National Laboratory, Berkeley California, 130 p.

Leeds and Associates, 1989, Seismic Effects/DuPont Sabine River Works, DuPont Sabine River Works HWDIR Exemption Petition.

Loizzo, M., Lecampion B., Mogilevskaya S., 2017, The role of geological barriers in achieving robust well integrity. Energy Procedia

Loucks, R. G., Dodge, M. M. and Galloway, W. E., 1986, Controls on porosity and permeability of hydrocarbon reservoirs in lower Tertiary sandstones along the Texas Gulf Coast: Bureau of Economic Geology, Report of Investigations No. 149.

Lowry, P., 1988, Stratigraphic Framework and Sedimentary Facies of a Clastic Shelf Margin: Wilcox Group Paleocene-Eocene, Central Louisiana; Louisiana State University and Agricultural and Mechanical College, PhD Dissertation

Lund Snee, J.E. and Zoback, M.D, 2016, State of Stress in Texas: Implications for induced

seismicity: AGU Publications Geophysical Research Letters, 43, 10,208 – 10,214

Lund Snee, J. E. and Zoback, M. D., 2020(b), Multiscale variations of the crustal stress field throughout North America: Nature Communications.

Mancini, E. A., and Puckett, T. M., 2002, Transgressive-regressive cycles in Lower Cretaceous strata, Mississippi Interior Salt Basin area of the northeastern Gulf of Mexico, USA: Cretaceous Research, v. 23, p. 409-438.

Mancini E.A., 2008, Basin Analysis and Petroleum System Characterization and Modeling, Interior Salt Basins, Central and Eastern Gulf of Mexico, DOE Report No. 15395.

Matthews, A. C., Weed, S. B., Coleman, N. T. 1955, The Effect of Acid and Heat Treatment on Montmorillonite: National Academy of Sciences, Washington DC.

Matthews, W. R. and Kelly, J., 1967, How to predict formation pressure and fracture gradient from electric and sonic logs: The Oil and Gas Journal, Figure 3, ADT 21

McClain, K. C., 2021, Mineralogical restrictions on porosity in the Taylor Sand of the Cotton Valley Group, Northern Louisiana Salt Basin, Claiborne Parish, Louisiana: Electronic Theses and Dissertations, Stephen F. Austin State University, p. 1-87.

Meckel, T.A., Nicholson, A.J., and Trevino, R.H., 2017, Capillary Aspects of Fault-Seal Capacity for CO<sub>2</sub> Storage, Lower Miocene, Texas Gulf of Mexico”, in Geological CO<sub>2</sub> Sequestration Atlas of Miocene Strata, Offshore Texas State Waters, Bureau of Economic Geology, 2017.

Merriman, D. , 2014, More motion, less e-motion—Is 2014 the year lithium regains its traction: Sixth Annual Lithium Supply & Markets Conference, Montreal, Quebec, Canada, May 20–22 2014, Presentation.

Miller, C., Hales C., Clark, J. E. and Collins, G., 1989, Density drive flow near salt domes: Underground Injection Practices Council Winter Meeting, San Antonio, Texas.

Murray, 1957, Hydrocarbons in Gulf Coastal Province of the United States: Gulf Coast Association of Geological Societies, Transactions, Vol. VII, and p. 254.

Murray, G.E., 1961, Geology of the Atlantic and Gulf coastal province of North America: Harper and Brothers, New York, p. 692.

National Academies of Sciences, Engineering, and Medicine, 2019, Negative Emissions Technologies and Reliable Sequestration: A Research Agenda. Washington, DC: The National Academies Press. <https://doi.org/10.17226/25259>

Nealon, D. J., 1982, A Hydrological Simulation of Hazardous Waste Injection in Mt. Simon, Ohio: Master's Thesis, Ohio University.

Neuman, S. P. and Witherspoon, P. A., 1969a, Theory of flow in a confined two aquifer system, Water Resources. Res., 5, 4, 803-816.

Neuman, S. P. and Witherspoon, P. A., 1969b, Applicability of current theories of flow in leaky aquifers, Water Resources. Res., 5, 4, 817-829.

Neuzil, C. E., 1986, Groundwater flow in low permeability environments: Water Resources Research, v. 22, no. 8, p. 1163-1195

Nichols, J. L., 1958, Sligo stratigraphy of North Louisiana, Arkansas and East Texas: Reference report on certain oil and gas fields, vol. 4, p. 1-52.

Nicholson, A., J., 2012, Empirical Analysis of Fault Seal Capacity for CO2 sequestration, Lower Miocene, Texas Gulf Coast: Master's Thesis, The University of Texas at Austin, 100 p.

Nuclear Regulatory Commission (NRC), 2019, Arkansas Nuclear One, Unit 2 Safety Analysis Report (SAR), p. 4270.

Ohio Department of Natural Resources, 2012, Executive Summary: Preliminary report on the Northstar I Class II injection well and the seismic events in the Youngstown, Ohio area: State Report, p 1- 23, Columbus, Ohio.

Ostermeier, R. M. 2001, Compaction effects on porosity and permeability: Deepwater Gulf of Mexico turbidite. *Journal of Petroleum Technology*, 53(02), 68-74.

Paulson, O. L., 1972, Various factors influence Wilcox deposits in the “Golden Triangle”: Oil and Gas Journal, 86-87.

Payne, J. N., 1972, Hydrogeologic significance of lithofacies of the Cane River Formation or equivalents of Arkansas, Louisiana, Mississippi, and Texas: Geological Survey Professional Paper 569-C, 17 p

Rainwater, E. H., 1964(a), Regional Stratigraphy of the Midway and Wilcox in Mississippi: Mississippi Geological Economic and Topographical Survey, Bulletin No. 102, 9-31 pp.

Rainwater, E. H., 1964(b), Stratigraphy Gulf Coast Miocene: Gulf Coast Association of Geological Societies Transactions, v. 14, 76-77.

Rutqvist, J., Wu, Y. S., Tsang, C. F. and Bodvarsson, G., 2002, A modeling approach for analysis of coupled multiphase fluid flow, heat transfer, and deformation in fractured porous rock: *International Journal of Rock Mechanics and Mining Sciences*, v. 39, no. 4, p. 429–442

Salvador, A., 1991, Origin and development of the Gulf of Mexico Basin, in A. Salvador ed., *The Gulf of Mexico Basin: Geological Society of America, The geology of North America*, v. J, p. 389 – 444.

Salvador, A., 1991, *The Geology of North America Vol. J, The Gulf of Mexico Basin; The Geological Society of America*

Salvador, A., 1991a, Chapter 8: Triassic-Jurassic, *The Geology of North America, Vol. J, The Gulf of Mexico Basin*. p. 131-180.

Sawyer, D. S., Buffler, R. T., and Pilger, R. H., Jr., 1991, The crust under Colorado, *Geological Society of America, The Geology of North America*, v. J. Gulf of Mexico basin, in Salvador, A., ed., *The Gulf of Mexico Basin: Boulder*

Schlumberger, 1987, Log Interpretation Principles/Applications, Schlumberger Educational Services, Houston, Texas, p. 198.

Schlumberger, 1988, Archie's Law: Electrical Conduction in Clean, Water-bearing Rock, The Technical Review, v. 36, n. 3, Schlumberger Educational Services, Houston, Texas, pp. 4-13.

Schrader, T. P., 2014, Water levels and water quality in the Sparta-Memphis aquifer (middle Claiborne aquifer) in Arkansas, spring–summer 2011: U.S. Geological Survey Scientific Investigations Report 2014–5044, p. 44, <http://dx.doi.org/10.3133/sir20145044>.

Schulz, K. J., DeYoung, J. H., Jr., Seal, R. R., II, and Bradley, D. C., eds., 2017, Critical mineral resources of the United States—Economic and environmental geology and prospects for future supply: U.S. Geological Survey Professional Paper 1802, p. 797, <https://doi.org/10.3133/pp1802>.

Slaughter, G. M., 1981, An Analysis of Ground Water Flow Times Near Seven Interior Salt Domes: Dept. of Energy for Battelle Memorial Institute Office of Nuclear Waste Isolation.

Sone, H. and Zoback, M., 2013, Mechanical properties of shale-gas reservoir rocks — Part 2: Ductile creep, brittle strength, and their relation to the elastic modulus. *Geophysics*, Vol. 78, No. 5 Sept-Oct; p. D393–D402.

Spain, D. R., Lie, S., BP America, Devier, C., PTS Laboratories, 2011, Petrophysical rock typing of tight gas sands – Beyond porosity and saturation: Example from the Cotton Valley Formation, East Texas: Society of Petroleum Engineers Middle East Unconventional Gas Conference, Muscat, Oman, p. 1-14.

Swain, F. M., 1943, Stratigraphy of the Cotton Valley beds of the Northern Gulf Coastal Plain: Dissertation, University of Kansas, p. 1-56.

Talman, S., 2015, Subsurface geochemical fate and effects of impurities contained in a CO<sub>2</sub> stream injected into a deep saline aquifer: What is known: *International Journal of Greenhouse Gas Control* p. 40.

Thomas, W.A. and Mann, J.C., 1966, Late Jurassic depositional environments, Louisiana and Arkansas, AAPG Bulletin (1966) 50(1) 178-182 pp.

Turner, R., 1964, Kinetic studies of Acid Dissolution of Montmorillonite and Kaolinite: Ph.D. thesis, Univ. of Calif. Davis.

U.S. Geological Survey (USGS), 2008, Monitoring of Sparta Aquifer recovery in southern Arkansas and northern Louisiana, 2003 – 07: Fact Sheet 2007 – 3102, p. 4.

Warner, D. L., 1988, Abandoned oil and gas industry wells and their environmental implications: prepared for the American Petroleum Institute.

Warner, D. L. and Syed, T., 1986, Confining layer study-supplemental report: prepared for U. S. EPA Region V, Chicago, Illinois.

Warren, J. K., 2016, Hydrocarbons and Evaporites. In: Evaporites A Geological Compendium. Springer International Publishing, p. 959-1079.

Wesson, R. L., and C. Nicholson, 1987, Earthquake hazard associated with deep well injection: U.S. Geological Survey Open-File Report 87-331, 72

Williams S., Carlsen T., Constable K., Guldahl, A., 2009, Identification and qualification of shale annular barriers using wireline logs

Wilson, D. A., and Hensel, W. M., 1982, The Cotton Valley sandstones of East Texas: A log-core study: SPWLA Twenty-Third Annual Logging Symposium, July 6-9, p. 1-27.

Wood, D. H. and Guerva, E. H., 1981, Regional Structural cross sections and general stratigraphy, East Texas basin: University of Texas at Austin, Bureau of Economic Geology, 21 p.

Worley and Standard Lithium LTD., 2019, NI 43 – 101 Technical Report, Preliminary economic assessment of Lanxess Smackover project, p. 230.

Zhang, J. and Roegiers, J. C., 2010, Integrating borehole-breakout dimensions, strength criteria and leak-off test results, to constrain the state of stress across the Chelungpu Fault, Taiwan. *Tectonophysics*, 24921–4, p. 295–8.

Zoback, M.L. and Zoback, M., 1980, States of Stress in the Conterminous United States. *Journal of Geophysical Research*, v. 85, no. B11, 6113-6156 pp.